FINAL TECHNICAL REPORT
Award Number: G13AP00046

Title: "Proposal in Support of the St. Louis Area Earthquake Hazards Mapping Project: Completion of the Final 12 SLAEHMP Seismic and Liquefaction Hazard Maps"

Chris H. Cramer, P.I.
Center for Earthquake Research and Information
University of Memphis
3890 Central Ave
Memphis, TN 38152-3050
901-678-4992
FAX: 901-678-4734
cramer@ceri.memphis.edu

July 1, 2013 – June 30, 2017

Total Funding: $85,329.00

Submitted: July 1, 2017

"Research supported by the U.S. Geological Survey (USGS), Department of Interior, under USGS award number G10AP0004. The views and conclusions contained in this document are those of the authors and should not be interpreted as necessarily representing the official policies, either expressed or implied, of the U.S. Government."

St. Louis Area Earthquake Hazards Mapping Project: Seismic and Liquefaction Hazard Maps

By C.H. Cramer, R.A. Bauer, J. Chung, J.D. Rogers, L. Pierce, V. Voigt, B. Mitchell, D. Gaunt, R.A. Williams, D. Hoffman, G.L. Hempen, P.J. Steckel, O.L. Boyd, C.M. Watkins, and N.S. McCallister

Summary

Probabilistic and deterministic (scenario) seismic hazard maps for the St. Louis metropolitan area, which include the effects of surficial geology on site response, have been prepared for the 29 USGS 7.5-minute quadrangles of the study area. The computer codes used in this study, which are similar to those used in the generation of the USGS national seismic hazard maps (Frankel and others, 2002; Petersen and others, 2008, 2014), were modified for use in this study by Cramer (2003, 2011, 2014). These codes, which were implemented for this project on a high performance computing (HPC) system at the University of Memphis, account for the fully-probabilistic approach in developing the maps and apply the median and natural logarithm standard deviation of site amplification estimates to the hard-rock ground motion attenuation relations in the probabilistic maps. Only the median of site amplification was applied in the deterministic maps. All of the seismic hazards were calculated based on a grid of 0.005°, or about every 500 m, the same spacing employed in the amplification distribution calculations. To account for some of the uncertainty found in St. Louis area shear-wave velocity measurements, shear modulus proxies, depth to bedrock calculations, earthquake time histories, and so on, a Monte Carlo randomization procedure was used to generate site-amplification distributions and provide an estimate of the uncertainty, in terms of mean, median, and standard deviation. These distributions were assumed to be lognormal in form.

In this study one-dimensional equivalent-linear response analysis was used to evaluate site-amplifications because of the following reasons: 1) high strain levels are not expected; 2) high excess water pressure development is not expected, and 3) the bedrock structure and overlying soft-sediment layering is near-horizontal in the St. Louis area. When compared to the USGS National Maps, the new probabilistic hazard levels calculated in the 29 quadrangle area for upland sites (loess covered till, drift, residuum) show up to 100 percent greater ground motion levels for peak ground acceleration (PGA), up to 150 percent greater ground motion levels for 0.2s spectral acceleration (SA), and up to 100 percent greater ground motion levels for 1.0s SA. Probabilistic hazard levels for lowland (alluvial) sites, generally the modern Mississippi and Missouri River floodplains, exhibit up to 175 percent greater ground motion levels for PGA, between 20 percent less to 20 percent greater ground motion levels for 0.2s SA, and up to 200 percent greater ground motion levels for 1.0s SA, when compared to the National Hazard Map. A simplified shaking hazard map, based on PGA estimates from 5%-in-50-year probabilistic hazard, which includes median ground motions from a M7.5 on the NE segment of the New Madrid seismic zone, shows generally moderate (> 0.1 g) shaking hazard (serious hazard for unreinforced masonry construction).

SLAEHMP also generated liquefaction hazard maps for the 29 quadrangles of the study area.

Liquefaction probability curves were developed from available SPT data for typical lowland and upland water levels. These liquefaction probability curves where then used with the probabilistic and scenario ground shaking hazard maps to calculate liquefaction hazard maps. Technical liquefaction hazard maps were developed for moderate and severe liquefaction hazard using the probability of the Liquefaction Potential Index (LPI) exceeding 5 and 12, respectively. A simplified liquefaction hazard map has been created from the same 5%-in-50-year probabilistic ground shaking as the simplified shaking hazard map and based on the expected % area showing liquefaction effects at the surface. The liquefaction hazard ranges from low (< 40% of area expected to liquefy) in the uplands to severe (> 60% of area expected to liquefy) in the lowlands. Artificial-fill deposits are common, and are assigned a "special study required" designation because of the difficulties associated with estimating their geotechnical and engineering properties, and thus restricts the ability to forecast their response to seismic shaking. Since many transportation routes, power and gas transmission lines, and population centers exist in or on the highly susceptible Holocene alluvium, these areas in the St. Louis region are at significant potential risk from seismically induced liquefaction and liquefaction-related ground deformation.

Introduction

The SLAEHMP is a key part of the USGS Earthquake Hazards Program, which seeks to reduce the Nation's risk from earthquake hazards; other metropolitan areas that are a part of this national program include Seattle, Washington; Evansville, Indiana; Memphis, Tennessee; Charleston, South Carolina; Reno, Nevada; and the Wasatch Front, Utah urban corridor. The project addresses earthquake hazards throughout the St. Louis metropolitan area, a densely populated urban zone, which is split between Missouri and Illinois (fig. 1). The region has experienced strong ground shaking as a result of pre-historic and contemporary seismicity associated with the major neighboring seismic source areas, including the Wabash Valley seismic zone (WVSZ) and New Madrid seismic zone (NMSZ) (fig. 1). The goal of the St. Louis project is to produce practical hazards maps and an internet-accessible database that can be used by those in the geosciences, design communities, and city and county planning agencies and would allow these groups to more accurately plan for events of this nature.

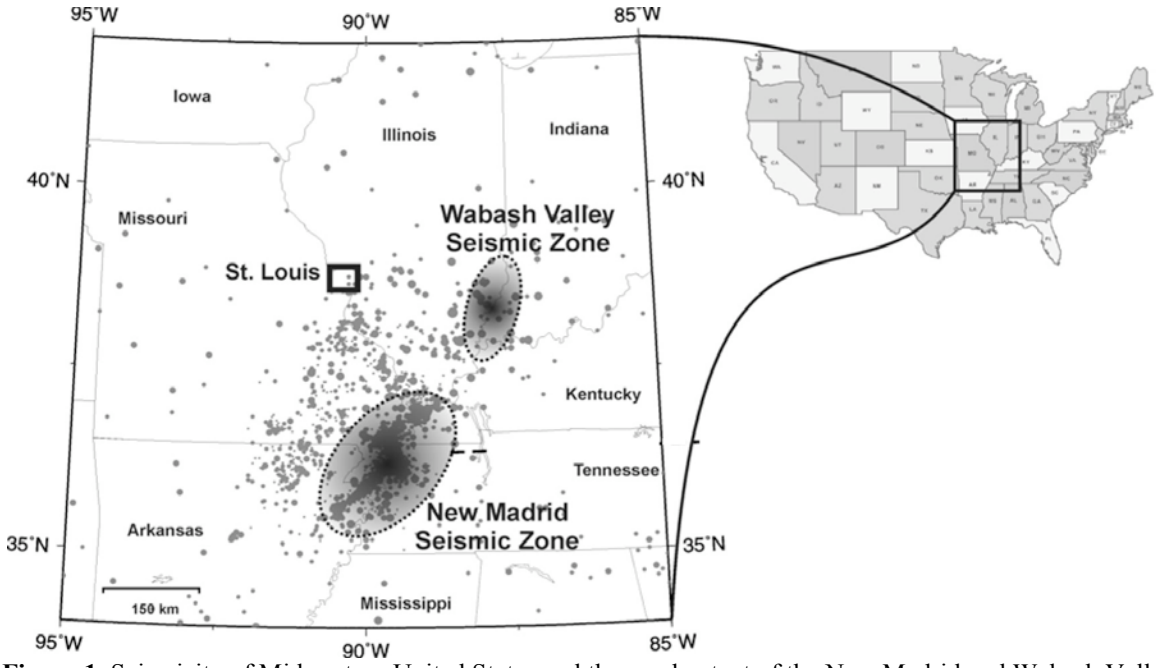

Figure 1. Seismicity of Midwestern United States and the areal extent of the New Madrid and Wabash Valley Seismic Zones relative to the St. Louis area. Dots represent the seismic activity recorded during historic time. The diameters of the circles represent earthquake epicenters, with increasing magnitude.

In response to earthquake hazard potential in other parts of the Midwest, in 2004 the USGS Memphis office organized the SLAEHMP. The project is guided by a Technical Working Group (TWG) consisting of earth scientists and engineers from local firms, universities, and government agencies. The TWG convenes four times a year to discuss mutual goals and assignments focusing on evaluating relative seismic risks and ground shaking hazards posed to the St. Louis Metropolitan area.

The study area encompasses about 4,000 square km across 29 USGS 7.5-minute quadrangles (fig. 2). The objectives of this project are to: 1) create detailed maps of earthquake hazards in the St. Louis area, 2) create a three-dimensional database of geological and geotechnical information, and 3) enlist practical input from stakeholders and end users of the hazard maps. The 29 quadrangles have been completed and are the subject of this report. The array of urban hazard maps and their format are very similar to the urban hazard maps established by the USGS for the Memphis/Shelby County Seismic Hazard Mapping project completed in 2004, with the addition of simplified seismic and liquefaction hazard maps (one of each) for use by non-technical users.

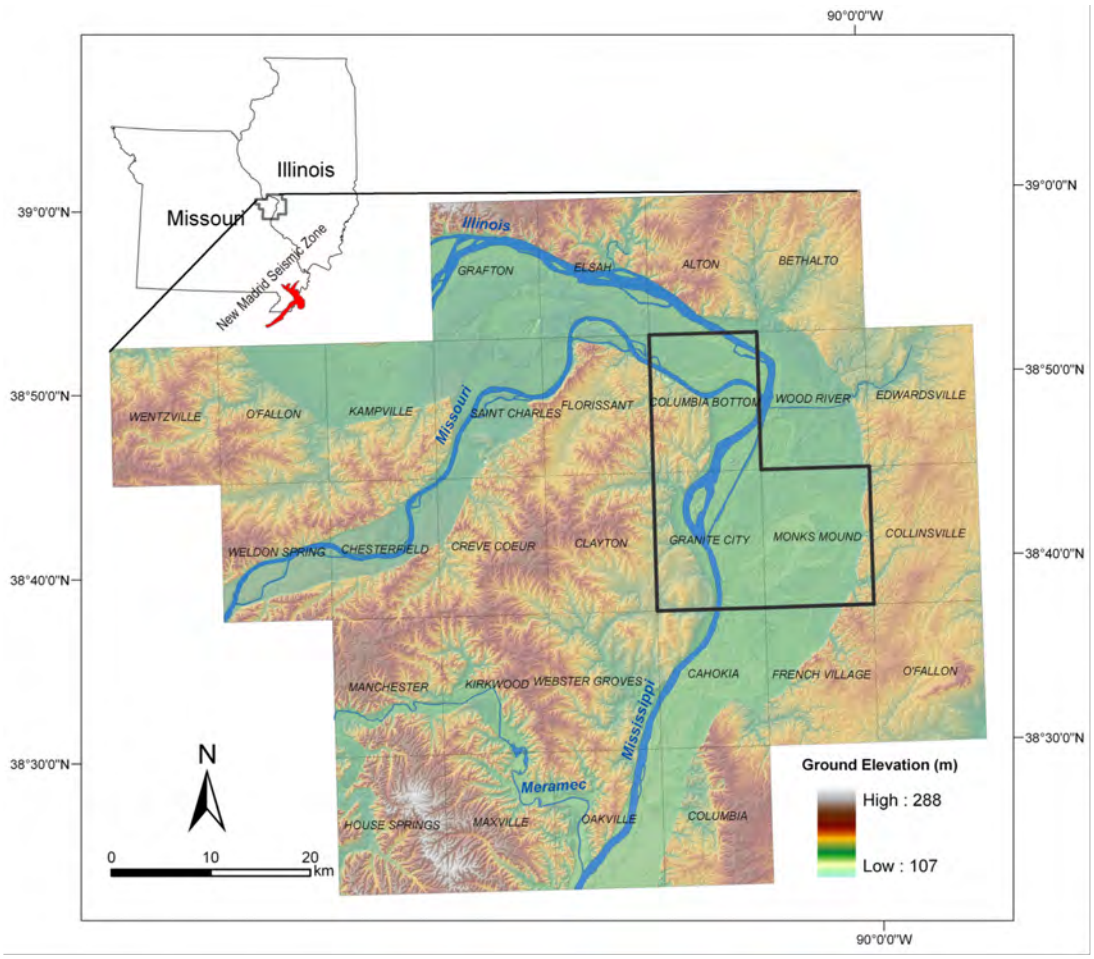

Figure 2. For this study, the St. Louis metropolitan area encompasses 29 USGS quadrangles as shown on this shaded relief map. The general outline of NMSZ seismicity is shown as the red area in the upper left (after Hoffman 2005, personal commun.; Chung, 2007). The black outlined three quadrangles are the original pilot study quadrangles of the project.

This region is, for the most part, located on unconsolidated Quaternary deposits which consists of: 1) lowlands of alluvial deposits in floodplains along four major rivers (Mississippi, Missouri, Illinois, and Meramec), and 2) uplands of loess over glacial till or drift deposits or residuum (Goodfield, 1965; Grimley and others, 2007b; Grimley and Phillips, 2006). Bedrock shallowly underlies the Quaternary deposits in the St Louis region and largely consists of flat-lying sedimentary rock formations, mostly Mississippian-age limestone and Pennsylvanian-age shale (Harrison, 1997). According to borehole data provided by the Missouri and Illinois Geological Surveys, the depths to bedrock are generally about 30 to 40 m and about 0 to 15 m in lowlands and uplands, respectively.

Methodology

The physical properties of the bedrock and Quaternary deposits in the St. Louis area will strongly

influence seismic wave transmission through the region. It is well known that the bedrock of the Central and Eastern United States (CEUS) is older and more indurated than that in the western United States, such as California, and partly as a result of this, seismic energy is transmitted much more efficiently in the CEUS. These properties of CEUS bedrock also lead to higher seismic wave speeds, less energy attenuation, and permit crustal earthquake waves to spread laterally over much larger areas (Nuttli, 1973).

The site response analyses used in this study considered the time-histories at the base of the Quaternary deposits and assume a flat (horizontal) boundary between the Quaternary and the underlying bedrock. In the St. Louis study area, the Quaternary-rock interface is nearly horizontal, so focusing effects are not expected to be a strong influence. Past experiences have demonstrated that the intensity of ground shaking may vary considerably during any given earthquake, depending on the underlying geology. Our seismic hazard analyses depend on ground shaking estimates, which, in turn, are based on accurate subsurface characterization of the geology. Some fundamental uncertainties always exist, however, with the accuracy of the subsurface models, which are estimates based on data from borings or other subsurface measurements that may be located some distance away. The uncertainty in estimated depths and thicknesses of geologic layers increases with increasing offset distances from the points of subsurface measurement. In this study the most important factors affecting ground-shaking estimates appear to be the physical properties and thickness of the Quaternary surficial materials overlying the bedrock.

In the Geology section, information on the compiled bedrock and surficial geology are summarized, as well as the methods employed to estimate the depth and thickness of the surficial units. In the Shear-Wave Velocity section, the approach of reference shear-wave velocity (Vs) profiles is reviewed. In the Specific Model Development section, the ISGS and MoDGS geologic models are presented. The ISGS and MoDGLS geologic models include specific Vs reference profiles developed for each state's geologic input to the hazard calculation process. In the Seismic Hazard Maps section, the methodology for the generation of the seismic hazard maps is presented along with representative seismic hazard maps. And in the Liquefaction Hazard Maps section, the investigation and development of the liquefaction potential curves and the approach for calculating the liquefaction hazard maps is presented along with representative liquefaction hazard maps.

Geology

Bedrock Geology

The term "bedrock" in the St. Louis area is used to describe those geologic formations of Paleozoic Era in the 29-quadrangle study area, which range in age between the Ordovician and Pennsylvanian Periods. This bedrock is only sparsely exposed in most quadrangles. Most of the information about the underlying bedrock was developed from available borehole logs and previously mapped and interpreted areas. Information concerning the bedrock geology is referenced from the studies and maps prepared by ISGS, USGS, and MDNR (Denny, 2003; Denny and Devera, 2001; Harrison, 1997; Grimley and others, 2007a; Lutzen and Rockaway, 1971). The bedrock is composed mainly of limestone, dolostone, chert, shale, and sandstone.

Pockets of individual sinkholes and karstic features in these limestones were identified by Goodfield (1965). In the hazard maps, however, karstic features were not taken into account because of the limited knowledge about the extent of these features.

Surficial Geology and Depth to Bedrock

The surficial geology of the St. Louis area varies widely, from thick alluvium (30 to 50 m) in the broad Mississippi River valley to thin glacial drift (usually < 15 m), and to thick loess in the areas east of the Mississippi River, in Illinois. The loess is thickest (up to 29 m) at the bluffs immediately east of the Mississippi River valley and thins to the east and northeast (Fehrenbacher and others, 1986; Grimley and others, 2007b). The modern river floodplains are comprised of alluvial sediment, mostly silts and silty clays, and a thick sequence of sands and gravels extending down to the bedrock (Goodfield, 1965). Seventeen quadrangles contain portions of this Mississippi River alluvial valley (fig. 3). Additionally, there are flood plain deposits along the Missouri (~ 30 m thick) and Meramac Rivers (< 20 m thick), which are tributaries to the Mississippi River.

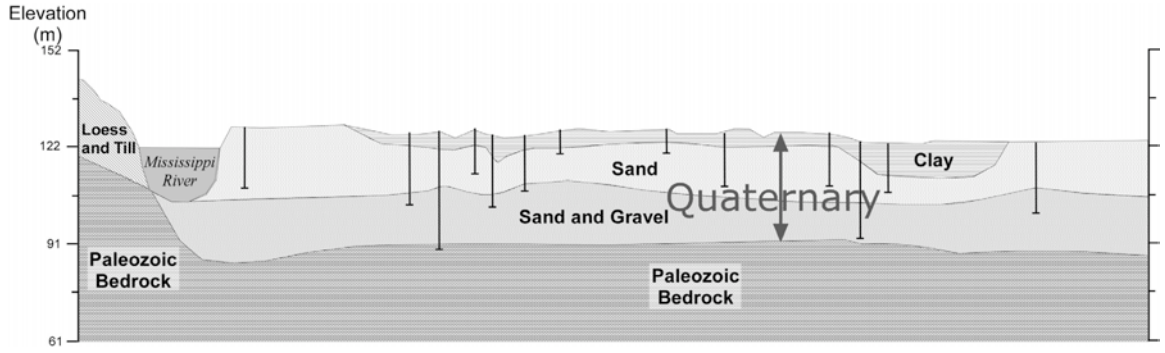

Figure 3. Schematic cross-section looking north showing the surficial geology in the study area (after Grimley and others, 2007a; Phillips and others, 2001). Thickness of Quaternary silty clay, sand, and gravel in the river lowland, overlying the Paleozoic bedrock, is constrained by borehole data (vertical black lines with horizontal bar at maximum depth).

In the study area the alluvial floodplains, being generally the area of lowest elevation, are identified as lowlands. Areas outside the floodplains generally covered by silt (loess), till over bedrock, and some bedrock exposures are identified as uplands. A Quaternary thickness map (or depth to bedrock) of the uplands and lowlands was prepared for the study area and used as input data in ground motion hazard calculations. Stratigraphic interpretations and geologic cross sections, used to estimate depth to bedrock, were prepared by MDNR and ISGS based on information gleaned from field exposures, geophysical surveys, and well logs [geotechnical, water wells, mining, and environmental; Missouri and Illinois Department of Transportation (MoDOT and IDOT) and other private geotechnical agencies; Palmer and others, 2006, written commun.; Palmer 2006, personal commun.; Bauer 2006, personal commun.].

The Quaternary thickness map shows that the bedrock surface is generally about 30- to 50-m deep below the ground surface in the lowlands, and 0- to 15-m deep in most of the uplands with

smaller areas as thick as 40 to 75 m. The bedrock surface changes most abruptly at the lateral margins of the modern day floodplain, which coincides with the boundary between lowlands and uplands. In limited sampling from seismic and boreholes the bedrock surface beneath the Mississippi River floodplain appears to be an even planated to slightly undulating surface, with an extensive area at an elevation of between 90 and 100 m MSL. The greatest uncertainties about depth to bedrock exist in the deep alluvial valleys bordering major rivers, where few borings pierce bedrock.

Shear-Wave Velocity

Shear-Wave Velocity Investigations

The seismic hazard maps require accurate site-amplification calculations that largely depend on the estimated shear-wave velocity (Vs) of the materials underlying the site. In most site response hazard studies Vs has emerged as the one index property that is well correlated, inversely, with earthquake ground motion (Borcherdt, 1970, Wills and others, 2000). Researchers at Missouri S&T, Saint Louis University, MDNR, ISGS, and USGS have collaborated to collect, analyze, and interpret Vs measurements in the upper 50 m at over 100 locations in the St. Louis metropolitan area. These data constrained the St. Louis area seismic velocity model used in the earthquake hazard map calculations.

For these seismic studies we used small hammers to gently shake the ground either vertically to generate surface waves or horizontally to produce shear waves. Vs data was extracted from a variety of field methods including primarily seismic reflection/refraction and multi-channel analysis of surface waves (MASW) measurements, a few seismic cone penetrometer tests, several downhole tests, and one ultrasonic lab test of St. Louis limestone. As described above, bedrock depth around St. Louis was supplemented by existing drillers logs, some older oil exploration wells, and a detailed map of bedrock in downtown St. Louis compiled by URS-St. Louis. Subsurface seismic velocity models at each test site were constructed which were then used to develop the generalized shear-wave reference profiles for the St. Louis area.

Validation of the results by the different methodologies was achieved by comparing the surface-based methods (MASW and reflection/refraction) against existing borehole and downhole data from the same location or a nearby site. Seismic velocities of the soft sediments determined by surface-based methods differed by 5 to 30 percent from the downhole data. Discussions within the SLAEHMP about the thickness of visible weathering of the bedrock around St. Louis indicates that it is generally about 1 m thick for the limestone bedrock and that it is probably non-existent at the top of bedrock within the Missouri and Mississippi River floodplains where it has been scoured off. Thus, for the purposes of the earthquake hazard maps in St. Louis, the depth to the “distinct” alluvium or residuum contact with bedrock by reflection/refraction methods was determined to within about 10 percent of the downhole or borehole result. Vertical resolution limits of the surface-based methods are on the order of 1.5 to 3 m and thus capable of detecting layering that would influence ground motions at the 1- to 5-Hz frequencies of the proposed hazard maps.

Uplands on the Illinois side of the Mississippi River and part of the bedrock below the river on the east side is Pennsylvanian strata, which consists mostly of shales and claystones and thin layers of coal and limestone. The TWG has placed a 25-m thick weathered zone in these shales based on other weathering zones in shales in other parts of the state of Illinois from shear wave velocity measurement and not visible weathering. Also on the Illinois side and under the Mississippi River valley, the TWG placed a 10-m thick weathered zone in the limestones, again based on ISGS experience in Illinois with shear wave velocity measurements.

Results of the Vs field studies show that the Paleozoic rock underlying softer alluvium and residuum in the St. Louis region is clearly identifiable in the reflection/refraction data at depths of generally 10 to 40 m. Indeed, in an analysis of St. Louis Advanced National Seismic System (ANSS) station recordings of a small earthquake, this important impedance boundary was shown to generate a prominent 2-Hz resonance in the 30-m thick alluvial section overlying bedrock in the Mississippi River floodplain (Williams and others, 2007a). A clear difference exists in the Vs profiles between lowland sites and upland urban areas of St. Louis. Vs30 (travel-time averaged Vs to 30-m depth) values in the lowlands range from 200 to 290 m/s (NEHRP category D) and contrast with upland sites, which have Vs30 values ranging from 410 to 785 m/s (NEHRP categories C and B). The lower Vs30 values and earthquake recordings in the floodplains suggest a greater potential for stronger and more prolonged ground shaking during an earthquake.

Despite all these measurements and extensive compilation, there are still ‘holes’ or areas of great uncertainty, especially about bedrock depth along the margins of the floodplain, in areas of the urban uplands not located near major highways and infrastructure. Some of these data ‘holes’ persist inspite of additional effort under SLAEHMP to gathering new data from geotechnical consulting companies, additional MoDOT and IDOT drilling, and using inexpensive shallow seismic methods, to target these areas of uncertainty.

Reference Vs Profiles

Here we summarize the methodology for determining average Vs profiles for the study area. The methodology used is similar to that of Romero and Rix (2001, 2005) and Gomberg and others (2003). Based on similar characteristics, an average Vs profile was assigned to several lowlands (alluvium) and uplands (loess, residuum, and till) surface geologic settings by both ISGS and MDNR. Local analyses were performed to ascertain variations, uncertainties, and randomness associated with the Vs profiles. This study used 76 site-specific Vs profiles to compile characteristic profiles needed for the hazard calculations. In summary, characteristic Vs profiles were determined following a three-step procedure: 1) investigation of geology from the available borehole logs and estimations of the stratigraphy underlying each point of calculation, 2) determination of mean Vs (with uncertainties) from local Vs profiles, in five-meter depth increments, and 3) comparing the variations in Vs values with borings and known limiting parameters, such as depth-to-bedrock.

Specifics of Geologic Model Development

Shear Wave Velocity Data

Alluvium materials

Downhole, crosshole and seismic cone penetrometer test (CPT) shear wave velocity data were collected/compiled from 13 sites in the mapping area and 2 at a great distance: Risco, Missouri and Marked Tree, Arkansas areas (Liu and others, 1997) (fig. 4). This distance covers more than 300 valley miles of Mississippi River sediments. Shear wave velocity values from the study area materials compared favorably to other similarly measured values throughout the Central U.S. Additionally data from some boreholes for the Stan Musial Veterans Memorial Bridge were discarded because of their non-reproducible (between two borehole measurement runs), large range in values (from 250 to 800 m/sec) in the same boreholes at the same depth (figs. 5a & 5b).

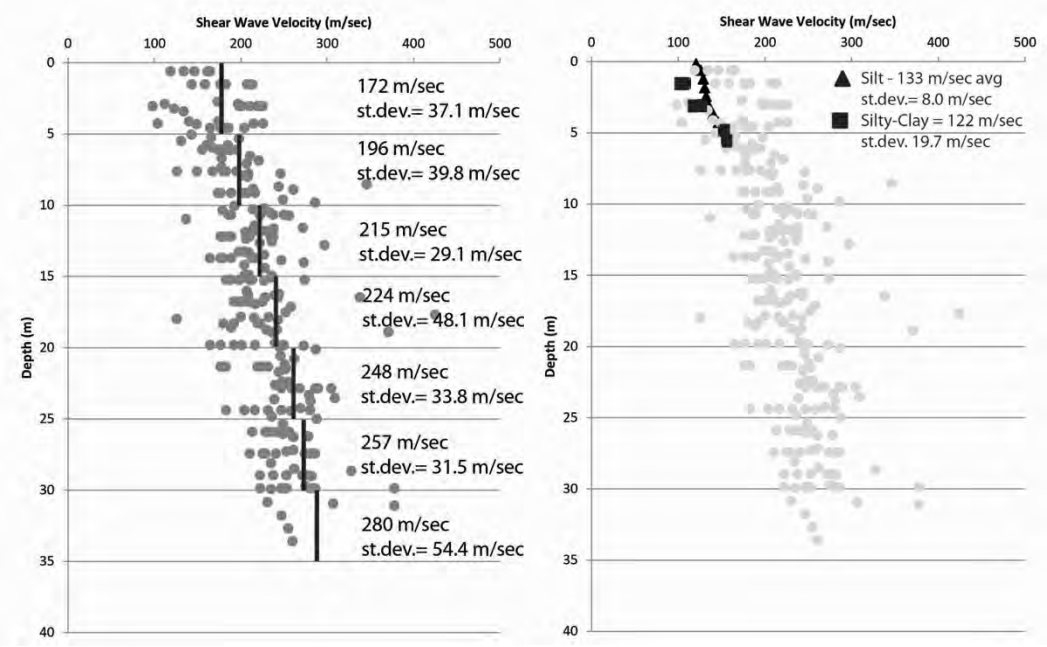

Figure 4. a) Shear wave velocity values from Mississippi River alluvium from downhole, crosshole and seismic CPT measurements. b) Comparison showing how various overbank deposits of silt and silty clay shear wave velocities near the ground surface compare to the alluvium sand.

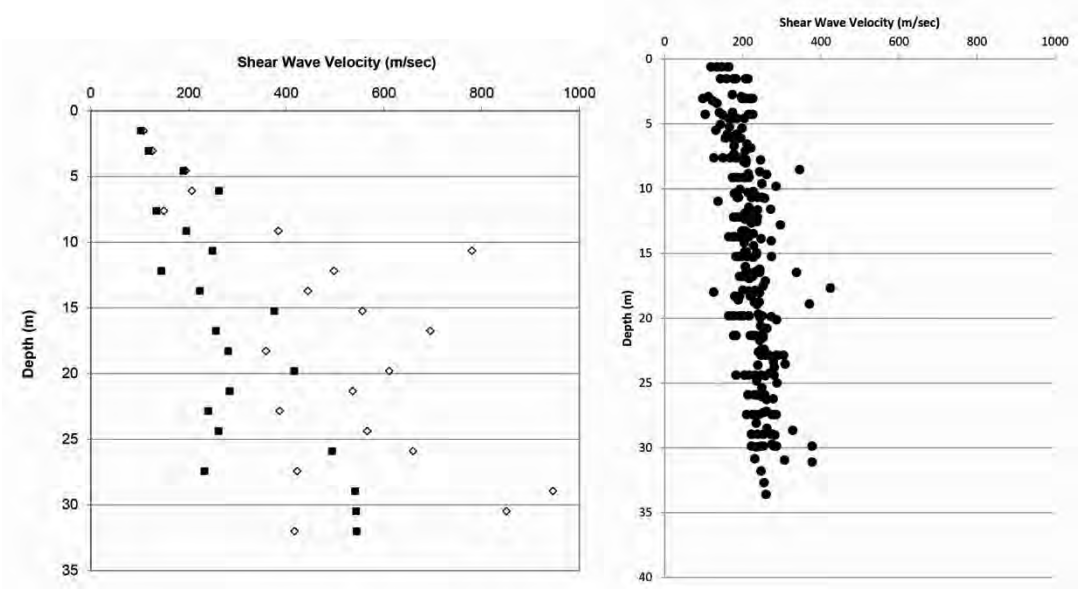

Figure 5. a) Measurements in one borehole at same depths for two different times (black vs. grey). b) Comparison to all other data from 14 boreholes in the same materials, which used several different measuring techniques.

Bedrock materials

Bedrock in the Illinois mapping area is either Mississippian limestone or Pennsylvanian strata which is predominately shale. Downhole measurements in Mississippian limestone exist in the mapping area on both sides of the Stan Musial Veterans Memorial Bridge crossing the Mississippi River (fig. 6). The Missouri data seems to show a fairly linear influence of depth of weathering on shear wave velocity values.

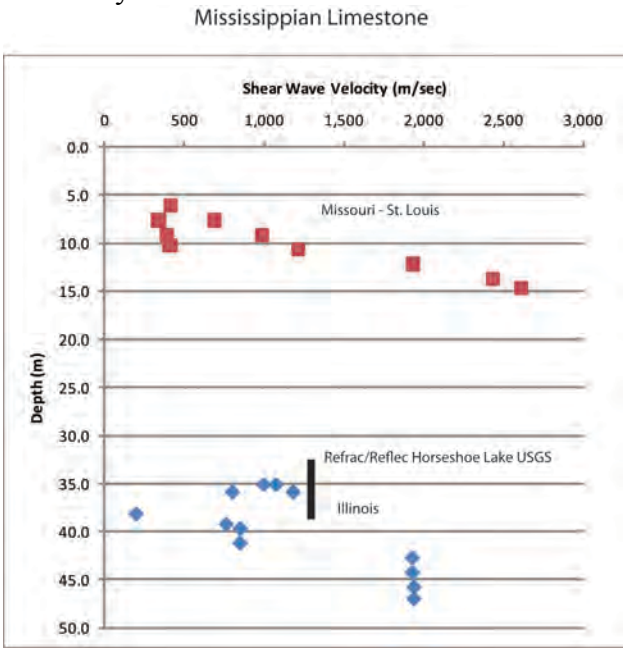

Figure 6. Shear wave velocity downhole measurements for Mississippian limestone on either side of the Mississippi River for the area of the Stan Musial Veterans Memorial Bridge and a refraction/reflection measurement in the area by USGS (Williams and others, 2007a).

Using refraction/reflection, Williams and others (2007a) found the limestone shear wave velocity at Horseshoe Lake State Park in Illinois to be about 1,350 m/sec. This method is not expected to show or detect small changes with depth (weathering profiles) as downhole or crosshole measurements. Using similar methods, shear wave velocity measurements for top of Pennsylvanian strata in the area (Williams and others, 2007a) was found to be about 1,300 m/sec near Collinsville, Illinois (within study area). Also in southern Illinois, Woolery (2005) reported on MASW measurements at surface mines or quarries. The average value is 1,487 m/sec for bedrock with a range of 1,030 to 1,820 m/sec.

Additional Pennsylvanian shear wave velocity values at three sites in Illinois using refraction/reflection and ReMi methods (Odum and others, 2010) show a weathered layer with values ranging between the two methods from 500 to 600 m/sec weathered shale with 950 to 1,250 m/sec unweathered below; 800 to 900 m/sec weathered over 1,100 to 1,600 m/sec unweathered and 1,200 m/sec unweathered.

Crosshole measurements at another site in Illinois show the weathering profile for shale bedrock, as shown by a consistent increase in shear wave velocity values with depth, down to about 20 meters into the shale (fig. 7). Data in the lower part of the graph shows 3-D sonic velocity (another downhole measuring technique) derived in several boreholes where the same shale was deep below the surface and any affects from weathering. The higher shear wave values at the tops of the deep layers are cementation found in the upper parts of the shale at depth.

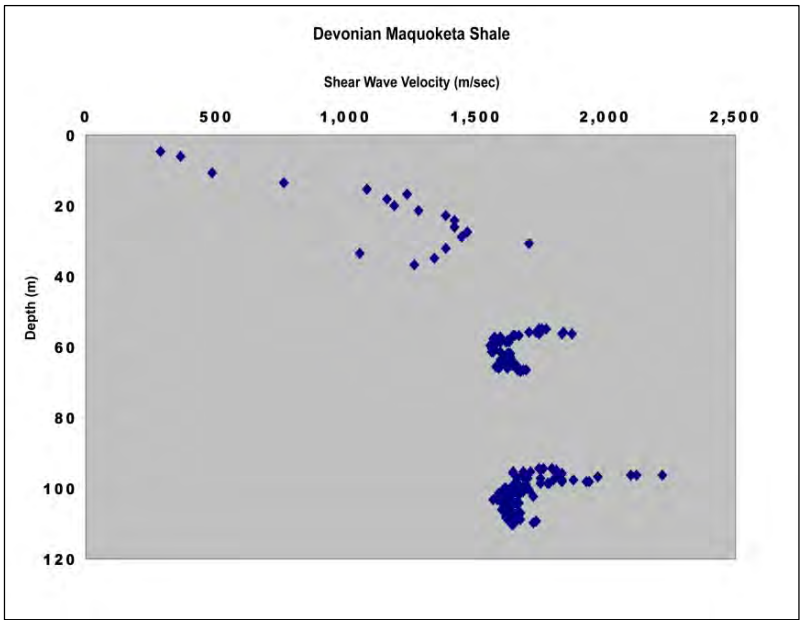

Figure 7. Shear wave velocity measurements from crosshole and 3-D sonic methods showing what is interpreted as the influence of depth of weathering in shale as shown by velocity values.

Upland deposits

Upland deposits throughout Madison and St. Clair Counties in Illinois have been mapped in detail and several locations had downhole shear wave velocity measurements performed in the two major differences in the deposits (figs. 8 & 9). The several major differences in deposits are the presence of the Pearl sand versus areas of till. The other difference is areas of Petersburg silt found near the base of the glacially derived sediments (fig. 9). There are also areas of thicker silt deposits where the Petersburg is found over Harkness silts and over Canten silts. In figure 8, the diamictons (tills and associated sands) show large ranges in shear wave velocity values which are related to the variation in environments of deposition for these deposits. Downhole shear wave velocity measurements in other diamicton locations in the state show this variation as normal (fig. 10). The location of the basal Petersburg silts is shown in plan view in figure 11 for St. Clair County and the study area.

The top layer of the study area materials is loess, which is wind-blown silts from the Mississippi River valley. These silts are thickest near the valley and thin going away from the valley. The thickness sections by the valley edge are over 20 meters thick and tapper to less than 4 meters thick in the study area. Based on downhole shear wave velocity measurements throughout the state, these too show a fairly tightly spaced range of values, which increase in velocity with depth (fig. 12).

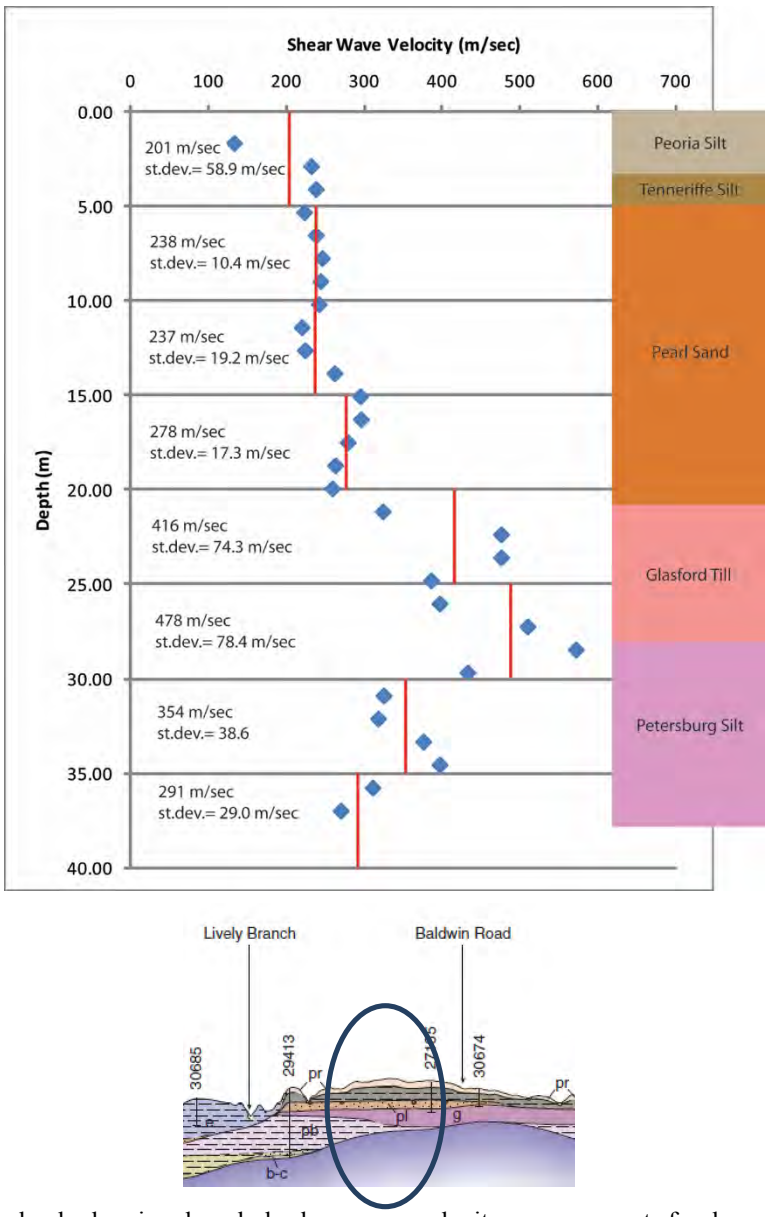

Figure 8. Cross section of uplands showing downhole shear wave velocity measurements for deposits represented in circled area dominated by the Pearl sand (pl) and the basal Petersburg silt (pb). Averages and standard deviations are shown for every 5 meters of depth.

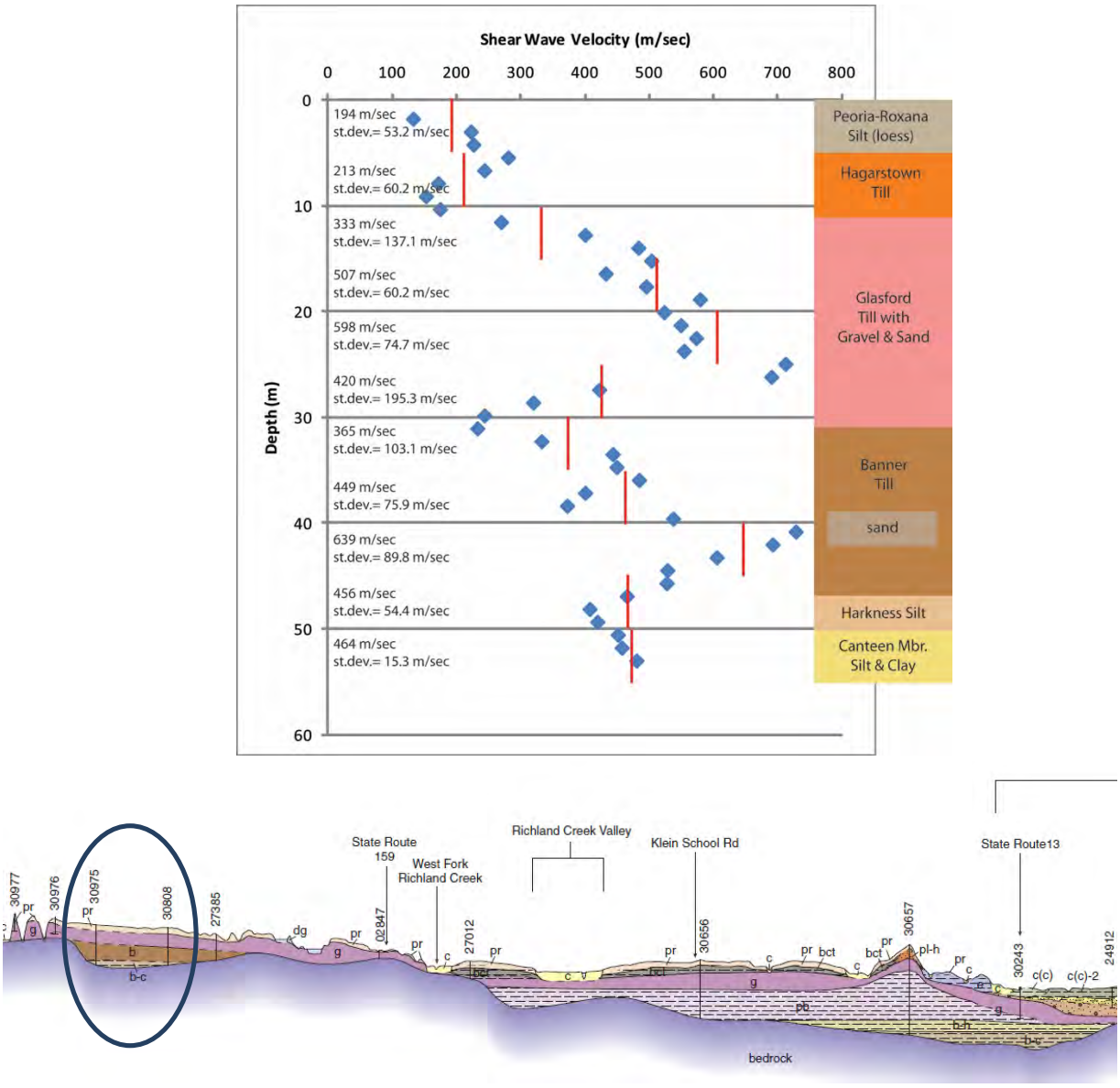

Figure 9. Cross section of uplands showing downhole shear wave velocity measurements for deposits represented in circled area dominated by the sequence of diamicton deposits. Averages and standard deviations are shown for every 5 meters of depth.

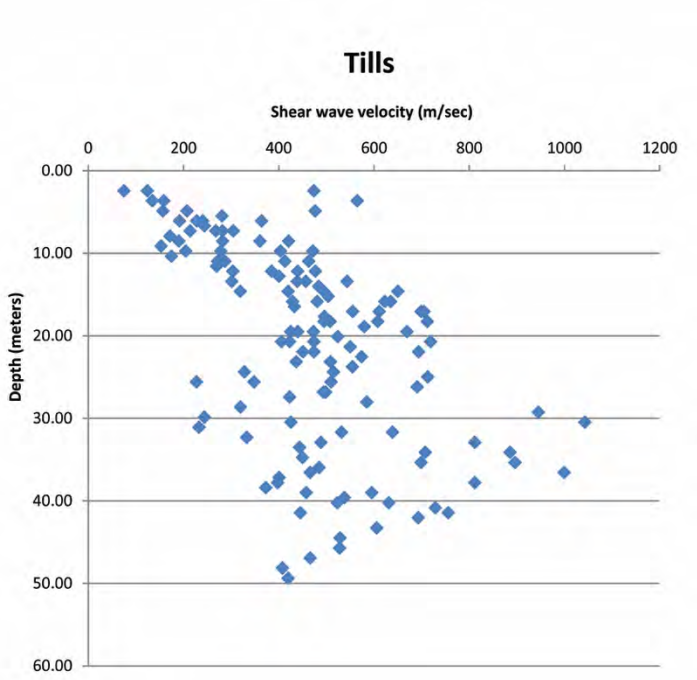

Figure 10. Graph showing the wide variation in downhole shear wave values found in diamictons (tills and associated sand/silt layers). Large variations are a reflection of the non-uniform environments of deposition for diamictons.

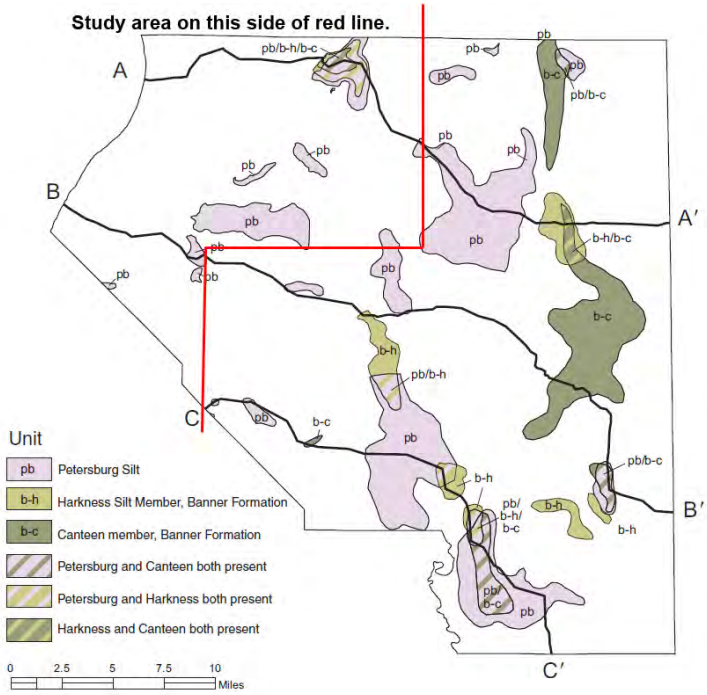

Figure 11. The basal silt (Petersburg silt-(pb)) has been mapped throughout St. Clair County, Illinois. The project area for the St. Louis Urban Hazard Mapping is the western half of this county; west of red line. Map from Grimley and Phillips (2011).

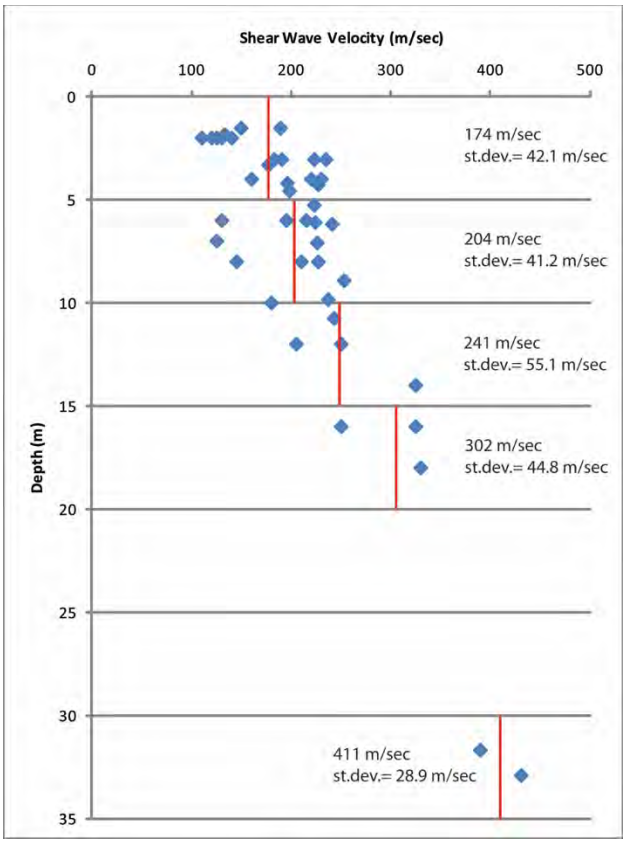

Figure 12. Loess shear wave velocity values from downhole measurements in Illinois. Data averaged with standard deviations for each 5 meters of depth.

Sensitivity Analysis

Multiple columns of the gross variations of the deposits in the alluvial floodplain and upland deposits were assembled and analyzed using the SHAKE91 program for an initial sensitivity analysis of their impact on ground motion amplification**.** Three columns for the alluvial floodplain included 35 meters of just sand over bedrock and two variations with a 5- and 15-meter silty-clay cap over the sand representing various environments of deposition. For the Uplands, first an analysis was run for the two major divisions shown in figures 8 & 9 representing the presence of the thick Pearl sand versus diamictons. The SHAKE91 analysis showed for similar thickness columns of 5 meters of loess cover over a Pearl vs. diamicton dominated sequence that the Pearl column produced an amplification of 3.08 versus 3.79 for the diamicton sequence. The Pearl dominated sequence in this area is mostly east of the study area. The other two major mapped differences are the presence and absence of the Petersburg basal silt and the variations in thickness of the loess top layer. An analysis for the basal silt had a column of 5 meters of loess over 40 meters of till over no silt and another over 10 meters of basal silt. For the loess thickness changes, three columns were used, each with 5, 10 and 20 meters of loess over till. The ground motion inputs were a magnitude 7.7 New Madrid event with the basal input fixed at 0.1 g for all the columns. Their results are shown in table 1.

Table 1. SHAKE91 analysis of various geologic settings in the study area showing amplification in relation to top of bedrock input. Ground motion input is a magnitude 7.7 New Madrid event with the basal input fixed at 0.1 g for the columns.

Alluvial sediments	Amplification		Amplification
35 m sand over bedrock	2.18		
5 m clay over 30 m sand	1.88		
15 m clay over 20 m sand	2.30		
Uplands Basal Silt comparison			
5 m loess over 25 m Pearl/diamicton	3.08	5 m loess over till only	3.79
5 m loess over 25 m Pearl/diamicton over 10 m silt	3.22	5 m loess over till over 10 m basal silt	2.67
		5 m loess over till over 20 m basal silt	2.64
Uplands with changing loess cover			
5 m loess over 50 m diamicton	3.07		
10 m loess over 50 m diamicton	3.49		
20 m loess over 45 m diamicton	2.55		

Similar columns were provided along with dynamic properties, shear wave velocities and standard deviations to Dr. Chris Cramer, University of Memphis who generated site amplification distributions using the randomization approach that was used in generating the St. Louis Area Earthquake Hazards Mapping Project (SLAEHMP) seismic hazard maps. A report on this work is Appendix A. All of these variations were analyzed for the purpose of a sensitivity analysis of what materials and what variations in thicknesses may impact amplification, leading to the generation of geologic provinces representing the materials in the area. The columns in table 1 and in the report in Appendix A are not the final reference profiles for geologic provinces in the study area, but were used for sensitivity analyses which guided the development of the final columns and reference profiles.

Uncertainty of Point Locations and Elevations and there Implications

The primary data for bedrock elevation are boring descriptions compiled from archives at the ISGS Geological Records Unit (GRU). The original boring records vary widely in the accuracy and precision of their locations and elevations. The related geologic descriptions also vary widely in reliability and detail. These attributes are partly classifiable by boring type ("Status"), such as water well, geotechnical boring, petroleum boring, etc., but there is variation within each Status category as well. After compiling the historic data, we perform quality assurance and control by checking well locations, assigning elevations when none were originally given, and interpreting the log descriptions. The quality of the result of the location verification depends upon supporting data found in the original records, supporting data added from other sources such as plat or tax maps, and the local topographic or geologic variability. The supporting data also vary in quality by the date of their acquisition and by their locale (especially county-county variability). A further complication in describing the entire data set is that these data were compiled by quadrangle over 12 years of mapping. The available supporting data, verification rubric, and effort expended varied with time. Missouri data used along the Illinois border was not verified for location or elevation. To the data compiled from archived records were added

new observations from our mapping, including outcrop descriptions, stratigraphic borings, and geophysical studies. These are relatively few compared to the historic information. Finally, synthetic data including points extrapolated from borings that do not reach bedrock, and contours and streamlines added by judgment are added to the data set to fit geomorphic principles and documented area characteristics.

Uncertainty of location

Point locations (fig. 13) were verified by examining all available locational information including GPS coordinates, driller's logs, water well permits, address matching, air photos, and conversations with drillers. Points were moved within a GIS environment, and the new locational information and coordinates were updated in the ISGS GRU Oracle database. The most accurate locations were obtained in the field using GPS devices or air photos. Classes of locational information and supplementary notes were attributed in the source data.

Water wells could be verified to varying degrees of accuracy. The least accurate locations could only be matched to property boundaries shown on plat maps or to quarter-quarter-quarter PLSS (public land survey system) descriptions. These may thus be only within 100 m of the actual location. Where a house could be identified for a particular property by examination of air photos, DOQs (digital orthophoto quadrangle), or a known street address and no additional information was available, the well was placed on the driveway. Such a point is probably within 50 m of the actual water well. Water wells drilled since about 1975 usually have a Water Permit. Some Water Permits in GRU include driving directions from which street addresses could be obtained, or large scale maps of drilling locations with distances to features observable on air photos such as house corners or property boundaries. These points are probably accurate to within a few meters. Other locations were described by the driller in telephone conversations. These may also be accurate to within a few meters.

Bridge boring records from the Illinois Department of Transportation could be matched to bridge locations on DOQs. Boring locations were placed relative to the bridge center based upon Station Number (footages) or accompanying technical drawings, when available. These locations are thus accurate from approximately 1.5 to 15 m. Stratigraphic borings and field observations were located by an ISGS geologist on a topographic map, air photo, or with differentially corrected GPS coordinates. These locations are probably accurate from within 0.3 to 15 m. The only records generally available for Coal borings are driller's logs. Locations described by PLSS and other descriptive information are assumed to be correct because the coal companies have a presumed interest in the accuracy of their data. Points were deleted from the analysis, however, when log descriptions conflicted strongly with, e.g., elevations on topographic maps, or reported bedrock elevations were much different than neighboring data points. The horizontal accuracy of coal borings used may thus vary from 3 to 100 m. Classes of locational information and supplementary notes were attributed in the source data.

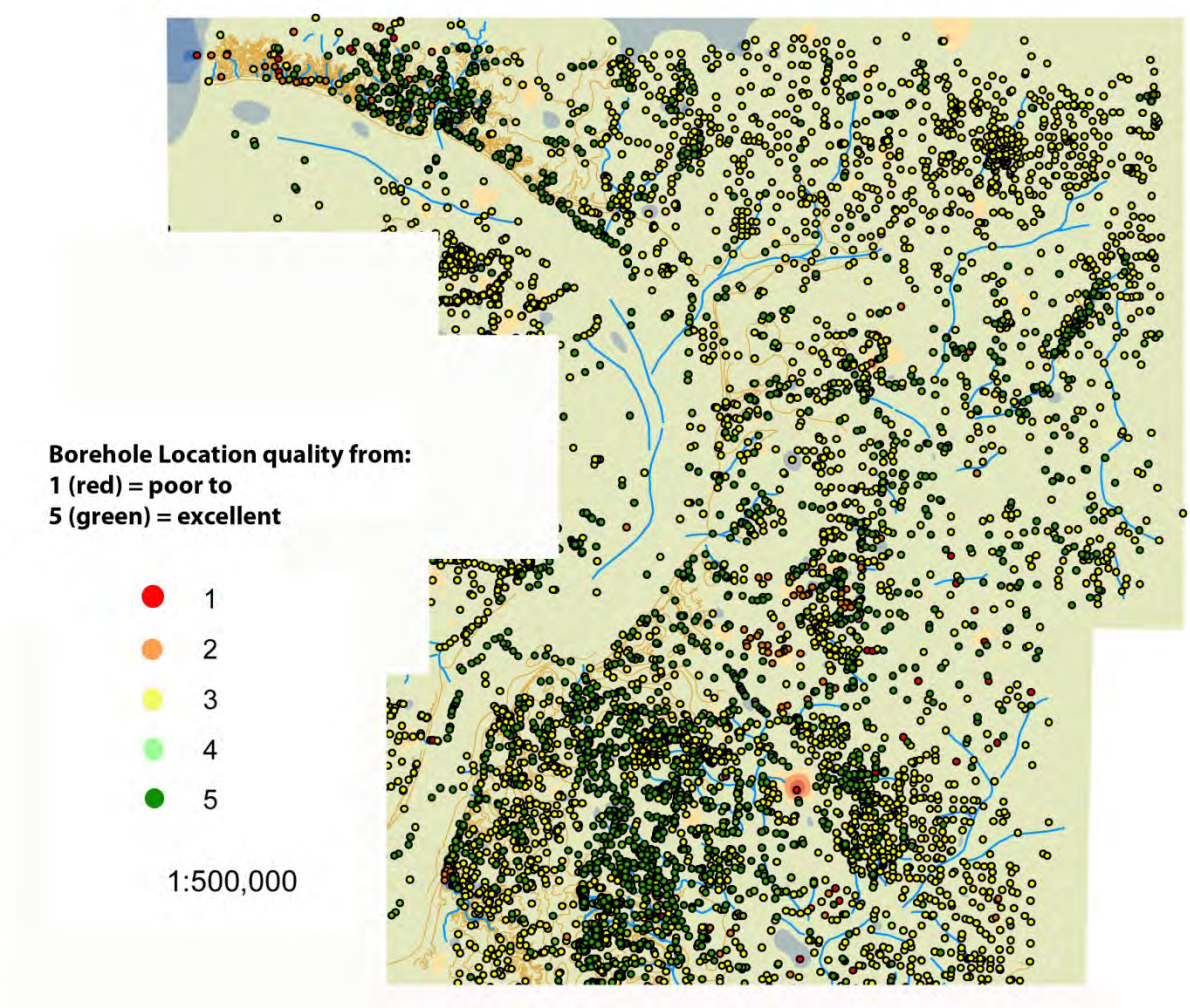

Figure 13. Map of study area showing borehole locations and location quality.

Uncertainty of elevation

Borings for which elevations were provided by the company, mainly geotechnical, coal, and petroleum borings, were assumed to have been surveyed and thus of high accuracy. This is true even when the horizontal location is not confirmed with high accuracy. Some elevations for stratigraphic borings were determined by differentially corrected GPS, and thus also have high accuracy.

Other elevations were assigned from topographic maps or digital elevation models to borings after horizontal locations were verified. The accuracy of those elevations thus depends upon the accuracy of the location, local topographic variability, and source map accuracy. Topographic variability is low on the American Bottoms and upland till plains, but high on transitional areas, incised uplands, and ridged uplands. Topographic map and digital elevation model vertical accuracy is nominally ~3 m, but the age of the map and the source of the data have a small effect. For example, elevations for the Cahokia Quadrangle have never been updated from plane table surveys in the 1950s that have known internal errors, and spot elevations in the Collinsville Quadrangle were observed to differ significantly from the topographic map.

Synthetic points were created to constrain the bedrock surface where insufficient observations occurred. An initial map of predicted bedrock outcrop was constructed by digitally comparing an early draft of the bedrock topography map to the surficial digital elevation model (USGS1997). Where predicted outcrop was known to not occur, the surface was forced down by 3 m, and where outcrop was expected but not predicted by the model the surface was raised by 1.5 m. Similarly, where early models of the bedrock surface intersected well-known borings that did not reach bedrock, the surface was depressed by 3 m. Synthetic points were added to some bedrock valley axes to remove interior depressions.

In sum, the typical range of point elevation uncertainty is 0.3 to about 7.6 m. Within the SLAEHMP area, half (1553/3423) of the borings used within the study area were geotechnical borings with surveyed elevations, whereas only one fourth (899/3423) were lower accuracy water wells.

Uncertainty in log interpretation

The interpretation of water well, geotechnical, and coal borings is not straightforward because of varying nomenclature, a tendency for various practitioners to value materials selectively, and variable care taken in log descriptions. Although the occurrence of limestone seems to be well recognized by most practitioners, weathered shale is often misidentified as till, and till can also be misidentified as shale. For corroborating evidence to descriptions of bedrock in geotechnical borings, blow counts typically rise abruptly to 100 blows per 6 in, and unconfined compressive strengths (Qu) also rise abruptly. Reevaluation of lithologies incorrectly described in logs requires familiarity with nearby geology and best professional judgment. Till misidentified as shale may be described as "blue shale", "soft gray slate", "clayey shale", and "soft shale". Shale can be also lumped into the "overburden" with till in coal borings. Weathered shale misidentified as till might be described as having "abundant soft pebbles", which are actually lenses of less weathered rock. Complicating that interpretation is the fact that some tills, especially the Omphghent member of the Banner Formation, contain abundant weathered shale clasts.

Uncertainty of bedrock elevation and sediment thickness

Bedrock elevations were determined by direct observation in outcrop, and by calculating from boring surface elevation minus depth to rock. Thus the uncertainty of the bedrock elevations is a function of the uncertainty of the surface elevations and some estimate of the roughness of the bedrock surface. Uncertainty of sediment thickness, determined by subtracting the bedrock topographic map from the surface topographic map, follows directly.

The most precise elevation measurements are for the Illinois Department of Transportation (IDOT) boreholes, which include measuring ground elevations and depths to lithologic changes to within 3.05 cm. This allows for an analysis of variations of the elevation of the eroded top of the limestone bedrock surface in the Mississippi River valley bottom over an area surrounding clusters of boreholes. These clusters are 1.4 to 1.7 km across and 2.24 km apart. The northern cluster has an average top of limestone bedrock elevation of 33.1 m with a standard deviation of

1.4 m with a range of 32.0 to 34.7 m. The southern cluster has an average top of limestone bedrock elevation of 35.4 m with a standard deviation of 1.2 m with a range of 31.8 to 36.8 m. This presents the variability (roughness) of the eroded limestone bedrock surface and the representation of an individual borehole for an area about 1.5 km across for this setting.

Sensitivity Analysis. We analyzed an earlier version of the point data set to characterize the uncertainty of the bedrock topographic model. Significantly missing from the data set but included in the final map (fig. 25) are 500 geotechnical borings from levee records (locations provided by Conor Watkins) and ~230 outcrop descriptions in the uplands. Our working data set covers all of Madison, St. Clair, and parts of Monroe County, Illinois, as well as selected borings in Missouri for edge control. Thus the following discussion addresses the entire map rather than only the Illinois SLAEHMP quadrangles, except where noted. The analysis was to determine the effects of the uncertainty of the horizontal positions on assigned borehole elevations, and thus the elevation of the bedrock surface.

The analysis was accomplished by allowing boring surface elevations, SURF_ELEV, and thus bedrock elevations to vary with local topography based on the horizontal precision of each boring. Bedrock topographic maps with 50 m cells using default and test point data as well as final contour data and streamlines were then modeled with the ESRI Topo to Raster algorithm. Input parameters were the same as the final product. Finally, the resulting maps were compared.

The analysis data set was obtained from the parent data set on June 3, 2011. Subsequent modifications that affect the deliverables for this project were the addition of 564 levee borings in the American Bottoms and 73 outcrop descriptions in the uplands from field notes in the ISGS archive. The horizontal precision of each boring was categorized in 6 classes by the quality of information used to verify it (table 2 & fig. 13).

Table 2. Horizontal Precision Classes

Location Quality ID	Description	Approximate Precision (m)
5	Best. Differential GPS, map, or diagram supported by DOQ	≤ 10 m
4	Street address or parcel number plus DOQ	10 - 30 m
3	Platbook, DOQ, or driller's description	30 - 100 m
2	In quarter Section or large plat	200 - 400 m
1	In section	600 - 1000 m
0	Worst. Conflicting information, probable bad location.	indeterminate

To simplify the analysis, the 6 classes were reduced to 4 (table 3). The highest precision points were mainly outcrops and geotechnical, stratigraphic, and exploration borings. Most of the lower precision points were water wells.

Table 3. Horizontal Precision Classes in Sensitivity Analysis

Precision Class (m)	Frequency	Frequency in SLAEHMP area
10 m	2265	1190
100 m	6290	1634
200 m	262	108
1000 m	86	6

The range of elevations within 10, 100, 200, and 1000 m search radii were obtained from a 30 m pixel DEM (Abert, 1995), and were extracted to each boring. Borings were also assigned a

random value, RAND1, between 0 and 1 using the ESRI *rand* function. Random signs, RAND_SIGN, were determined from even or odd values of that random number. Test elevations, TEST_Z1, were then calculated as

$$TEST\_Z1 = SURF\_ELEV*RAND1*RAND\_SIGN$$

However, elevations provided by companies were assumed to be correct despite possible uncertainty in horizontal position, and so were not allowed to vary in the test model. Nearly one half of the elevations, 4062/8903, were thus taken as highly accurate.

The default and test surfaces are shown in figure 14. The default surface comprises the point, contour, and streamline data used in the final map, but not passed through the surface topography intersection step. Extreme clustering of the data is evident. Although the test surface shows greater variability than the default, there is very little difference in the major features. Over the most of the area, the elevation differs by 3 m or less (fig. 15A). Differences between 3 and 8 meters are distributed uniformly across the area, and appear to be controlled by individual data points. Larger differences occur mainly on the Missouri side of the river where we did little quality checking, and in the south-central area. The points that control those larger differences include both higher quality (surveyed elevations) and lower quality (assigned elevations with low verification precision and high local relief) borings (fig. 15B). All occur where bedrock is near the surface and features rugged topography.

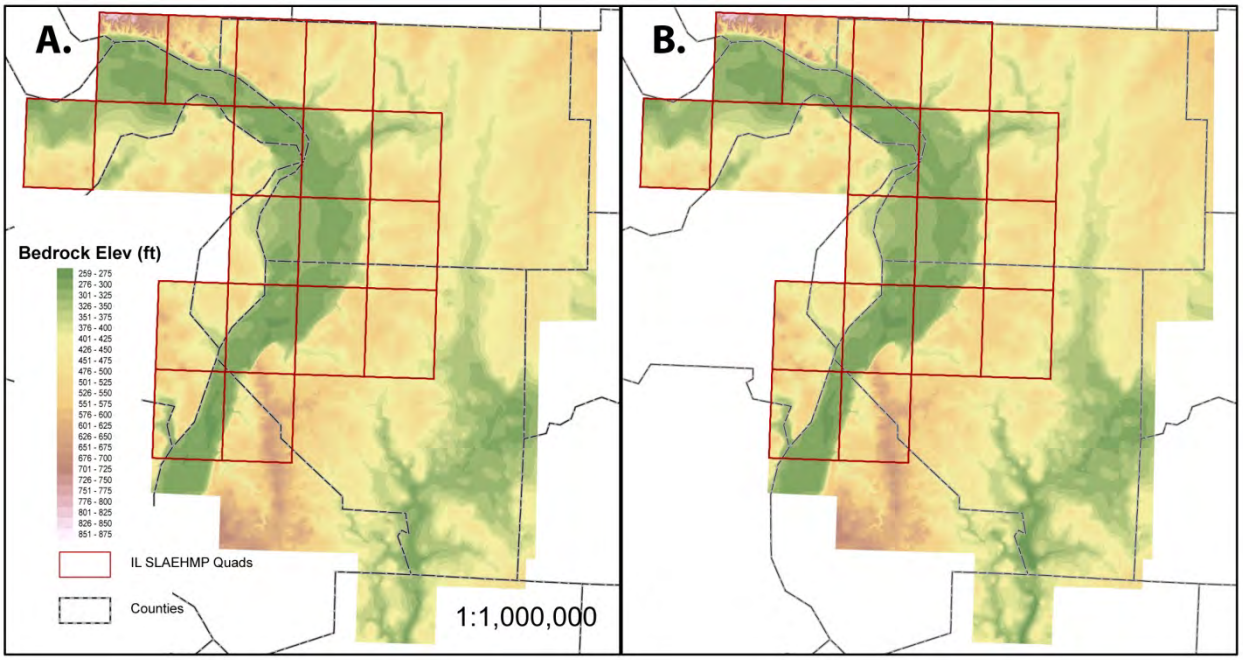

Figure 14. Bedrock topography models using original (A) and randomized (B) point elevations. Just over half of the data were randomized. Contour and streamline inputs were the same for each. Rasters have been clipped to the data extent. Missouri data not verified.

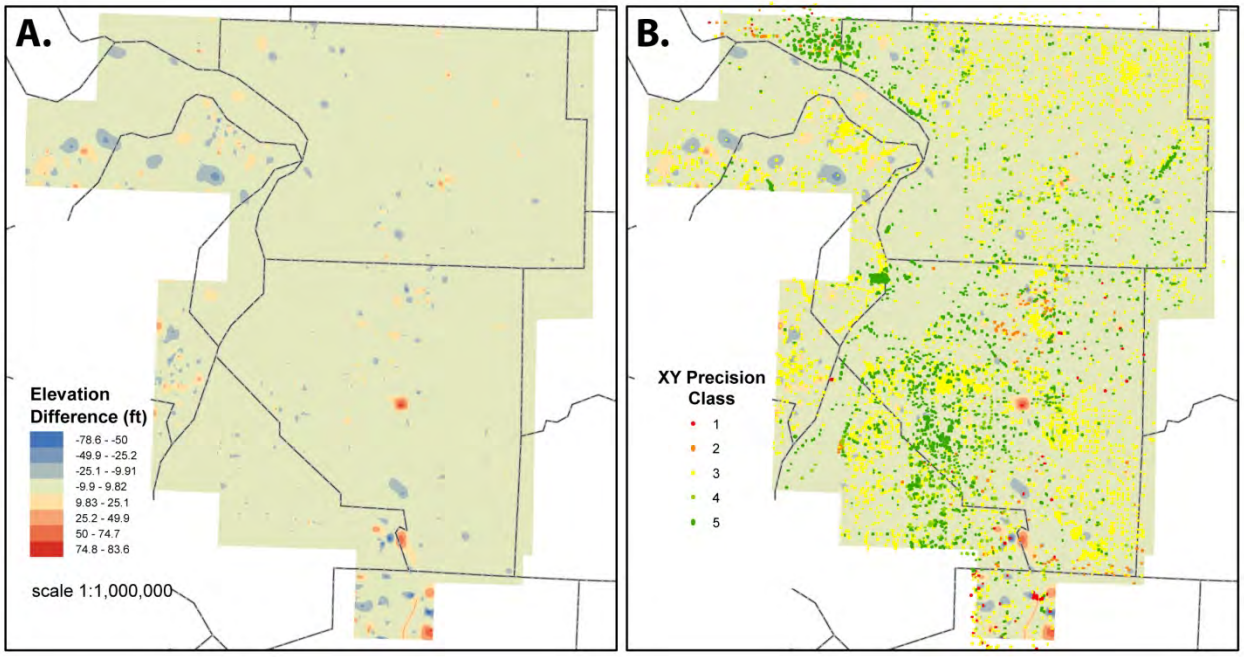

Figure 15. (A) Difference between original and randomized bedrock elevation models. (B) The same difference map overlain by point data classed by precision of location, where 5 is best and 1 is worst. Rasters have been clipped to the data extent. Missouri data not verified.

A krige-interpolated map of the residuals, the difference between the input test values and the interpolated values, shows that the Topo to Raster model closely honors the input data (fig. 16A). The only areas where the residuals exceed ± 3 m are along the rocky limestone bluffs at the extreme northern and southern ends of the American Bottoms, and near dissected river valleys in the northern and eastern portions of the study area.

A krige-interpolated map of the residuals of only the higher-quality points (presumably surveyed locations and points known within 10 m in the horizontal) is shown in figure 16B. The fact that nearly half of the data are high quality is evident in low residuals ± 3 m over most of the area. Only in the southwest corner does the map differ markedly from figure 16A. There, it appears that the high quality data are delineating some feature in the bedrock, possibly related to the Waterloo-Dupo Anticline (Phillips 2010; Nelson 1995), but the feature is obscured within the lower quality data.

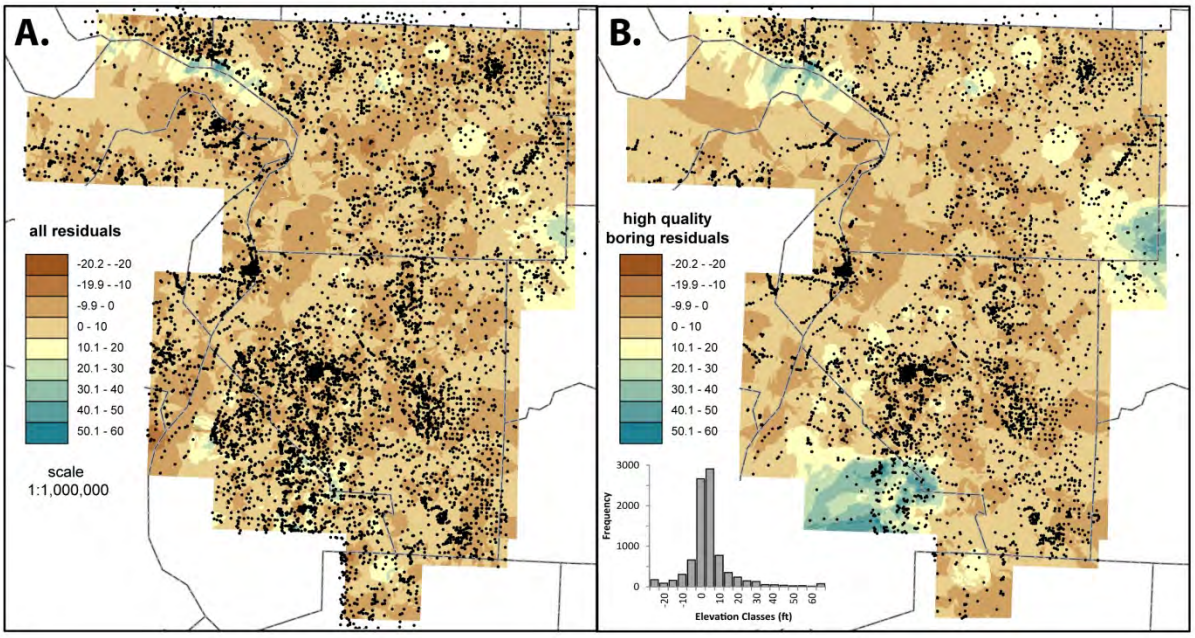

Figure 23. Krige interpolation maps of residuals between test values and output. (A) Residuals for all points. (B) Residuals for only the highest quality data, for which elevations were provided by the company or location precision was within 10 m. Missouri data not verified.

We can conclude that the largely office-based methods used to verify the well and boring locations are reasonably effective, at least for regional-scale maps. In fact, except for the bluffs between Alton and Grafton, the larger areas of uncertainty in the depth to rock lie outside the SLAEHMP area. Not considered here is the variable quality of the descriptive data from with the depth to rock is determined. However, all of the data are the best available for the area despite the reliance on some descriptions.

Geologic Provinces Methodology

Table 4 is a generalization of Quaternary (surficial) geologic mapping units from detailed 1:24,000 mapping in the St. Louis Metro East region from 1998-2011 (maps listed after references). The divisions were categorized based on an attempt to group areas with a fairly similar column of sediment that would have similar properties and the decision on mappable areas to include as provinces based on the 500-meter grid sampling size that will be used for analysis. Size and shape of the province would have to be large enough to include multiple grid points and not just one or two points. The provinces were generated based on the sensitivity analysis and iterations between producing geologic provinces and running statistics for each province on ranges and averages of column thickness (table 5). The site-amplification analysis process uses the data at a grid point for the geologic province and its shear wave reference profile and cuts off the bottom of the shear wave velocity profile based on the overburden thickness at that point. Therefore a number of geologic provinces (columns) had to be generated to maintain the geology found at the location while having its lower section as represented by the shear wave profile, cut off/changed over the range of thicknesses found in that province.

The process to create these groupings was as follows:

1.) Map polygons of upland loess units (Peoria and Roxana Silts), loess covered Illinoian terraces (loess over Teneriffe Silt or Pearl Fm.), colluvium (Peyton Fm.), near-surface till (Glasford Fm.) and near-surface bedrock (Paleozoic shale/limestone/sandstone/coal) were merged together.

2.) Map polygons of lowland sandy deposits (Henry Fm. and Cahokia sandy facies) were merged together because they are materially similar.

3.) Map polygons of last glacial fine-grained slackwater terraces (Equality Fm.) and adjacent deposits of fine-grained Holocene alluvium over such deposits (Cahokia over Equality) were merged together into a TRIBUTARY VALLEYS unit (Code #12).

4.) The merged upland polygons were split into 3 categories based on typical maximum values for loess thickness. Three contour lines (40-foot, 20-foot, and 10-foot) were used from a regional GIS dataset from previous detailed mapping in order to delineate into categories of 12 to 27 m (40 to 90 feet) loess thickness, 6 to 12 m (20 to 40 feet) loess thickness, and 3 to 6 m (10 to 20 feet) loess thickness.

5.) The 3 upland loess categories were further subdivided into those having thick basal silt deposits (2 to 25 m thick) and those that do not. This resulted in 6 categories (Code #'s 5, 6, 7, 8, 9, 10, 11). The basal silt delineation was mainly based on areas that were known to contain subsurface deposits of the Illinoian Petersburg silt and older pre-Illinoian silt deposits (Harkness and Canteen Members of the Banner Fm.) from Grimley and Phillips (2011) in St. Clair County and other published maps for the other areas.

6.) A category was made for one polygon based on the unusually thick deposits of fine sand and diamicton (debris flows and till) in an ice-marginal ridge called Shiloh Ridge. The deposits here can be as much as 76 m thick and are generally sandier in the subsurface than the surrounding loess/till areas. This area, delineated mainly because of the thick glacial drift was decided to have its own unit (Code #13) so that it could be modeled more accurately.

7.) Disturbed land was split into three categories. Code #1 includes urban and industrial fill less than 5 m thick in the American Bottoms over generally sand alluvium. Code #99 is largely undifferentiated disturbed land. It includes a wide variety of urban, industrial, excavated, and made land such as quarries, landfills, and fill of indeterminate origin. The fill ranges from silt and sand to rubble, asphalt, and other anthropogenic materials. It lies over both sandy and clayey alluvium as well as glacial (loess and till) strata. Code #100 includes levee and road interchange fill and excavations over both alluvial and glacial strata.

The map showing the 15 geological provinces as defined above and in table 4 is shown in figure 17.

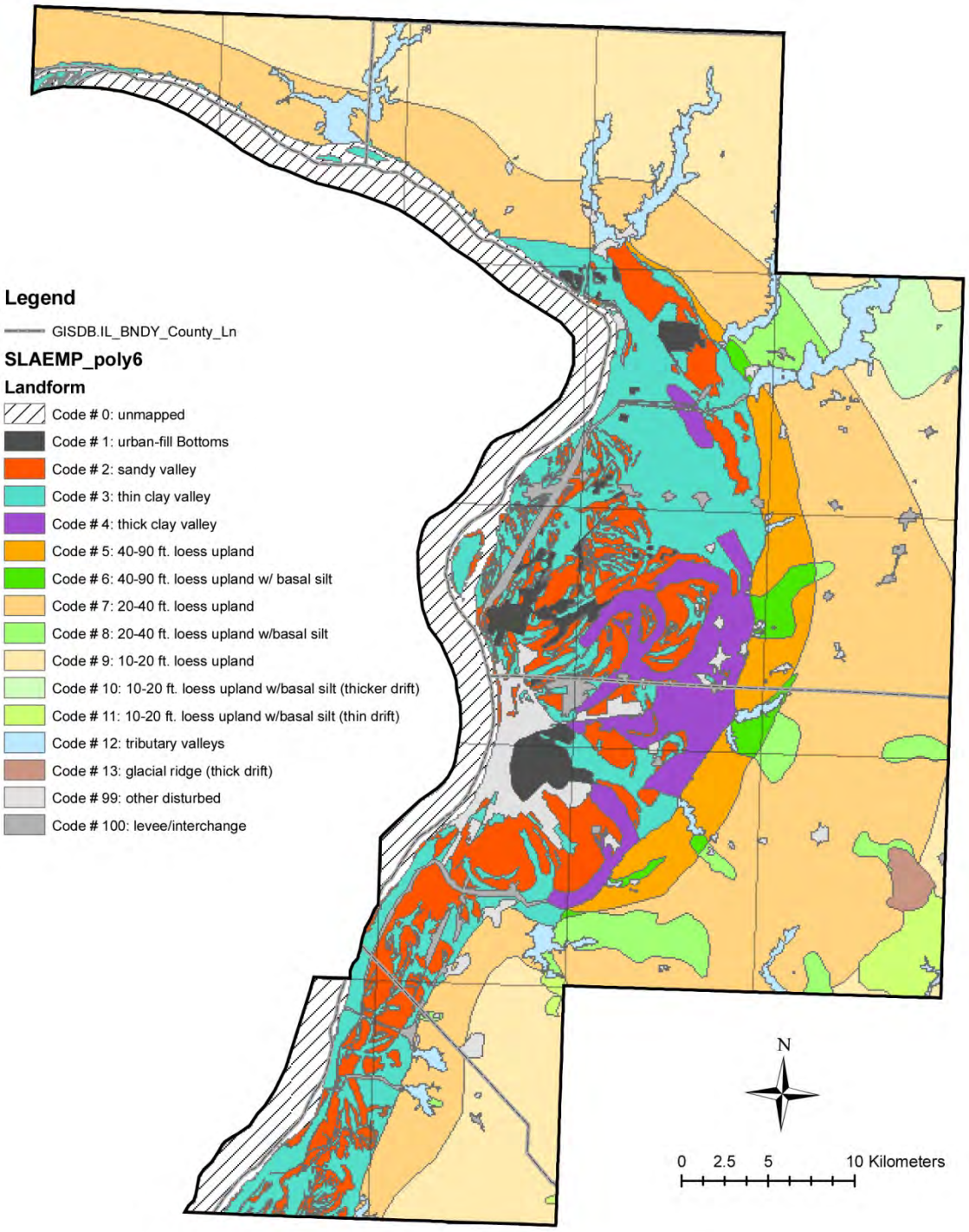

Figure 17. Geologic province map showing 15 provinces with complete descriptions of each in table 4.

Table 4. Characteristics of geologic provinces

# Code	Generalized Unit Name	Typical Profile	Explanation	Predominant Landform	Average Unconsolidated Sediment Thickness
0	unmapped areas	----------	mostly in Missouri buffer zone	----------	----------
1	disturbed ground: < 3 m fill over alluvium	A) 3m mixed fill/ B) sand or thin clay over sand	Rubble and fill over mixed alluvial sediment	Urban and industrial land (American Bottoms)	35 m (+/- 3m)
2	sandy valley deposits	A) 15m fine to medium sand/ B) 20m medium to coarse sand	Cahokia Formation (meandering stream) over Henry Formation (outwash), or Henry Formation terraces	Mississippi River Valley (American Bottoms)	35 m (+/- 5m)
3	thin alluvial clay (< 30 ft [9 m]) over sand	A) 5m clay B) 30m sand	Cahokia (backswamp deposits) or Peyton Formation (alluvial fan) over Henry Formation (outwash)	Mississippi River Valley (American Bottoms)	35 m (+/- 8m)
4	thick alluvial clay (> 30 ft [9 m]) over sand	A) 10m clay/ B) 25m sand	Cahokia (meander fill) Formation over Henry Formation (outwash)	Mississippi River Valley (American Bottoms)	35 m (+/- 6m)
5	thick loess (40-90 ft* [12 – 27m]) over till#	A) 15m loess/ B) till	Peoria and Roxana Silts (loess) over Glasford Fm. till and ice-marginal sediment	Upland, dissected to varying degree	20 m (+/- 10m)
6	thick loess (40-90 ft* [12 – 27 m]) over till with basal silt**	A) 15m loess/ B) 10m till/ C) 10m silt	Peoria and Roxana Silts (loess) over Glasford Fm. till and ice-marginal sediment over Petersburg Silt / Banner Fm. silty	Upland, with buried bedrock valley in subsurface.	35 m (+/- 13m)
7	moderate loess (20-40 ft* [6 – 12 m]) over till	A) 10m loess/ B) till	Peoria and Roxana Silts (loess) over Glasford Fm. till and ice-marginal sediment	Upland, dissected to varying degree	15 m (+/- 8m)
8	moderate loess (20-40 ft* [6 – 12 m]) over till with basal silt	A) 10m loess/ B) 10m till/ C) 15m silt	Peoria and Roxana Silts (loess) over Glasford Fm. till and ice-marginal sediment over Petersburg Silt / Banner Fm. silty	Upland, with buried bedrock valley in subsurface.	35 m (+/- 12m)

9	thin loess (10-20 ft* [3 – 6 m]) over till	A) 5m loess/ B) till	Peoria and Roxana Silts (loess) over Glasford Fm. till and ice-marginal sediment	Upland, dissected to varying degree	15 m (+/- 10m)
10	thin loess (10-20 ft*[3 – 6 m]) over thick till and basal silt	A) 5m loess/ B) 20m till / C) 20m silt	Peoria and Roxana Silts (loess) over Glasford Fm. till and ice-marginal sediment over Petersburg Silt / Banner Fm. silty	Upland, with buried bedrock valley in subsurface.	45 m (+/- 7m)
11	thin loess (10-20 ft*[3 – 6 m]) over thin till and basal silt	A) 5m loess/ B) 10m till/ C) 5m silt	Peoria and Roxana Silts (loess) over Glasford Fm. till and ice-marginal sediment over Petersburg Silt / Banner Fm. silty	Upland, with buried bedrock valley in subsurface.	20 m (+/- 6m)
12	tributary valleys	15m silt	Cahokia Formation (mainly silty stream sediment) or Equality Formation (lacustrine) overlying other Quaternary sediment or bedrock	Valleys draining uplands	15 m (+/- 9m)
13	glacial ridge	A) 5m loess B) 20m sand C) 15m till ? D) 15m silt ?	Peoria and Roxana Silts (loess) over Hagarstown Member sand-diamicton over Glasford Fm. till and ice-marginal sediment over Petersburg Silt / Banner Fm. silty	Glacial ridge on upland, with buried bedrock valley in subsurface.	50 m (+/- 11m)
99	Disturbed ground - indeterminate	undifferentiated	Wide variety of fill and excavation over any other units	Urban land, industrial land, landfills, quarries	30 m (+/- 11m)
100	Disturbed ground – levees and road interchanges	undifferentiated	Silty to sandy fill and excavations over any other units	Levees and road interchanges	30 m (+/- 9m)

* loess thickness is maximum value range on uneroded landscapes. Actual loess thickness can be much less.

till may include sand and silt lenses or even sandy terrace deposits over till; some areas are eroded and have exposed bedrock; also includes areas with Sangamon paleosol alteration.

** basal silt includes Petersburg Silt, Lierle Clay (Yarmouth paleosol and accretion-gley) and Banner Formation till, lake sediment, and alluvium

Table 5. Statistics on thickness of entire column per landform/geologic province.

PROV_CODE	Land Forms	MIN (m)	MAX (m)	RANGE (m)	Mean (metric)	STD (metric)
1	Disturbed <3m over alluvium	21	47	26	35	3
2	sandy valley deposits	5	49	44	35	5
3	< 9 m clay /sand	0	51	51	33	8
4	>9 m clay/sand	0	47	47	32	6
5	12-27 m loess/till	0	63	63	20	10
6	12-27 m loess/till/silt	0	65	65	32	13
7	6-12 m loess/till	0	52	52	15	8
8	6-12 m loess/till/silt	0	61	61	33	12
9	3-6 m loess/till	0	61	61	16	10
10	3-6 m loess/till/silt	15	66	51	43	7
11	3-6 m loess/thin till/silt	0	44	44	18	6
12	tributary valley	0	53	53	16	9
13	glacial ridge	26	79	53	53	11
99	Disturbed ground	0	68	68	31	11
100	Disturbed - levee, interchange	0	53	53	32	9

Shear Wave Reference Profiles

Shear wave reference profiles were produced to match the geologic provinces listed in table 4 with thicknesses of lithologies as shown in the Typical Profile column. Shear wave velocities were averaged for 5 m depths for the various lithologies found in the mapped area. Some values had to be extrapolated to greater depths than the data available. These assigned values can be found in Appendix B in the Text format used in the analysis.

Unconsolidated Sediment Thickness Map Methodology

An unconsolidated sediment thickness (or depth to bedrock) map for the St. Louis Metro East region in Illinois (16-quad area) was created using a multi-step process. This process involved multiple steps that included development of a regional bedrock surface topography map (fig. 25) (50 m grid size), followed by subtraction of this surface from the land surface digital elevation model (10 m grid size). Lastly, the resulting thickness (or depth to bedrock) map was corrected for negative thickness areas, where the bedrock surface protruded above the actual land surface.

1.) Creation of a bedrock surface topography map.
This map is based on data from which a reliable bedrock elevation could be determined. Data within about one km of the quadrangles were also utilized to limit edge effects. Within the analysis area, a total of a few thousand data locations were used, including 536 outcrops, 52 stratigraphic tests, 1553 engineering borings, 899 water-well borings, and 353 coal borings and 82 oil and gas test borings. In addition, contour data were included where bedrock outcrop was observed. The bedrock surface was

modeled utilizing a “Topo to Raster” program in ArcMap 9.3 (ESRI) using a vertical standard error of 1.5 m and with "drainage enforcement" which attempts to make a hydrologically correct surface. This program incorporated a combination of three information types: (1) data points coded with bedrock top elevations, (2) digitized contour lines coded with bedrock top elevations to incorporate extensive outcrops of bedrock or surface topographic expression of near-surface bedrock, and (3) digitized “streams” (ESRI ArcMap term) that forced the bedrock surface model to conform to a typical stream drainage, guided by geological insights and surface topography. The final bedrock topography map output was a 50 m grid in the horizontal --- chosen as a reasonable cell size that would incorporate a fair amount of detail but without creating an extraordinarily large file. The locational accuracy of much of the point data is not much beyond 50 m so more detail was not deemed necessary.

2.) Subtraction of bedrock surface topography map from the land surface digital elevation model (DEM).
In order to create the thickness map, the 50 m grid of the bedrock topography surface was subtracted from a land surface digital elevation model (DEM), of 10 m cell size. The land surface DEM was acquired from the USGS website (http://seamless.usgs.gov/ned13.php), downloaded as a 1/3 arc-second (approximately10m) DEM. Some areas of the DEM are derived from oversampling of 30-meter Digital Elevation Model (DEM) source data. Thus, the original precision of the land surface DEM varies from areas with lower-quality resolution, including many upland areas, to areas with LIDAR data proximal to the Mississippi River.

3.) Correction of the thickness map.
Next, any remaining areas with bedrock surface elevations higher than the surface DEM (drift thickness < 0) were replaced with the value of the surface DEM using a conditional (“con”) statement in ArcMap 9.3. This both corrected the final bedrock topography map and provided for a recalculated drift thickness map with all values ≥ 0. The resulting thickness map thus has a small proportion of areas with drift thickness = 0 where bedrock is outcropping or close to it. The final cell size, or grid size, for the Thickness map is also 50 m [Illinois (eastern) portion of fig. 31]. The vertical precision is at best 1.5 m (5 feet), since the vertical standard error for the bedrock topography source data was set to this value. Due to additional locational inaccuracies and geologic description imprecision in the source point data and in the topographic map, the real vertical precision of the map probably averages more like 3 or 4.5 m.

MDNR Missouri Geologic Model

Geologic Provinces Methodology

The mapping area (St. Louis and St Charles counties) is underlain by Paleozoic-age bedrock comprised primarily of limestone and shale within the Mississippian and Pennsylvanian subsystem. Surficial material units in the mapping area were described by Missouri Division of Geology and Land Survey (DGLS) staff in a series of surficial materials maps (Kaden and Starbuck, 2008a and 2008b; Gaunt and others, 2009a and 2009b; Gaunt and Carr, 2010a, 2010b, 2010c, 2010d, 2010e). Figure 18 shows the distribution of simplified surficial materials units across the mapping area. Table 6 generalizes these units. A more in-depth description of the surficial material units is as follows:

Quaternary Alluvium – This unit is a fluvial deposit emplaced by the Mississippi, Missouri and Meramec rivers or their tributaries. The upper 5 meters of these deposits are composed predominately of silt with variable amounts of clay and organic material. The material underlying the silt is predominately sand and

gravel to the top of bedrock. Thickness of this unit ranges from 12 to 30 meters across the mapping area. The water table is approximately 2 to 5 meters below ground surface, resulting in an interval of saturated sand and gravel greater than 25 meters thick.

Quaternary Loess – This unit is a wind-blown deposit consisting of silt and clayey silt with occasional pockets of clay, sand and gravel. The deposit is composed of two separate loess units, the Roxana Loess overlying the Peoria Loess. Total thickness of the two units may reach 18 meters. The Roxana Loess is higher in clay content and may have a paleosol developed at higher elevations. The Quaternary loess unit overlies Mississippian-age bedrock comprised of limestone and shale creating two unique environments. Where the loess is thin, the limestone may exhibit solution weathering and be karstic in nature. Where the underlying unit is predominately shale, water will perch and destabilize the contact zone. Where the loess rests upon shale, the landslide potential is increased.

Quaternary Till – The Quaternary till unit was deposited as a blanket of outwash during glaciation north of the Missouri River. The till is a mixture of clay, silt, sand, gravel and cobbles that covers the bedrock surface. The unit varies in thickness from 0 to 16 meters with the thickest deposits inland from the river and in depressions of the bedrock surface. The thickest deposits are located in eastern St. Louis and St. Charles counties and the City of St. Louis.

Quaternary Terrace Deposit – The unit mapped as Quaternary terrace deposits were deposited during fluvial events, leaving the terrace above low flow stage of the river. However, the terrace deposits in this area have a lacustrine signature of sensitive organic clays approximately 6 meters below the surface. After high stage flow returned to normal, low-lying areas within the terrace were filled with organic clay material. This zone has a very low shear wave velocity and underlies considerable infrastructure.

Karst – These areas have high concentrations of sinkholes, caves and other karst features due to solutional weathering of the Mississippian-age limestone underlying this area. These areas are typically found in the upland regions.

Paleozoic Bedrock – This mapping unit is typically found in areas of high topographic relief.

Residuum – The areas mapped as the residuum unit consist of residual material found on the slope and toe slope of high relief upland areas. Texture of the unit is dependent on the bedrock parent material but typically has high clay content with fragments of the underlying bedrock.

Artificial Fill – This unit comprises artificially emplaced fill material and is composed of a mixture of heterogeneous clay, silt, sand and gravel in various quantities. This unit may reach up to 12 meters in total thickness and has typically been placed on undisturbed materials.

Table 6. Generalized Missouri surficial materials map units.

Generalized Unit Name	Typical Profile	Explanation
Quaternary Alluvium	12-30m of silt and clay on top of sand and gravel	Deposited by the Missouri, Mississippi and Meramec rivers and their tributaries.
Quaternary Loess	Up to 18m of silt and clayey silt with occasional pockets of clay, sand and gravel	A wind-blown deposit of two separate layers, the Roxana below and Peoria above, found on the uplands. The Roxana is higher in clay content than the Peoria.
Quaternary Till	Up to 16m of clay, silt, sand, gravel and cobbles, with the thickest deposits inland from the rivers and in depressions of the bedrock surface	Deposited as a drift blanket during glaciation north of the Missouri River.
Quaternary Terrace Deposit	Primarily organic clay material with lacustrian organic clays approximately 6m below the surface	Deposited during fluvial events, up-slope of the Quaternary Alluvium.
Karst	Generally less than 7m of surficial materials over bedrock. Surficial materials may be composed of loess or residuum.	High concentrations of sinkholes, caves and other karst features due to solution weathering of Mississippian-age limestone. Typically found in the upland regions.
Paleozoic Bedrock	undifferentiated	Typically found in areas of high topographic relief, near tributaries or in quarries.
Residuum	undifferentiated	Content is dependent on bedrock parent material but typically has high clay content with fragments of parent material.
Artificial Fill	undifferentiated	Artificially emplaced fill material composed of a mixture of clay, silt, sand and gravel for levees, highway and railroad beds.

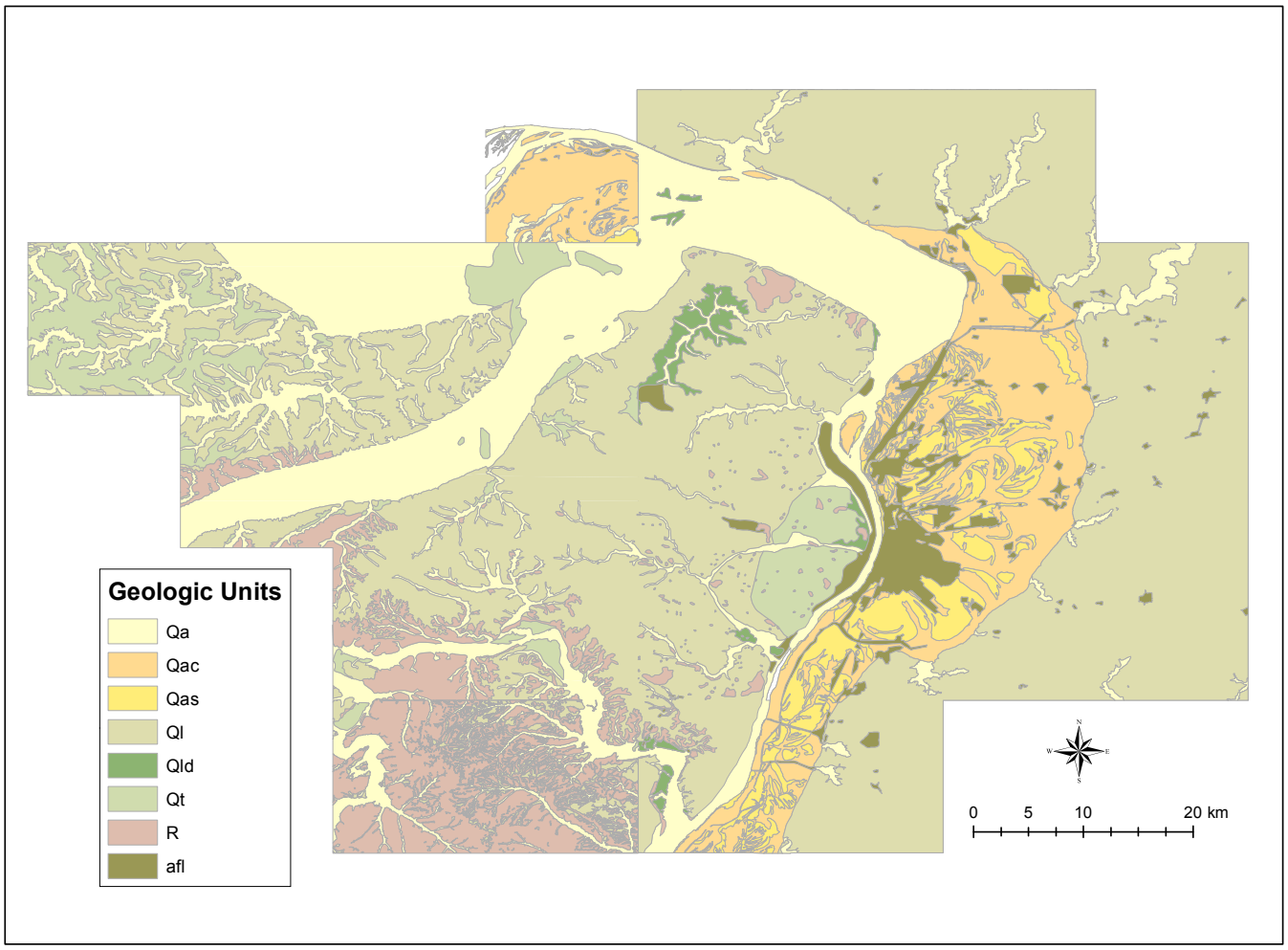

Figure 18. Simplified Missouri/Illinois Surficial Materials Map

Bedrock Surface Topography Map Methodology

Missouri DGLS supplied a bedrock surface topography map to be used in the model. More than 3500 data points were used to create the bedrock topography map for the 29-quadrangle area. The bedrock surface was modeled using a "Topo to Raster" program in ArcMap 9.3 (ESRI) using a vertical standard error of 5 feet and with "drainage reinforcement." Bedrock topography was produced with a 50 m horizontal grid. The bedrock surface topography map was based on bedrock elevation data extrapolated from well logs and field observations. Data was only used where reliability could be collaborated. Various agencies, including the Missouri University of Science and Technology (MST) and Illinois State Geological Survey (ISGS) provided data. Data within five kilometers of the mapping area were also used to limit edge effects. Table 7 shows the data sources used to populate the bedrock surface elevation file titled PR_Borings (Mitchell, personal communication, May 21, 2013).

Table 7. Missouri bedrock depth data sources

Input By	Well Type	State	Data Source
MST	other studies	MO	
MST	boring	MO/IL	Geotechnology_USGS
ISGS	Log/highway log	IL	ISGS drilling records
DGLS	Well log/certified wells	MO	MoDNR-DGLS (2007)
MST	Borings/well field development	MO	Reitz & Jens, Inc.
MST	borings	MO	Shannon & Wilson, Inc.
DGLS	borings	MO	Palmer and others (2006)
MST	borings	MO	Sverdrup Corp.
MST	URS Isopleth	MO	URS Corp (2007, written communication)
MST		MO	USACE
DGLS		MO	Outcrop files
MST		MO	USGS Mo River Map
MST	Borings	MO	Virginia Stone Property
MST	borings	MO	Williams (USGS)

Shear Wave Velocity Data and Reference Profiles

Shear wave velocity (Vs) data has been collected throughout the study area using various techniques (Chung and Rogers, 2012b). Techniques include seismic cone penetrometer tests and seismic reflection/refraction. Early in the investigation, the Multi-Channel Analysis of Surface Waves (MASW) geophysical technique was used to collect shear wave velocity data for 20 locations on the Wentzville 7.5' quadrangle (Hoffman and others, 2008). During the winter of 2009 and the summer of 2010 seismic cone penetrometer investigations were conducted along portions of Interstates 44 and 70, U.S. Highway 40, and State Highways 79, 94, 109 and 364. A Hogentogler cone penetrometer owned and operated by the Missouri Department of Transportation (MoDOT) was used to measure the geophysical properties of 27 boreholes near bridges, overpasses and areas of geologic interest (Siemens, personal communication, May 20, 2013). Table 8 is an example of a SCPT data sheet for one borehole measured by MoDOT. Standard deviation was calculated for the shear wave velocity data for each general surficial geology type. Values far from the mean were closely examined and, in some cases, determined to be of a different surficial geology type or unusable. Determination of generalized shear wave velocity profiles for each surficial material type was done in collaboration with the members of the Technical Working Group of the St. Louis Area Earthquake Hazards Mapping Program. Twelve generalized profiles were used to create the Vs model and are presented in Table 9.

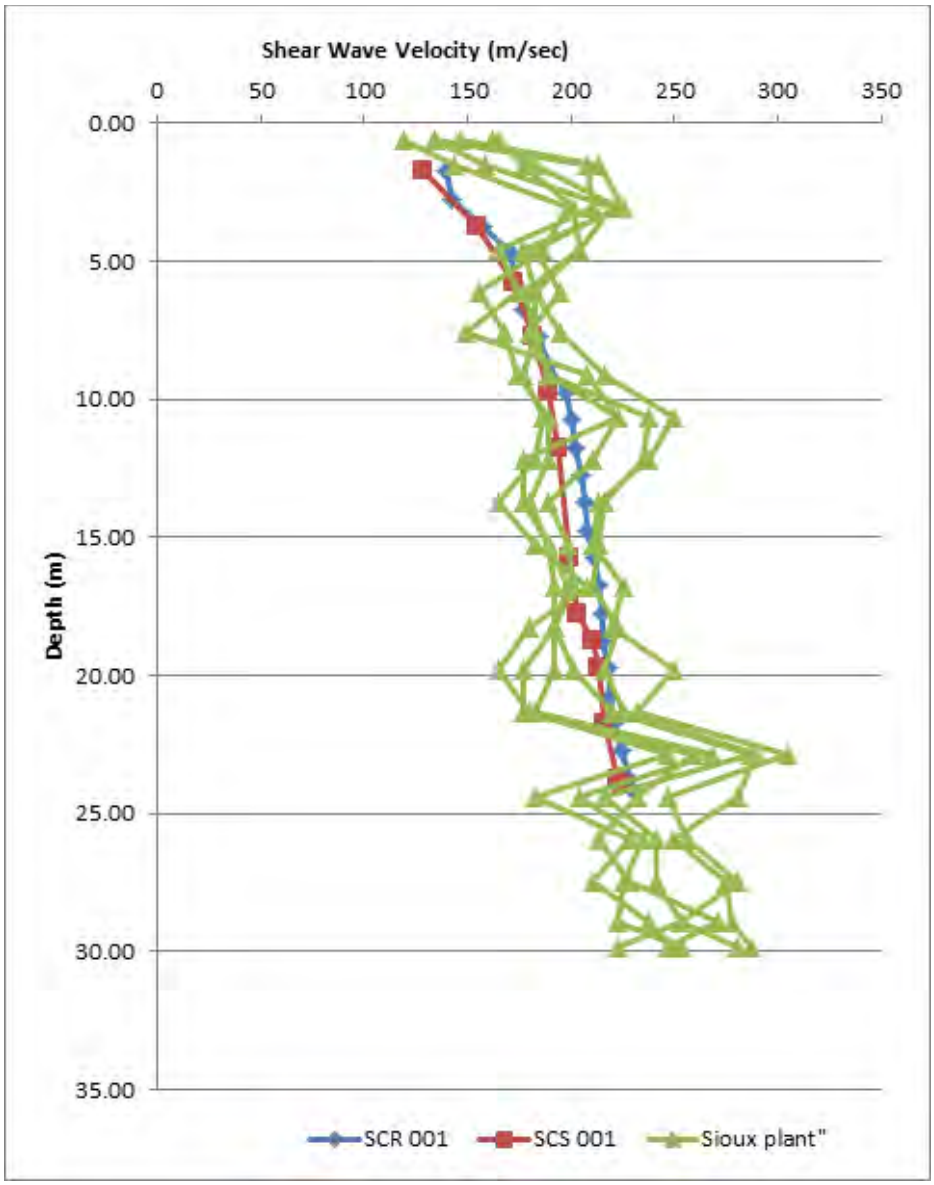

Figure 19. USGS data (SCR 001 & SCS 001) compared to Sioux plant crosshole data for Shearwave Velocity in relation to depth for the Mississippi and Missouri River Floodplains. (Williams, personal communication, July 11, 2012).

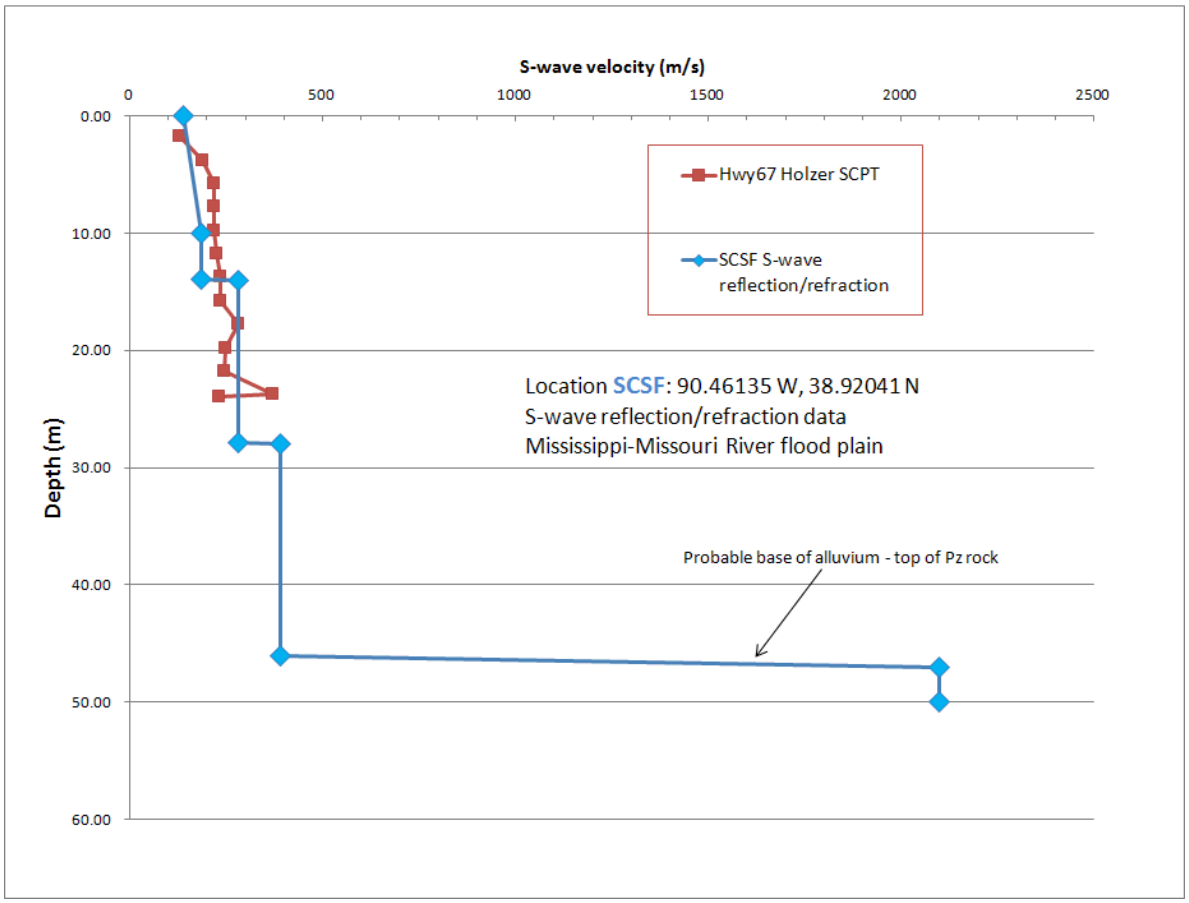

Figure 20. Comparison of reflection/refraction and SCPT – USGS data (Williams, personal communication, July 11, 2012).

Table 8. Example of MoDOT SCPT data sheet.

Depth Velocity (ft)	Depth Velocity (m)	QC TSF	FS TSF	FS/QC %	zone	Soil Behavior Type UBC-1983	Seismic (ft/s)	Seismic (m/s)
3.44	1.049	105.14	1.5453	1.470	8	sand to silty sand	1296.850	395.2799
6.73	2.051	27.62	0.3183	1.152	6	sandy silt to clayey silt	810.105	246.92
10.17	3.100	21.50	0.2515	1.170	6	sandy silt to clayey silt	738.287	225.0299
13.29	4.051	51.71	0.3580	0.692	7	silty sand to sandy silt	641.765	195.61
16.73	5.099	111.17	0.6255	0.563	9	sand	1037.533	316.2401
20.01	6.099	114.46	0.5016	0.438	9	sand	507.808	154.7799
23.29	7.099	106.96	0.2951	0.276	8	sand to silty sand	604.724	184.3199
26.57	8.099	140.41	0.4953	0.353	9	sand	438.780	133.7401
30.02	9.150	196.68	0.6786	0.345	9	sand	663.944	202.3701
33.30	10.150	101.34	0.3280	0.324	9	sand	813.944	248.0901
36.75	11.201	78.74	0.2811	0.357	8	sand to silty sand	709.318	216.2001
40.19	12.250	150.01	0.5683	0.379	9	sand	754.987	230.12
43.47	13.250	285.48	1.1808	0.414	10	gravelly sand to sand	952.592	290.35
46.75	14.249	278.08	0.7999	0.288	9	sand	612.763	186.7702
49.87	15.200	83.07	0.2176	0.262	8	sand to silty sand	1176.214	358.51
53.64	16.349	239.35	0.9433	0.394	9	sand	542.749	165.4299

Table 9. Missouri shear-wave reference velocity profiles (in m/sec) for generalized surficial geology types.

Profile_ID	Vs_L1m	Vs_L2m	Vs_L3m	Vs_L4m	Vs_L5m	Vs_L6m	Vs_L7m	Vs_L8m	Vs_L9m	Vs_L10m
F1	121.375119	132.309921	124.145040	177.599238	199.489670	186.895842	238.756749	285.284672	278.593499	385.727651
F2	119.784876	107.968237	150.355859	124.538842	158.687872	197.738390	216.380111	232.325266	252.054360	372.428719
F3	143.123673	139.415433	132.102323	168.952077	195.236679	224.626671	279.587467	327.321541	342.612399	487.427887
L1	251.641729	224.413362	313.467422	346.945025	408.758701	554.478242	637.969241	751.089838	852.610860	1199.459925
L2	201.143870	189.539372	156.804487	204.141629	230.053007	284.305146	337.975753	400.743776	454.420199	659.523243
L3	197.213265	188.584343	162.923296	202.749811	230.054776	285.509443	336.640926	394.133101	443.509260	646.275763
Td1	118.628283	117.151245	156.711811	158.317305	178.959779	204.757219	229.396395	260.334456	285.460728	413.118208
Td2	196.033644	203.375362	195.569738	165.471043	143.204184	207.502963	269.826638	318.247776	374.416320	526.560288
T	185.855141	158.523895	184.434224	227.326704	228.643221	271.361038	347.910961	403.849064	456.993833	650.391067
Qsnd	132.885028	142.263622	159.027419	157.194555	186.214055	206.971646	228.199086	266.281306	294.224202	427.600618
Qslt	114.133213	128.721795	131.151173	185.150577	191.957736	175.259817	226.395930	273.618716	277.495041	388.636520
Qcly	139.370958	137.045426	146.611391	163.460735	161.593439	183.030724	222.597726	244.004135	252.258515	376.698510

Alluvium materials

Work done by the United States Geological Survey (USGS) and Missouri Division of Geology and Land Survey (DGLS) in the confluence area of the Mississippi and Missouri rivers indicates variation in the Vs profile with variation in surface (cap) material (fig. 19) resulting in the three profile types, Qcly, Qslt and Qsnd. Alluvium materials in the Missouri River valley upstream from the confluence area as well as in the floodplain-upland transition were determined to have different average Vs profiles. Table 10 shows five profiles that were used for alluvium in the seismic response model.

Table 10. Missouri generalized alluvium deposit surficial types with Vs profile IDs.

Profile_ID	**Surficial Geology Type**	**Soil Profile Layer Type**	**Average Surficial Material Thickness**
F1	Floodplain-Upland Transition	12-30 m alluvium with stratified sands, gravels, silts and clays over bedrock	19m (+/- 8m)
F2	Alluvium	12-30 m alluvium with stratified sands, gravels, silts and clays over bedrock	18m (+/- 6m)
F3	Artificial fill	Artificially emplaced fill over alluvium or terrace deposits	19m (+/- 8m)
Qcly	Clay-capped Alluvium	5 m clay with silt and organic material over sand and gravel	29m (+/- 10m)
Qslt	Silt-capped Alluvium	5 m silt with clay and organic material over sand and gravel	25m (+/- 12m)
Qsnd	Sand-capped Alluvium	5 m sand with clay, silt and organic material over sand and gravel	32m (+/- 9m)

Terrace deposits

Average shear wave velocity profiles for terrace deposits along the Missouri and Mississippi Rivers were determined (table 11). These terrace deposits include lacustrine silts, clays and organic material in some locations; notably, much of the Lambert-St. Louis International Airport is located on a large lake/terrace deposit (Goodfield, 1965). Shear wave velocities for Missouri River terrace deposits are significantly lower than those for Mississippi River terraces.

Table 11. Missouri generalized terrace deposit surficial types with Vs profile IDs.

Profile_ID	Surficial Geology Type	Soil Profile Layer Type	Average Surficial Material Thickness
Td1	MO River terrace	0-50 m lacustrine silts and clays and some organic material over bedrock	22m (+/- 9m)
Td2	MS River terrace	0-50 m lacustrine silts and clays and some organic material over bedrock	18m (+/- 11m)

Bedrock materials

Bedrock in the Missouri portion of the 29-quadrangle area is generally Paleozoic-age and consists primarily of the Mississippian or Pennsylvanian subsystem. The Mississippian bedrock units are composed primarily of limestone with some shale in the Warsaw Formation. The Pennsylvanian bedrock units are comprised primarily of clastic rocks (predominately shale) but also includes limestone and coal. An exception occurs in the southern extent of the mapped area where Ordovician and Devonian limestone with some shale is exposed near the surface. The area of Ordovician and Devonian outcrop in the 29-quadrangle area is less than one square kilometer and is therefore insignificant. Properties are similar to Mississippian bedrock. In general, an abrupt change in shear wave velocity is encountered at the top of bedrock (fig. 20). Presence of a weathered zone at the top of bedrock was not incorporated into the model.

Upland deposits

Upland deposits in the Missouri portion of the 29-quadrangle area consist of loess and glacial till. Large variation in the Vs profiles for the loess indicated that at least three distinct surficial geology types and three generalized Vs profiles (L1, L2, and L3) are required to characterize seismic response in this material. These three profiles are outlined in Table 12. Areas mapped as “Karst” may fall into either the L1 or L2 Profile_ID class.

Table 12. Missouri generalized upland deposit surficial types with Vs profile IDs.

Profile_ID	Surficial Geology Type	Soil Profile Layer Type	Average Surficial Material Thickness
L1	Thin loess/residuum	0-5 m loess over residuum, cherty clay	13m (+/- 10m)
L2	Loess	2-3 m silty loess over 9-15 m clayey loess over variable residuum and carbonate	18m (+/- 11m)
L3	Loess	0-3 m silty loess over 6-15 m clayey loess over variable residuum and carbonate	13m (+/- 8m)
T	Till	0-3 m silty loess over 6-15 m clayey till over variable residuum and carbonate	16m (+/- 7m)

Combined Geologic Maps

The surface and subsurface geology maps from Illinois and Missouri have been combined for use in the seismic and liquefaction hazard analysis. Figure 18 (above) presents the combined surface geology map used to generate the urban hazard maps of the next section. Figure 21 present the combined bedrock sediment thickness maps used in the site amplification analysis in the next section.

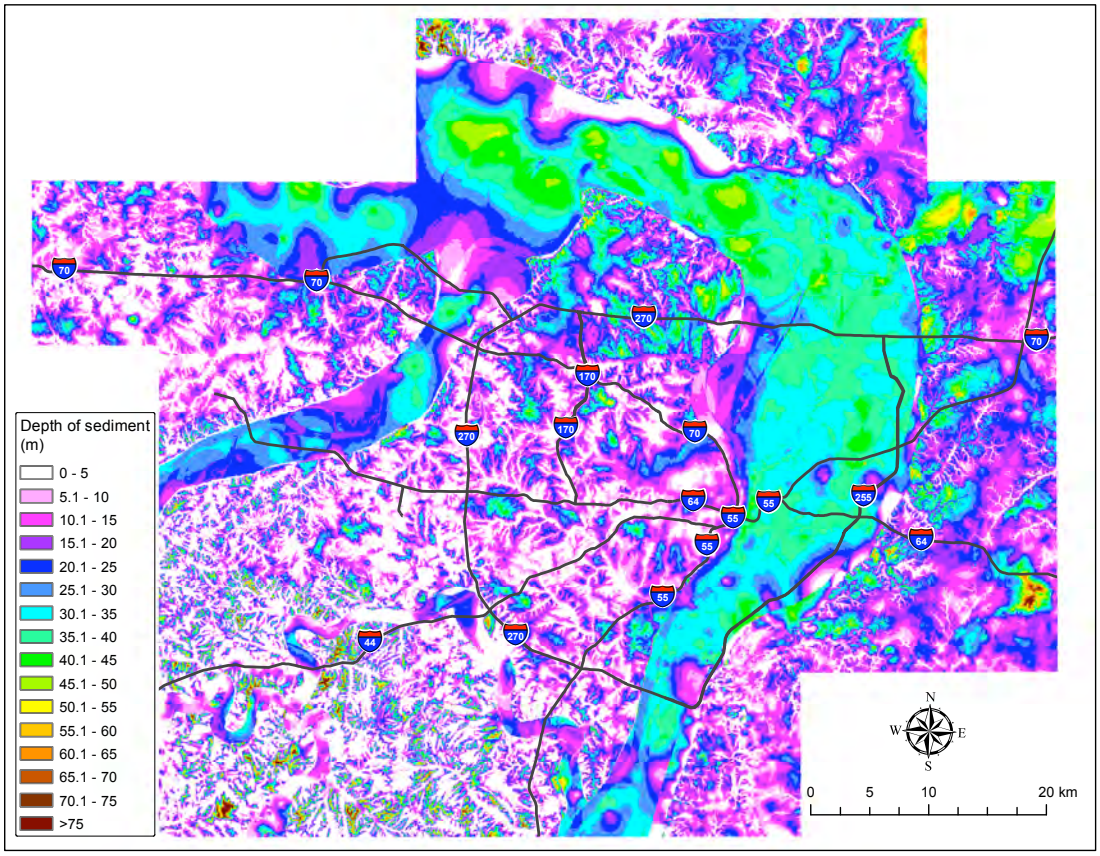

Figure 21. 29-quadrangle sediment thickness map with major highways.

Seismic Hazard Maps

Site Amplification

The method used to calculate site amplification was similar to those employed in the Memphis seismic hazard maps, summarized in Cramer and others (2004). Time histories (see below) were input into the one-dimensional site-response software program SHAKE91, which calculates the propagation of the wave through the soil column and estimates the site-specific amplification factors and other parameters.

Anytime we perform a series of calculations that utilize a series of input variables, uncertainties with each of those variables will be compounded, leading to a greater range of uncertainty, bracketing the calculated/reported values. In the assessment of site amplification, uncertainties exist in the following input parameters: 1) natural variations in shear-wave velocity (for example, horizontal versus vertically propagating shear waves, effects of fracture intensity, weathering, and so forth), 2) natural variations in bulk density (especially, with preferential weathering), 3) the techniques used to estimate the depth and thickness of the soil layers, and 4) the differences in the earthquake time-history records used in the 1-D shaking analyses. When combined together, these uncertainties may cause large differences in amplification calculations. To account for

this variability and uncertainties, a random sampling method is usually applied. Cramer and others (2004) used amplification distributions to account for the uncertainties associated with the amplification calculations. Cramer (2003) asserted that this method of calculating the hazard was the most dependable because it incorporates the uncertainties in the amplification factor. When a truly probabilistic site-specific ground motion is desired, the state-of-the-art approach should be used to estimate the site-specific amplification factor distributions for use in the probabilistic calculations (Cramer, 2003; Cramer and others 2004).

The site amplification calculations for peak ground acceleration, 0.1 s, 0.2 s, 0.3 s, 0.5 s, 1.0 s and 2.0 s spectral accelerations (Sa) were performed using the site amplification code (siteampunc.f) developed by Chris Cramer. In this code, input site response parameters are randomly selected from a range of Vs profiles, dynamic soil properties, geologic boundaries, and a set of earthquake acceleration time-histories. The code then inputs these randomly selected parameters into SHAKE91 and calculates the response. The process for selecting input parameters is explained in the following sections and the results are summarized.

The amplification distributions were calculated based on a grid of 0.005° or for about every 500 m. There were a total of 18,452 grid points encompassing the 29 quadrangles. For every grid point the site amplifications and distributions were calculated first, then the seismic hazard calculations. The amplification distributions were generated for 26 distinct geologic units (see geology section above), and the 500-m grid is thought to be sufficient enough to capture the differences between these units. The amplification values were then smoothed using GIS-based software and drawn as smooth color contours.

The magnitude dependent distribution of earthquake sources (deaggregation of seismic hazard) affecting the St. Louis area indicate that M5s and M6s are predominately within 50 km and M7s are predominately from the 180 to 200 km distance range. In this study, the recordings from the database developed for this project by Cramer (2009) were selected to capture the complexity of earthquake-time histories at epicentral distances up to 200 km. These recordings are a mix of real earthquake and synthetic earthquake records to better capture natural variability in earthquake ground motions. Separate site amplification distributions were generated for M5, M6, and M7 earthquake sources, with the M5 and M6 amplifications based on records within 50 km and the M7 amplifications based on records in the 150 to 200 km epicentral distance range.

To characterize the ground shaking in a fully probabilistic approach, the areal distribution of site amplification was required. To capture the amplification distributions, the above mentioned earthquake time-histories were scaled. This was accomplished on the actual ground-motion records at ten different shaking levels (0.01, 0.05, 0.1, 0.2, 0.3, 0.4, 0.5, 0.6, 0.8, and 1.0 g) at specific periods (PGA, 0.1 s Sa, 0.2 s Sa, 0.3 s Sa, 0.5 s Sa, 1.0 s Sa, and 2.0 s Sa) to obtain input, or base rock ground-motions. The SHAKE91 program was run for each of these shaking levels and the predicted site amplifications were determined for each level. In this study we used the shear modulus and damping ratio relations published by Electric Power Research Institute (1993) with an uncertainty of

0.30 natural log units.

Technical Seismic Hazard Maps

Technical seismic hazard maps were generated using the approach of Cramer and others (2004) with the modifications for this project by Cramer (2011, 2014). Because of the variation in predominant magnitude with distance cited above (predominant M5s and M6s within 50 km and predominant M7s in the 180 to 200 km epicentral distance range), probabilistic hardrock seismic hazard were calculated for M5s (including down to M4.5), M6s, and M7s separately and then the appropriate magnitude dependent site amplification distributions applied in an outside-the-hazard-integral approach (Cramer, 2011, 2014) and the hazard curves combined to obtain the total hazard curve for each site. Obviously for scenario (deterministic) hazard maps, the appropriate M5, M6, or M7 site amplification distributions were used to convert mean hardrock scenario hazard to mean site-specific scenario hazard.

Technical seismic hazard maps were generated for both probabilistic and scenario cases. The probabilistic maps are for 2%, 5%, and 10% in 50 years. The scenario seismic hazard maps are for five scenarios: M7.5 on the NE segment of the New Madrid seismic zone, a M6.0 south of St. Louis near St. Genevieve, a M6.0 east of St. Louis near the Shoal Creek paleoseismic site, a M5.8 beneath St. Louis, and a M7.1 near Vincennes, IN at the location of a large paleoseismic earthquake in the Wabash Valley seismic zone (fig. 22). The scenario hazard maps are for median ground motion hazard for the specified earthquake. All technical seismic hazard maps were generated at seven periods, including PGA.

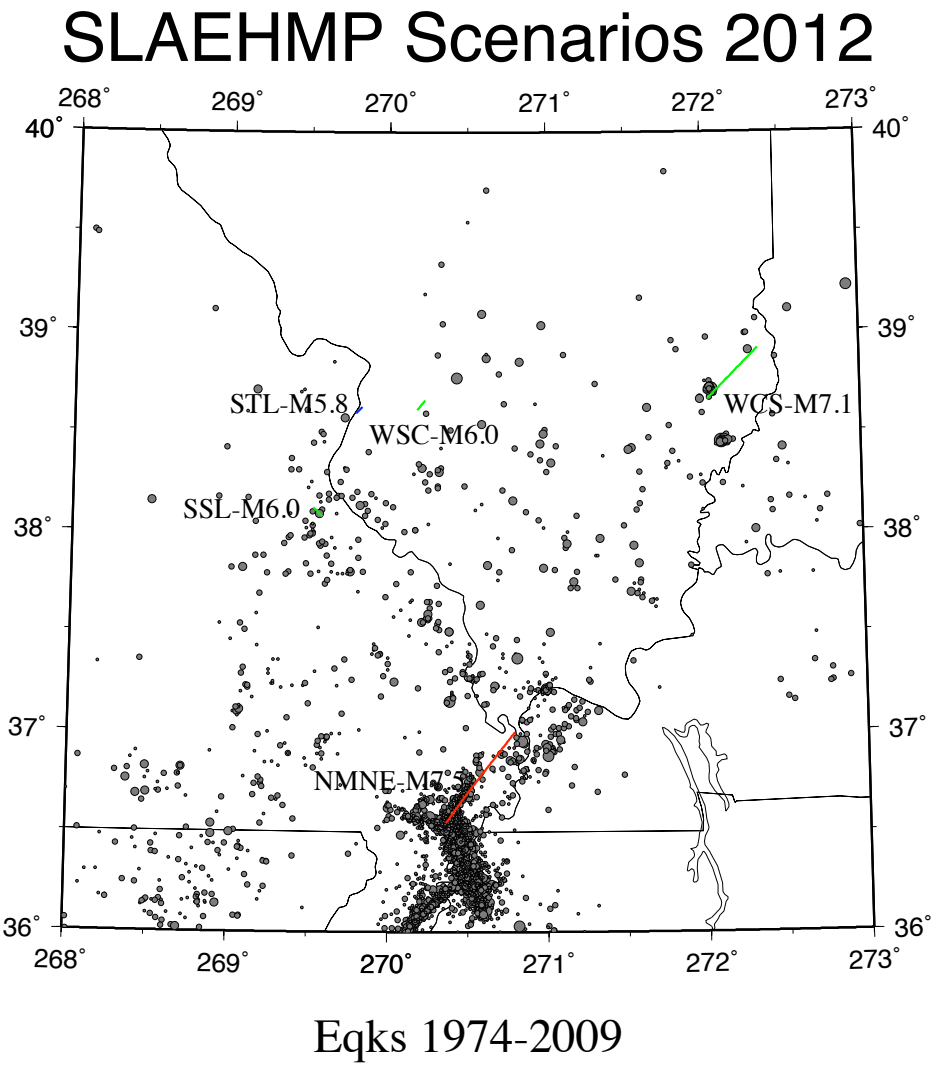

Figure 22: Location map for the five SLAEHMP earthquake scenarios. The grey dots are earthquakes in the region between 1974 and 2009. The line segments (red, green, and blue) are the locations of the ruptures for the scenarios.

Figure 23 shows 0.2 s and 1.0 s hazard maps for 2%-in 50-year ground motion hazard, with the PGA hazard map shown with the liquefaction hazard maps (figure 30). The 2%-in-50-year ground motion hazard maps show the NSHMP B/C boundary maps in the background for comparison. Generally, the SLAEHMP maps show higher hazard than the NSHMP maps due to the effects of local geology and the ground motion levels not being high enough for strong nonlinear soil effects at short periods.

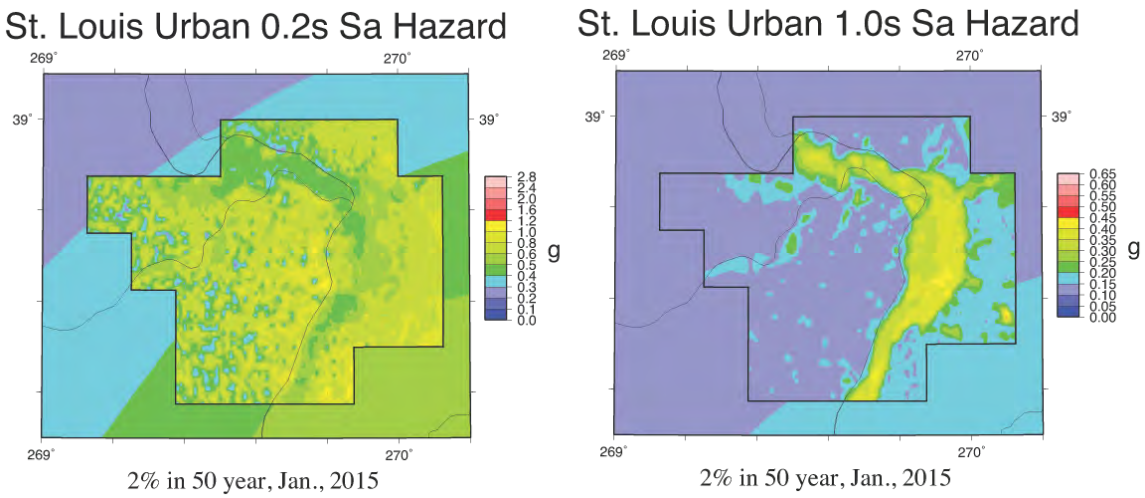

Figure 23: 2% in 50-year 0.2 s and 1.0 s spectral acceleration hazard maps.

Figures 24 shows 0.2 s and 1.0 s scenario maps for the M7.5 New Madrid NE segment scenario, with the PGA hazard map shown with the liquefaction hazard maps (figure 29). The most likely earthquake scenario is the M7.5 on the NE segment of the New Madrid seismic zone and corresponds to a probability of occurring of 0.002 (1 in 500 years). The other scenarios are extremely rare earthquake scenarios with much lower likelihoods of occurring and are not shown in this report.

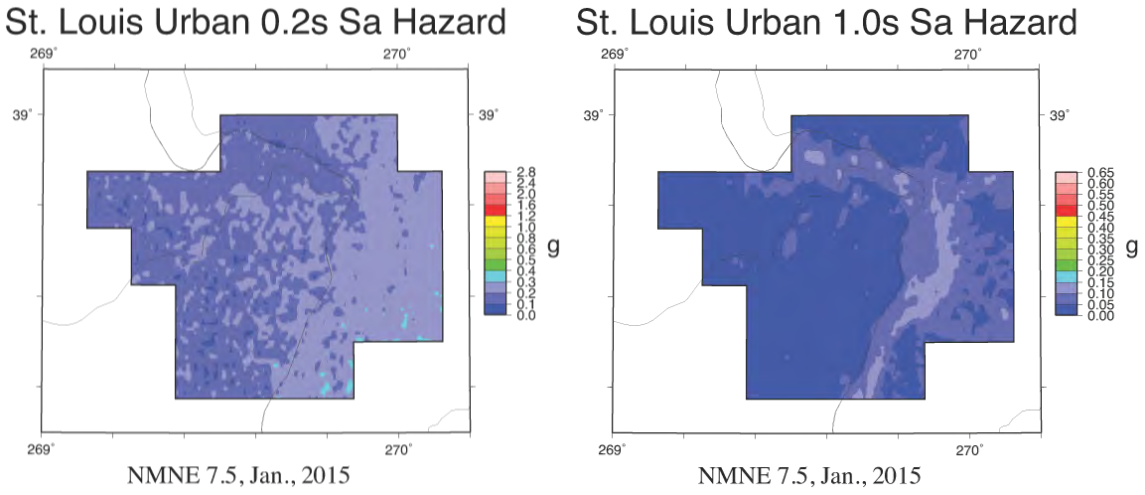

Figure 24: Scenario 0.2 s and 1.0 s spectral acceleration hazard map for the NE segment of the New Madrid seismic zone.

Simplified Shaking Hazard Map

A simplified shaking hazard map for the non-technical user community has been generated from the 5%-in-50yr PGA hazard map, which represents the likely shaking hazard from all major earthquakes including the median ground motion from a M7.5 on the NE arm of the New Madrid seismic zone (the most likely earthquake with the highest ground motion affecting St. Louis). Because the 5%-in-50yr ground motions are mean ground motions, the simplified shaking hazard map represents the 1000-year ground motion levels, including median ground motions from the 500-year New Madrid earthquakes. Median ground motions (half the ground motions are below and half above) for the 500-year earthquake are represented (up to the 60^{th} percentile New Madrid ground motions are included). If the simplified shaking hazard map was based on the 10%-in-50yr PGA hazard, the median (and even above the 35th percentile) ground motions from the New Madrid seismic zone would not be represented.

The technical scenario seismic hazard map was simplified by specifying that a low seismic hazard is for mean PGAs below 0.1 g, moderate seismic hazard is for mean PGAs from 0.1 g to 0.3 g, and severe seismic hazard is for mean PGAs above 0.3 g. Moderate seismic hazard would include severe damage to unreinforced masonry structures but little if any damage to engineered structures. Examples of severe damage to unreinforced masonry structures from recent earthquakes include the damage in Port-au-Prince from the 2010 M7.0 Haiti earthquake and damage in Kathmandu from the 2015 M7.8 Nepal earthquake where a strong motion recorder in Kathmandu only recorded a PGA of 0.15 g. Additionally, URM damage in downtown Christchurch, New Zealand from the 2010 M7.1 Darfield earthquake (epicenter 40 km away) was significant for recorded PGAs of 0.1-0.2 g, but from the 2011 M6.3 Christchurch earthquake (epicenter 10 km away) URM damage was severe from recorded PGAs exceeding 0.3 g (Moon et al., 2014). For engineered structures in downtown Christchurch, only PGAs exceeding 0.3g resulted in some significant damage (Fleischman et al., 2014). Possible significant damage to engineered structures begins at about 0.3 g. Figure 25 presents the simplified shaking hazard map.

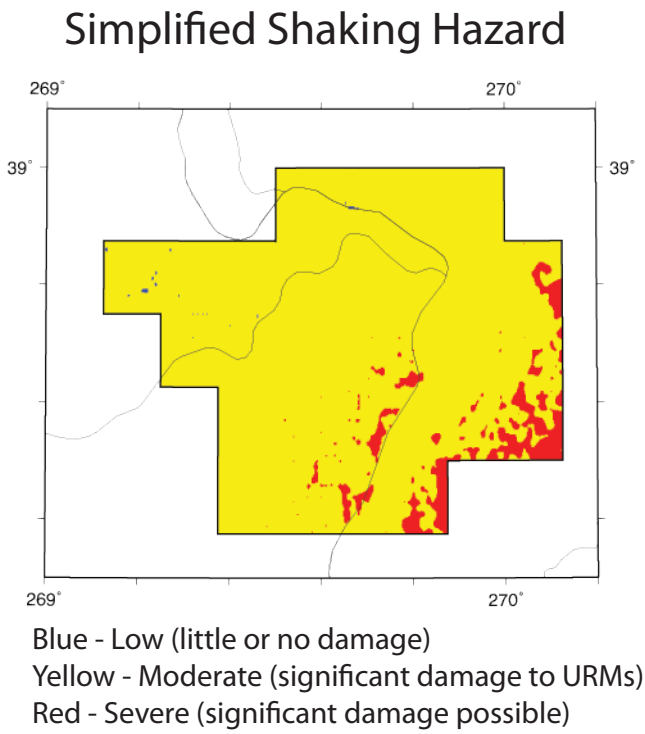

Figure 25: Simplified earthquake shaking hazard map for St. Louis where low shaking hazard indicates little or no damage, moderate shaking hazard indicates severe damage to unreinforced masonry (URM) structures but little or no damage to engineered structures, and severe shaking hazard indicates possible significant damage to engineered structures.

Liquefaction Hazard Maps

Liquefaction Potential

The liquefaction potential index (LPI; Iwasaki and others, 1978 and 1982) has been increasingly applied to evaluate liquefaction risk, worldwide (Holzer and others, 2005; Papathanassiou 2008; Hayati and Andrus 2008; Haase and others, 2011). Its risk criteria (zero to minor liquefaction risk when LPI < 5; severe liquefaction risk when LPI > 15) generally correlate well with liquefaction case histories (Iwasaki and others, 1982; Toprak and Holzer 2003).

Exceeding LPI value of 15 represents the median figure extracted from post-quake evaluations of liquefied sites over the past half-century (Iwasaki et al. 1978 and 1982). Recently, Toprak and Holzer (2003) related LPIs with ground damage for the 1989 Loma Prieta Earthquake, and they found that LPI > 12 were associated with more than 50% of ground cracking as severe hazards and LPI > 5 for sand boils as moderate hazards. Exceeding LPI values of 12 as the lower limit of severe liquefaction should be adopted if a conservative estimate is sought, as is typical of planning documents. Thus exceeding LPI values of 12 was adopted as the lower limit of severe liquefaction by the SLAEHMP Technical Working Group (TWG).

Cumulative Frequency Distributions

Holzer and others (2006) grouped 202 cone penetration test-based liquefaction potential index (LPI) values in surficial geologic units along the margins of San Francisco Bay (140 km^2), California. Cumulative frequency distributions of LPI > 5 for surficial geologic units were then analyzed. The percentage of LPI > 5 were interpreted as the probability to estimate surface manifestations of liquefaction at a random location.

This method estimates the threshold PGA for specific LPI values and its probability, for a scenario earthquake magnitude (e.g., Mw = 7.5). Cramer and others (2008) modified the approach to map liquefaction hazards in the Memphis area (six 7.5-minute quadrangles, 950 km^2). They adjusted the PGA values with various earthquake magnitudes, by applying correction factors termed 'magnitude scaling factors' (MSF).

Groundwater Depth

The depth of the groundwater table is a controlling factor for assessing liquefaction potential, because liquefaction only occurs in saturated soils. High groundwater levels increase the liquefaction potential and increase the LPI values. Liquefaction seldom occurs where the groundwater table is deeper than 12 m below ground surface (Youd, 1973). To demonstrate the effect of water table depth on liquefaction probability, Holzer and others (2011) showed that the liquefaction probabilities decrease significantly, for groundwater table depths of 1.5 m to 5 m.

Previous probabilistic liquefaction hazard maps (Holzer and others, 2006, Cramer and others, 2008) have been prepared using scenario earthquakes and groundwater levels for an entire study area (e.g., 1.5 m depth for San Francisco Bay; 6 m depth for Memphis). Such blanket assumptions tend to oversimplify liquefaction probability of regional areas. For example, the St. Louis metro area is situated on contrasting geomorphic settings: alluvial floodplains and dissected loess-covered uplands, which exhibit different groundwater depths. The depths-to-groundwater in the uplands are highly variable, ranging from 1 m to 30 m or more (Pearce and Baldwin 2008; Chung and Rogers, 2011 and 2012a).

To determine the liquefaction probability curves under the most likely conditions, we considered high and normal water table scenarios for both geomorphic provinces (lowlands and uplands), then calculated the liquefaction probabilities for LPI > 5 (moderate) and >12 (severe liquefaction hazard) at the differing seismic demand of PGA/MSF. Information from the Illinois State Geological Survey (Bauer, 2012) in both the lowlands of the Mississippi flood plain and the uplands provided the estimates for high and normal water table depths used in this study. In the lowlands water table depths of 0.5m and 2.0m were used for the high and normal depths. In the uplands water table depths of 1.0m and 4.0 m were used.

Data

The input data for mapping liquefaction hazard in this study consists of the following components:

- Surficial geologic map: The Quaternary surficial geologic maps (fig. 26 and table 13) were collected from: 1) the USGS (Schultz, 1993), and 2) the Illinois Geological Survey (ISGS; Grimley and Phillips, 2006; and Grimley, 2009). Different map units and mapping techniques have traditionally been employed by Missouri (depositional models) and Illinois (formational models). These were unified and simplified for this study, based on sediment types and genesis (Chung and Rogers, 2010, 2011).

- SPT profiles: The logs of 1,923 engineering boreholes (fig. 26 and table 13) including soil descriptions, respective thickness, and SPT (standard penetration test) blow counts, with sampling intervals of 0.76 m to 1.5 m were utilized in this study. These were collected from the Missouri Division of Geology and Land Survey (MODGLS; Palmer and others, 2006), the ISGS, and the USGS (Conor Watkins 2011, personal communication). These SPT profiles were used to calculate the LPI values.

- Assumed depth-to-groundwater (DTW): DTW estimates were based on data gleaned from monitoring wells (USGS, 2011), engineering boreholes (Chung and Rogers, 2012a), and local experience (Robert Bauer, 2011, personal communication; Brad Mitchell 2011, personal communication, Bauer, 2012). After review by the SLAEHMP Technical Working Group (TWG) we assumed two depths-to-groundwater scenarios for each landform:

    - High level: 0.5 m (95^{th} percentile) for floodplains and 1.0 m (95^{th} percentile) for uplands;
    - Normal level: 2.0 m (the median) for the floodplains and 4.0 m (the mode) for uplands.

The curves of liquefaction probability were established for both assumed water table depths and for floodplains and uplands.

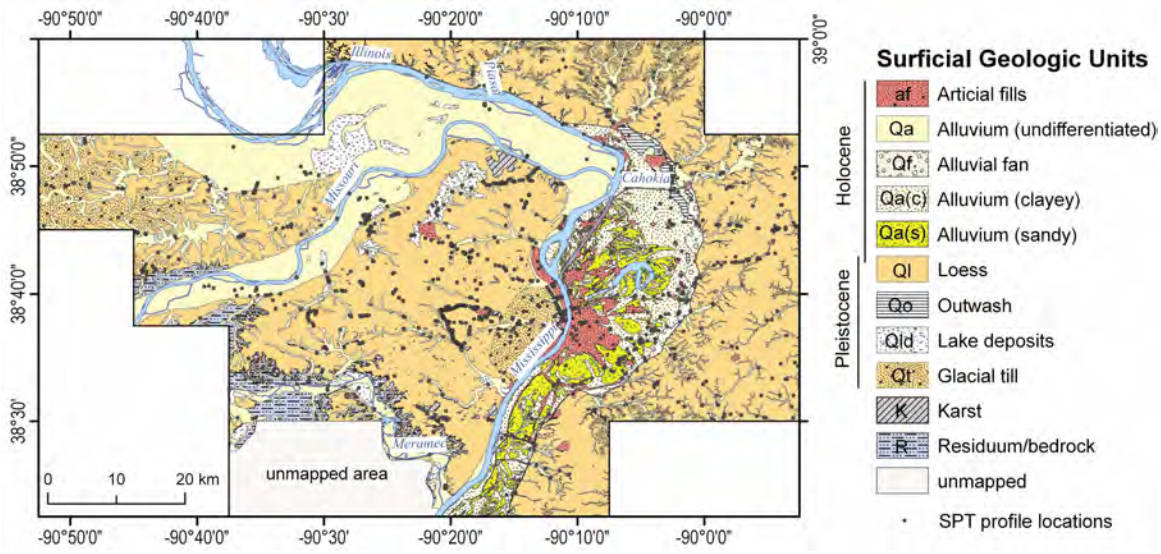

Figure 50. Simplified surficial geology map of the St. Louis area (modified from Schultz 1993; Grimley and Phillips, 2006; and Grimley, 2009), with overlay showing the locations of engineering borings used to assess liquefaction probability.

Table 13. Surficial Geologic Units and Distributions of Engineering Borings

Landform	Geologic Unit	Symbol	Materials	Number of Boreholes
Low-lying floodplains	Artificial fills	af	Various soil or rock types	150
	Alluvium	Qa	Silt loam	439
	Alluvial fan	Qf	Silt loam	17
	Alluvium (clayey facies)	Qa (C)	Silty to silty clay loam	74
	Alluvium (sandy facies)	Qa (S)	Very fine to medium sand	38
	Glacial outwash	Qo	Medium to coarse sand	8
	Lake deposits	Qld	Silty clay loam	120
Uplands	Artificial fill	af	Various soil or rock types	14
	Loess	Ql	Silt to silt loam	959
	Till	Qt	Mixed of clay, gravel, and rock fragment	87
	Residuum	R	Clay, silt and sand with rock fragments derived from the underlying bedrock	17

LPI Calculation

Following the approach of Romero-Huddock and Rix (2005), the simplified SPT-based procedure of Seed and Idriss (1971) and liquefaction resistance curve of Seed and others (1985) were applied to evaluate the critical PGA/MSF sufficient to exceed LPI's of 5 (moderate) and 12 (severe liquefaction effects).

MSF: among various proposed equations of a magnitude scaling factor (MSF), we employed the MSF suggested by Youd and others (2001):

$$MSF = 10^{2.24}/Mw^{2.56}$$

where Mw is moment magnitude.

PGA/MSF: 45 combinations of PGA (0.10, 0.15, 0.20, 0.25, 0.30, 0.35, 0.40, 0.45, 0.50 g) and Mw (6.0, 6.5, 7.0, 7.5, 8.0) were used to calculate LPI values for each of the surficial geologic units shown in table 13.

Liquefaction Probability Curves

Figures 27 and 28 present the probability of exceeding LPI's of 5 and 12, for high and normal groundwater levels, for the floodplain and upland geomorphic provinces, respectively. The liquefaction probability, as a function of the PGA/MSF, was fitted with a four-parameter Weibull's model, using SigmaPlot software (2006):

$$p = \begin{cases} 1 \quad e^{-\left(\frac{x \quad xo+b\ln 2^{1/c}}{b}\right)^c} & for\ x > x_0 \quad b\ln 2^{\frac{1}{c}} \\ 0 & for\ x \quad x_0 \quad b\ln 2^{\frac{1}{c}} \end{cases}$$

where a*p = the liquefaction probability (LPI >5 or >12), x = PGA/MSF, a, b, c, and x_0 = fitted coefficients.

The Weibull cumulative probability model is suitable for analyzing the failure probability of composites or layered materials under a given stress (Weibull, 1951; Jibson and others, 2000). This model produces the most versatile sigmoid curve, and is sufficiently flexible to accommodate most data sets. Regression analyses for Weibull's model are presented in figures 27 and 28, and the data is summarized in table C1 of appendix C.

Updating Liquefaction Computer Codes

The approach used by Cramer and others (2008) for producing liquefaction hazard maps for Memphis, TN has been applied to generating liquefaction hazard maps for SLAEHMP. The computer programs used to generate liquefaction hazard maps were updated from the 2002 to the 2008 and then the 2014 USGS national seismic hazard model (Petersen and others, 2008, 2014) to remain compatible with the seismic hazard maps being generated for SLAEHMP. This involved not only updating map generation programs to the 2008 and 2014 hazard model, but also transferring the national map codes to the University of Memphis High Performance Computing (HPC) facility. The HPC is needed to calculate both the site amplification distributions and the probabilistic liquefaction hazard in a reasonable time period (days instead of months) due to the 0.005-degree (~500 m) grid used and the number of quadrangles (29) included in the calculations.

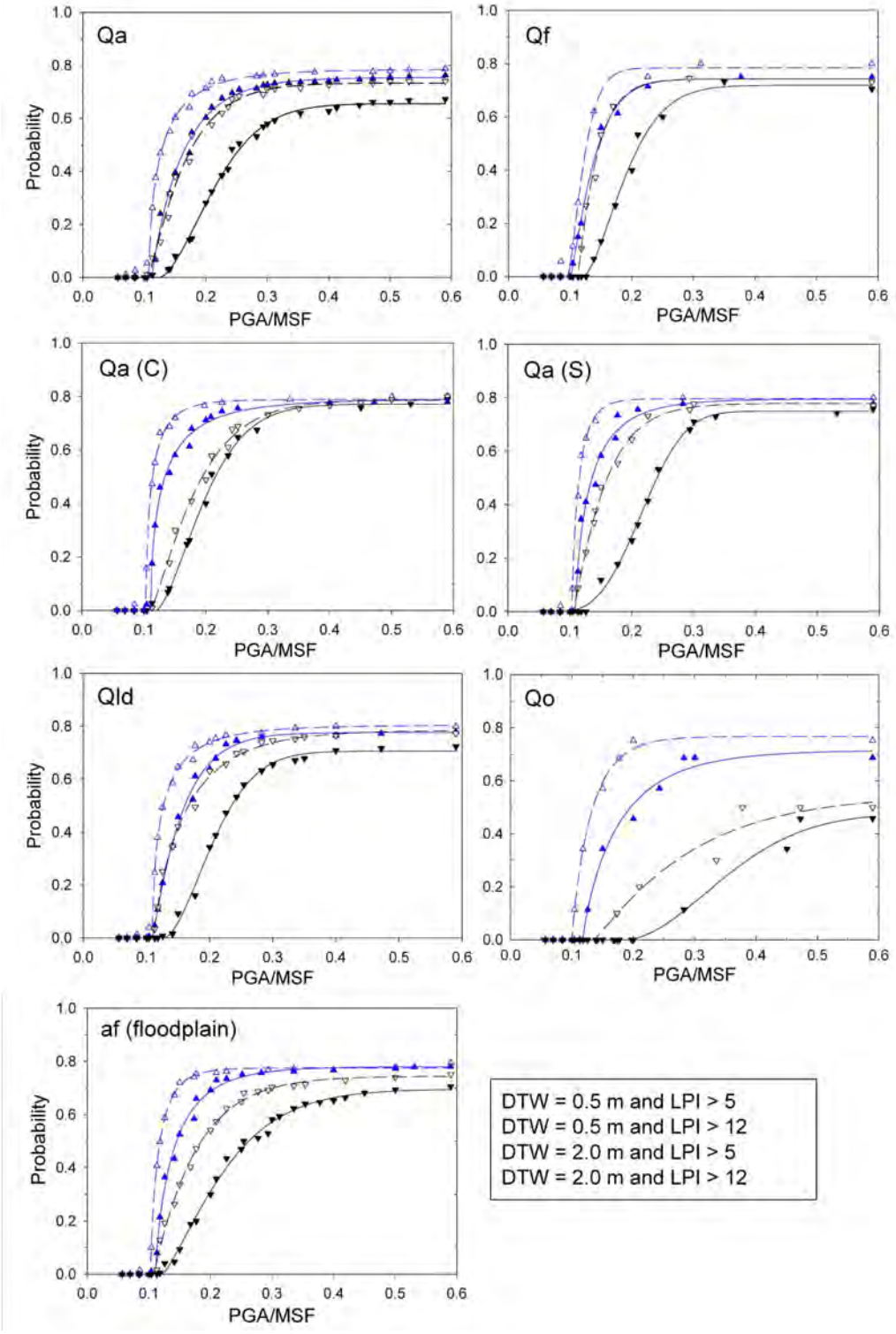

Figure 51. Curves of liquefaction probability of LPI > 5 (open) and LPI >12 (filled) for surficial geologic units, floodplains within St. Louis area. DWT = depth-to-groundwater (blue – 0.5m, black – 2.0m); Qa = alluvium; Qf = alluvial fan; Qa(C) = clayey alluvium; Qa(S) = sandy alluvium; Qld = lake deposits; Qo = glacial outwash; af = artificial fills.

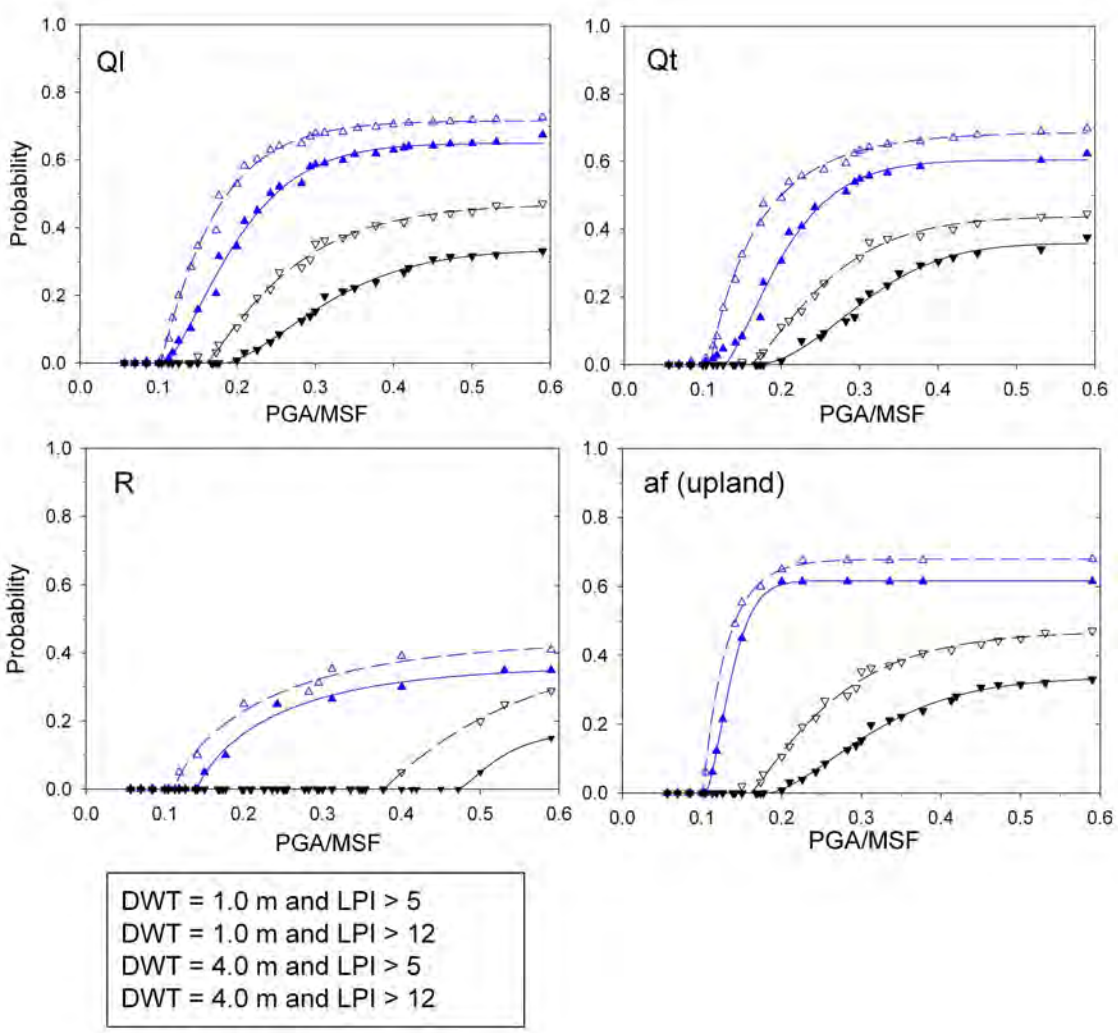

Figure 52. Curves of liquefaction probability of LPI > 5 (open) and LPI > 12 (filled) for surficial geologic units, uplands within St. Louis area. DWT = depth-to-groundwater (blue – 1.0 m, black – 4.0 m); Ql = loess; Qt = till; R = residuum; af = artificial fills.

The approach of Cramer and others (2008) uses the liquefaction cumulative probability curves generated in the previous section. Note that the liquefaction cumulative probability curves are a function of magnitude and hence are used inside the hazard integral to calculate probabilistic liquefaction hazard maps as indicated in the following equation from Cramer and others (2008):

$$P(P_{LPI>n} > Po) = \Sigma_i \alpha_i \int_M \int_R f_i(M)\, f_i(R)\, P(P_{LPI>n} > Po \mid A > Ao,M)\, P(A > Ao \mid M,R)\, dR\, dM$$

where $P(P_{LPI>n} > Po)$ is the liquefaction hazard curve for LPI>n, α_i is the rate of source i, M and R are magnitude and distance, $f_i(M)$ and $f_i(R)$ are the ith source magnitude and distance distribution functions, $P(P_{LPI>n} > Po \mid A > Ao,M)$ is the liquefaction cumulative probability curve for the site and LPI>n, and $P(A > Ao \mid M,R)$ is the site-specific attenuation relation. The site-specific attenuation relation is generated using the approach of Cramer (2003,2005).

Liquefaction Hazard Maps

The generation of final liquefaction hazard maps requires the use of a GIS, guided by the surface geology map, to piece together liquefaction hazard maps for each surface soil type into a scenario or probabilistic liquefaction hazard map. Figure 18 (in the MDNR geology section) show the detailed surface geology maps for Illinois and Missouri used to generate the liquefaction hazard maps. With the assistance of Illinois and Missouri geologists, surface geology units in figure 18 were related to the simplified surface geology units of figure 26 and table 13 to assign the appropriate liquefaction cumulative probability curves to the detailed surface geology.

Scenario liquefaction hazard maps have been generated by taking SLAEHMP scenario median peak ground acceleration (PGA) hazard maps that include the effects of local geology and applying the median liquefaction cumulative potential curve for the scenario magnitude. At each grid point, the median PGA scaled by the magnitude-scaling factor is used to select the probability of exceeding LPI 5 or 12 from the curve for the surface geology at that grid point. SLAEHMP scenario PGA maps available are for (1) a M7.5 earthquake on the northeast arm of the New Madrid seismic zone, (2) a M6.0 40 km east of St. Louis near the Shoal Creek, IL paleoliquefaction feature, (3) a M6.0 50 km SSW of St. Louis near Sainte Genevieve, MO, (4) a M5.8 beneath downtown St. Louis, and (5) a M7.1 near Vincennes, IN.

Once the liquefaction hazard maps for a given scenario or probability of exceedance for each LPI exceedance level, surface geology type, and depth to water table (DTW - high or normal) have been calculated, the two depth to water table alternatives are combined using a weighted average. The SLAEHMP technical working group (TWG) discussed the weighting to be used in combining high and normal water table alternative maps. After reviewing the water table evidence of Bauer (2012), the TWG weighted the flood plain high DTW map 1.0 and the normal DTW map 0.0, as the reliable evidence in Bauer (2012) showed the flood plain water tables to fluctuate between 0.5 to 1.0 m and rarely fall below 1.0 m. For the uplands, the high and normal DTW maps were weighted equally (0.5 each). Thus for the floodplain surface geologies, only the 0.5 m DTW map was used, while for the uplands the 1.0m and 4.0 m maps were averaged together.

An example scenario liquefaction hazard map for the M7.5 New Madrid scenario is shown in figure 29 for LPI>5 and LPI>12 along with its PGA scenario hazard map. As is noticeable in figure 29, for some surface geology types and near 10% probability of exceedance the LPI>5 values are similar to or slightly less than, instead of being greater than, the LPI> 12 values due to curve fitting to the liquefaction probability curve values (see figure 27). This inaccuracy in the curve fitting is not significant at these very low probabilities of exceedance and is within the calculation uncertainty. Scenario liquefaction hazard maps for the remaining SLAEHMP earthquake scenarios are not shown in this report.

Probabilistic liquefaction hazard maps have also been generated for LPI>5 and LPI>12. Again these maps were generated according to the method of Cramer and others (2008), as briefly described above. Figure 30 presents the 2% in 50-year liquefaction hazard maps along with their accompanying PGA probabilistic seismic hazard maps.

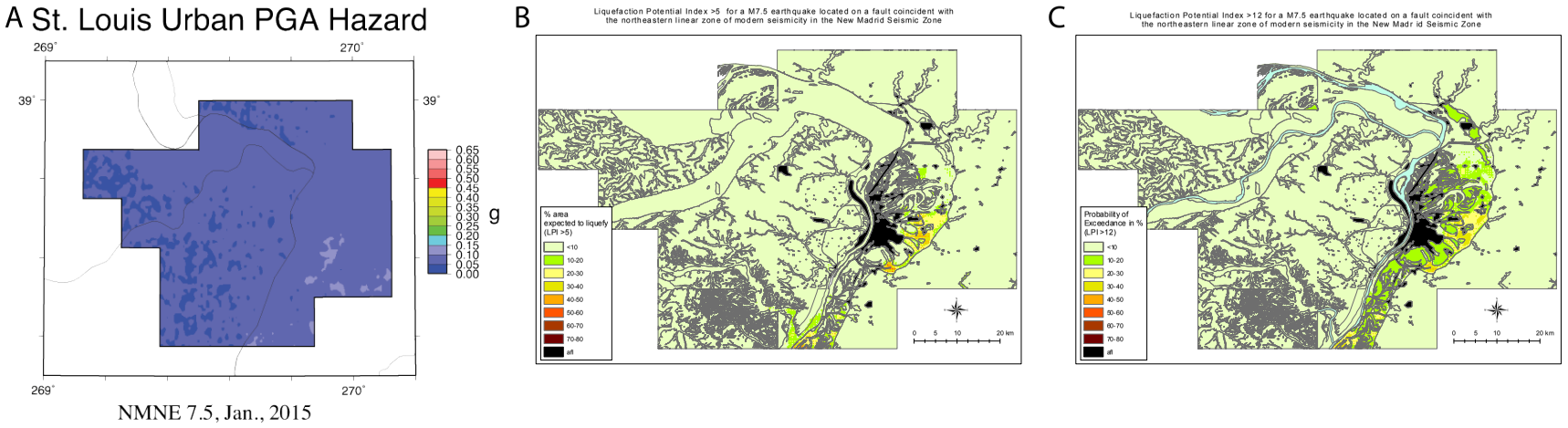

Figure 53. (A) PGA, (B) LPI>5, and (C) LPI>12 ground motion / liquefaction hazard maps for a scenario M7.5 earthquake on the NE segment of the New Madrid seismic zone.

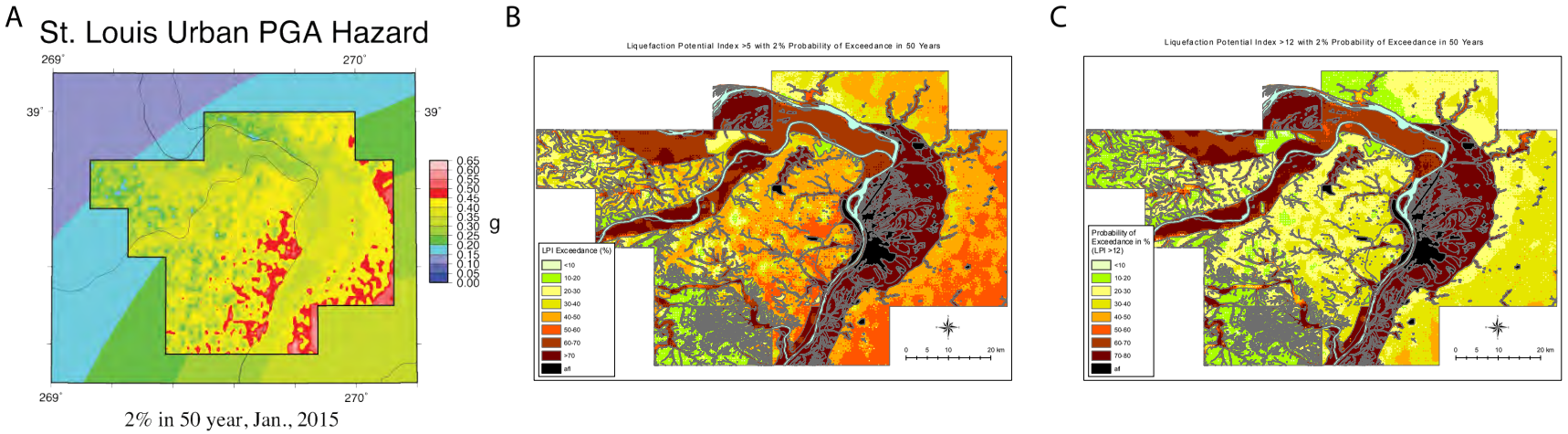

Figure 59. (A) PGA, (B) LPI>5, and (C) LPI>12 ground motion / liquefaction probabilistic hazard maps for 2% in 50 year exceedance.

An alternative interpretation of the LPI>5 liquefaction hazard maps is that they represent the percent area that will liquefy in the indicated surface geology formation during the scenario event or, in the case of the probabilistic maps, with the stated probability of being exceeded. LPI>5 is the threshold for the onset of liquefaction per our introductory discussion. Areas showing a probability for LPI exceeding 5 of less than 10% have very low likelihood of liquefaction effects at the surface. Probability of LPI>5 between 10% and 40% should have a low likelihood of liquefaction. For a probability of LPI>5 between 40% and 60%, the likelihood of liquefaction is moderate. It is severe for probabilities of LPI>5 exceeding 60%.

A simplified liquefaction hazard map has been generated using the above criteria for very low, low, moderate, and severe liquefaction hazard. As described above, the 5%-in-50yr hazard has been selected to best represent the general hazard level and hence the liquefaction hazard in the St. Louis area. Figure 31 presents this simplified liquefaction hazard map, which is designed for use by the non-technical user community to indicate the liquefaction hazard faced in the region.

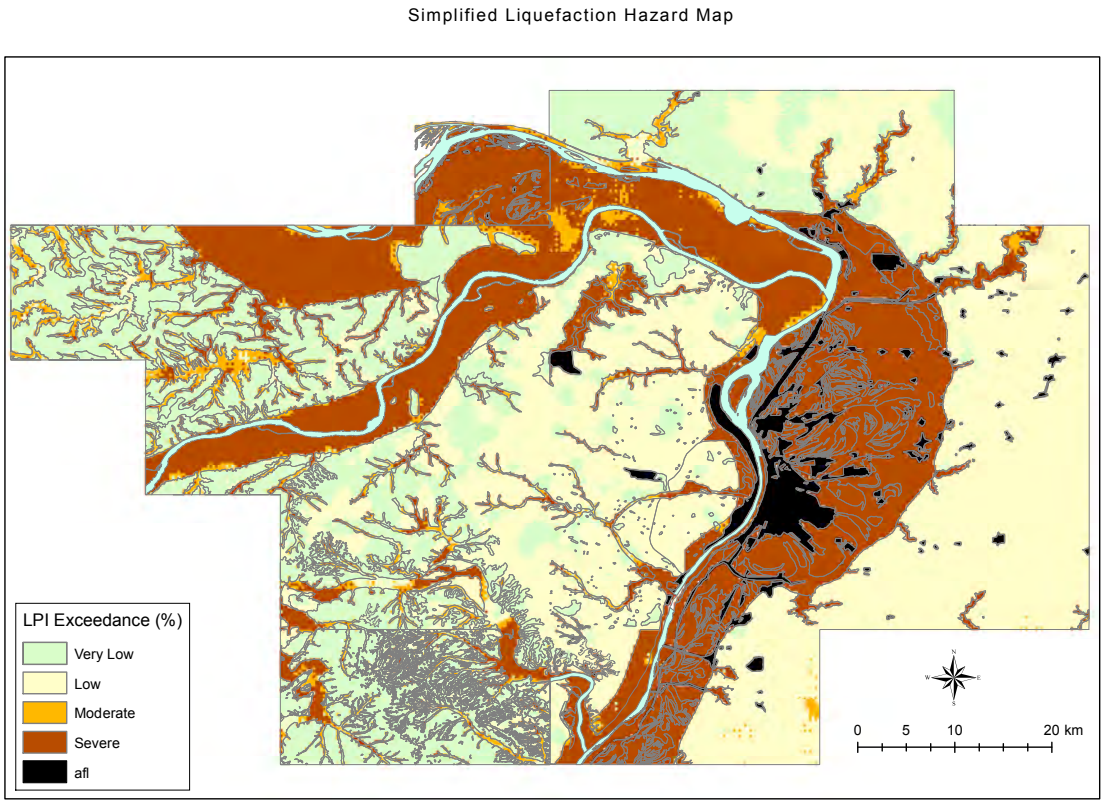

Figure 60. Simplified Liquefaction Hazard Map for the St. Louis area. Brown areas have severe liquefaction hazard, orange areas have moderate liquefaction hazard, the light yellow areas have low liquefaction hazard, and light green areas have very low liquefaction hazard. Black areas are areas of artificial fill with unknown liquefaction potential and hence are "special study" areas requiring further site-specific analysis.

Outreach Meetings

Two outreach presentations were conducted in the Spring of 2017, one in Kansas City, MO and the other in St Louis, MO. On February 8, 2017 a teleconference presentation of the St. Louis urban hazard maps was presented to 39 federal agency representatives of the Kansas City Continuity of Operations (COOP) interagency group. Rob Williams present on the seismic hazard setting of the New Madrid seismic zone and Chris Cramer presented the St. Louis urban seismic and liquefaction hazard maps.

On March 16, 2017 presentations were made at a joint meeting of the St. Louis Metropolitan Area COOP group (federal agencies) and the Mid-America Association of Contingency Planners (private and business organizations). There were three presentations to 50 attendees from these organizations. The joint meeting was held at the St. Louis Emergency Management Operations Center. Rob Williams and Chris Cramer again presented on the New Madrid seismic hazard and St. Louis urban hazard maps, respectively. They were joined by Nathan Gould who presented on resilience and hazard mitigation.

Both outreach presentations were well received.

Conclusions

Urban seismic hazard maps have been generated for the 29 quadrangles of the St. Louis Area Earthquake Hazards Mapping Project study area. Both technical and simplified seismic and liquefaction hazard maps have been produced that include the effects of local geology. The simplified hazard maps are for 5%-in-50yr hazard, which includes the median ground motion from a M7.5 earthquake on the NE segment of the New Madrid seismic zone (the most-likely damaging earthquake to affect the St. Louis area). 10%-in-50yr hazard does not contain ground motions above the 35th percentile from New Madrid earthquakes and hence is not sufficiently conservative for hazard mitigation. The simplified shaking hazard map is derived from the peak ground acceleration 5%-in-50yr hazard map and the simplified liquefaction hazard map is derived from the percent of area affected by liquefaction at the surface (Liquefaction Potential Index greater than 5) 5%-in-50yr liquefaction hazard map. Earthquake shaking hazard is characterized as moderate (significant damage to unreinforced masonry structures) to severe (potentially significant damage to all structures), depending on location. Liquefaction hazard is characterized as very low (liquefaction unlikely) to severe (liquefaction very likely), with the severe liquefaction hazard occurring in the Mississippi, Missouri, and Meramec River floodplains.

Both probabilistic and scenario (deterministic) seismic and liquefaction hazard maps have been produced. The probabilistic hazard maps are for 10%, 5%, and 2% probability of being exceeded in 50 years. The scenario hazard maps are for the most-likely damaging earthquake (M7.5 on the NE NMSZ), and for four other much less likely or theoretical earthquake scenarios: a M6.0 near St. Genevieve, MO, a M6.0 near the Shoal Creek, IL paleoliquefaction site, a M5.8 beneath St. Louis, and a M7.1 near Vincennes, IN centered on a large Wabash Valley paleoliquefaction field.

There are two major caveats associated with the St. Louis area urban hazard maps. The first is that they are still regional hazard maps and are not site-specific hazard maps due to the

mapping uncertainties, mainly associated with the ~500 m grid used in the calculations and the limitations of the geologic model. Second, these maps, while useful for guidance in developing a site-specific analysis, are not building code maps and are not to be used in the building code regulatory process.

The St. Louis urban seismic and liquefaction hazard maps were well received at two meetings of emergency management officials and contingency planners in February and March, 2017 in Kansas City MO and St. Louis MO.

References Cited

Abert, C., 1995, Digital Elevation Model of Illinois: Illinois State Geological Survey, Champaign, online access at http://www.isgs.illinois.edu/nsdihome/webdocs/st-geolq.html, scale 1:250,000.

Bauer, R. A., 2012, Cooperative agreement proposal to the USGS to complete St. Louis area earthquake hazards mapping projects's seismic and liquefaction hazard maps: Illinois State Geological Survey depth to groundwater report, ISGS final technical report, 15 pp.

Borcherdt, R.D., 1970, Effects of local geology on ground motion near San Francisco Bay: Bulletin of the Seismological Society of America, v. 60(1), p. 29–61.

Chung, J., 2007, Development of a geographic information system-based virtual geotechnical database and assessment of liquefaction potential for the St. Louis metropolitan area: Rolla, Missouri University of Science and Technology, Ph.D. dissertation, University of Missouri-Rolla, 169 p.

Chung, J.-W., and Rogers, J.D., 2010, GIS-based virtual geotechnical database for the St. Louis metro area, Environmental & Engineering Geoscience, 16(2), 143-162

Chung, J.-W., and Rogers, J.D., 2011, Simplified method for spatial evaluation of liquefaction potential in the St. Louis area, Journal of Geotechnical and Geoenvironmental Engineering, 137(5), 505-515.

Chung, J.-W. and Rogers, J.D., 2012a, Interpolations of groundwater table elevation in dissected uplands. Ground Water, in press, DOI: 10.1111/j.1745-6584.2011.00889.x.

Chung, Jae-won and J. David Rogers, 2012b, Seismic site classifications for the St. Louis urban area; Bulletin of the Seismological Society of America, Vol. 102, No. 3, pp. 980–990.

Cramer, C.H., 2003, Site-specific seismic-hazard analysis that is completely probabilistic, Bulletin of the Seismological Society of America, v. 93(4), p. 1841–1846.

Cramer, C.H., 2005, Erratum: Site-specific seismic-hazard analysis that is completely probabilistic, *Bull. Seism. Soc. Am.* **95**, 2026.

Cramer, C.H., 2009, Final Technical Report, a proposal in support of the St. Louis Area Earthquake Hazards Mapping Project: suite of CEUS-specific hard-rock time-histories and seismic hazard model updates, USGS grant 08HQGR0016, February 20, 2009, CERI, 24 pp (available at http://earthquake.usgs.gov/research/external/reports/08HQGR0016.pdf).

Cramer, C.H., 2011, Final Technical Report, a proposal in support of the St. Louis Area Earthquake Hazards Mapping Project: Update to Methodology and Urban Hazard Map Uncertainty Analysis, USGS grant G09AP00008, February 14, 2011, CERI, 26 pp (available at http://earthquake.usgs.gov/research/external/reports/G09AP00008.pdf).

Cramer, C.H., 2014, Magnitude dependent site amplification seismic hazard calculation outside the hazard integral for St. Louis, MO (abstract), *Seism. Res. Lett.* **85**, 542.

Cramer, C.H, Gomberg, J.S, Schweig, E.S., Waldron, B.A., and Tucker, K., 2004, The Memphis Shelby County Tennessee seismic hazard maps: United States Geological Survey Open-File Report 2004–1294, 41 p.

Cramer, C.H., Rix, G.J., and Tucker, K, 2008, Probailistic liquefaction hazard maps for Memphis, Tennessee, Seismological Research Letters, 79(3), 416-423.

Denny, F.B., 2003, Bedrock geology of Granite City quadrangle, Madison and St. Clair Counties, Illinois and St. Louis County, Missouri: Department of Natural Resources, Illinois State Geological Survey, scale 1:24,000, access at http://www.isgs.illinois.edu/maps-data-pub/statemap/pdf-files/granite_city_bg_sm.pdf.

Denny, F.B., and Devera, J.A., 2001, Bedrock geologic map of Monks Mound quadrangle, Madison and St. Clair Counties, Illinois, Department of Natural Resources: Illinois State Geological Survey, scale 1:24,000, access at http://www.isgs.illinois.edu/maps-data-pub/statemap/pdf-files/monks_mound_bg_sm.pdf.

Electric Power Research Institute, 1993, Guidelines for determining design basis ground motions, Palo Alto, Calif: Electric Power Research Institute, v. 1-5, EPRI TR-102293.

Fehrenbacher, J.B., Jansen, I.J., and Olson, K.R., 1986, Loess thickness and its effect on soils in Illinois: University of Illinois Agricultural Experiment Station Bulletin 782, 13 p.

Fleischman, R.B., Restrepo, J.I., Pampanin, S., Maffei, J.R., Seeber, K., and Zahn, F.A., 2014, Damage evaluations of precast concrete structures in the 2010-2011 Canterbury earthquake sequence, Earthquake Spectra, 30(1), 272-306.

Frankel, A.F., Petersen, M.D., Mueller, C., Haller, K.M., Wheeler, R.L., Leyendecker, E.V., Wesson, R.L., Harmsen, S.C., Cramer, C.H., Perkins, D., and Rukstales, K.S., 2002, National seismic hazard maps: documentation: United States Geological Survey

Open-File Report 02–420, 33 p.

Gaunt, David A., Travis Carr, Vicki Dove and Edith Starbuck, 2009a, Surficial material geologic map of the Alton 7.5' quadrangle St. Charles County, Missouri; Missouri Department of Natural Resources, Division of Geology and Land Survey, Open File Map OFM-09-543-GS, scale 1:24,000, 1 sheet.

Gaunt, David A., Travis Carr, Vicki Dove and Edith Starbuck, 2009b, Surficial material geologic map of the Elsah 7.5' quadrangle St. Louis and St. Charles counties, Missouri; Missouri Department of Natural Resources, Division of Geology and Land Survey, Open File Map OFM-09-544-GS, scale 1:24,000, 1 sheet.

Gaunt, David A. and Travis Carr, 2010a, Surficial material geologic map of the Florissant 7.5' quadrangle St. Charles County, Missouri; Missouri Department of Natural Resources, Division of Geology and Land Survey, Open File Map OFM-10-560-GS, scale 1:24,000, 1 sheet.

Gaunt, David A. and Travis Carr, 2010b, Surficial material geologic map of the Clayton 7.5' quadrangle St. Charles and St. Louis counties, Missouri; Missouri Department of Natural Resources, Division of Geology and Land Survey, Open File Map OFM-10-561-GS, scale 1:24,000, 1 sheet.

Gaunt, David A. and Travis Carr, 2010c, Surficial material geologic map of the Webster Groves 7.5' quadrangle St. Louis City and County, Missouri and Illinois; Missouri Department of Natural Resources, Division of Geology and Land Survey, Open File Map OFM-10-562-GS, scale 1:24,000, 1 sheet.

Gaunt, David A. and Travis Carr, 2010d, Surficial material geologic map of the Oakville 7.5' quadrangle St. Louis and Jefferson counties, Missouri and Illinois; Missouri Department of Natural Resources, Division of Geology and Land Survey, Open File Map OFM-10-563-GS, scale 1:24,000, 1 sheet.

Gaunt, David A. and Travis Carr, 2010e, Surficial material geologic map of the Cahokia 7.5' quadrangle St. Louis City, Missouri and Illinois; Missouri Department of Natural Resources, Division of Geology and Land Survey, Open File Map OFM-10-564-GS, scale 1:24,000, 1 sheet.

Gomberg, J.S., Waldron, B., Schweig, E.S., Hwang, H., Webbers, A., Van Arsdale, R.B., Tucker, K., Williams, R.A., Street, R., Mayne, P.W., Stephenson, W.J., Odum, J.K., Cramer, C.H., Updike, R.G., Hutson, S.S., and Bradley, M.W., 2003, Lithology and shear-wave velocity in Memphis, Tennessee: Bulletin of the Seismological Society of America, v. 93(3), p. 986–997.

Goodfield, A.G., 1965, Pleistocene and surficial geology of the city of St. Louis and the adjacent St. Louis County, Missouri: University of Illinois at Urbana-Champaign, Ph.D. thesis, 214 p.

Grimley, D.A., 2009, Surficial geology of Columbia Quadrangle, St. Clair and Monroe Counties, Illinois, Illinois State Geological Survey, Champaign, IL, available at http://www.isgs.illinois.edu/maps-data-pub/isgs-quads/c/pdf-files/columbia-sg.pdf.

Grimley, D.A., and Phillips A.C., 2006, Surficial geology of Madison County, Illinois: Illinois State Geological Survey, Illinois Preliminary Geologic Map IPGM Madison County-SG, scale 1:100,000, access at http://www.isgs.illinois.edu/maps-data-pub/ipgm/pdf-files/madison-co-sg.pdf.

Grimley, D.A. and A.C. Phillips, 2011, Surficial Geology of St. Clair County, Illinois: Illinois State Geological Survey, Illinois County Geologic Map, ICGM St. Clair County-SG, 2 sheets, 1:62,500.

Grimley, D.A., A.C. Phillips, and S.W. Lepley, 2007a, Surficial Geology of Monks Mound Quadrangle, Madison and St. Clair Counties, Illinois: Illinois State Geological Survey, Illinois Preliminary Geologic Map, IPGM Monks Mound-SG, 1:24,000.

Grimley, D.A., Phillips A.C., Follmer L.R., Wang H., and Nelson R.S., 2007b, Quaternary and environmental geology of the St. Louis metro east area, in Malone, David, ed., Guidebook for Field Trip for the 35th Annual Meeting of the North-Central Section of the Geological Society of America: Illinois State Geological Survey Guidebook 33, p. 21–73.

Haase, J.S., Y.S. Choi, R.L. Nowack, C.H. Cramer, O.S. Boyd, and R.A. Bauer, 2011, Liquefaction hazard for the region of Evansville, Indiana: U.S. Geological Survey Open-File Report 2011–1203, 38 p.

Harrison, R.W., 1997, Bedrock geologic map of the St. Louis, 30'x 60' quadrangle, Missouri and Illinois: United States Geological Survey, Miscellaneous Investigation Series Map I-2533, scale 1:100,000.

Hayati, H., and Andrus, R.D., 2008, Liquefaction potential map of Charleston, South Carolina based on the 1886 earthquake, Journal of Geotechnical and Geoenvironmental Engineering,134(6), 815–828.

Hoffman, David, Neil Anderson and J. David Rogers, 2008, St. Louis metro area shear wave velocity testing; Final technical report for External Grant Award Number 06HQGR0026, 24 p.

Holzer, T.L., Noce, T.E., Bennett, M.J., Tinsley, J.C., III, and Rosenberg, L.I., 2005, Liquefaction at Oceano, California, during the 2003 San Simeon earthquake, Bulletin of the Seismological .Society of America, 95(6), 2396-2411.

Holzer, T.L., Bennett, M.J., Noce, T. E., Padovani, A.C., and Tinsley, J.C., 2006, Liquefaction hazard mapping with LPI in the Greater Oakland, California, area, Earthquake Spectra, 22(3), 693-708.

Holzer, T. L., Noce, T. E., and Bennett, M. J., 2011, Liquefaction probability curves for surficial geologic deposits, Environmental & Engineering Geoscience, 17(1), 1-21.

Iwasaki, T., Tokida, K., Tatsuko, F., and Yasuda, S., 1978, A practical method for assessing soil liquefaction potential based on case studies at various site in Japan, 2nd International Conference on Microzonation, San Francisco, November 26 – December 1, 1978, 885-896.

Iwasaki, T., Tokida, K., Tatsuoka, F., Watanabe, S., Yasuda, S., and Sato, H., 1982, Microzonation for soil liquefaction potential using simplified methods. Proceedings of 3rd International Conference on microzonation, Seattle, USA, June 28 – July 1, 1982, 1319-1330.

Jibson, R.D., Harp, E.L., and Michael, J.A., 2000, A method for producing digital probabilistic seismic landslide hazard maps, Engineering Geology, 58(3-4), 271-289.

Kaden, Scott and Edith Starbuck, 2008a, Surficial material geologic map of the Columbia Bottom 7.5' quadrangle St. Charles and St. Louis counties and St. Louis City, Missouri; Missouri Department of Natural Resources, Division of Geology and Land Survey, Open File Map OFM-08-531-GS, scale 1:24,000, 1 sheet.

Kaden, Scott and Edith Starbuck, 2008b, Surficial material geologic map of the Granite City 7.5' quadrangle St. Louis City and County, Missouri; Missouri Department of Natural Resources, Division of Geology and Land Survey, Open File Map OFM-08-532-GS, scale 1:24,000, 1 sheet.

Liu, H-P, Y. Hue, J Dorman, T-S Chang, and J-M Chiu, 1997, Upper Mississippi Embayment Shallow Seismic Velocities Measured in situ, Engineering Geology 46, pp. 313-330.

Lutzen, E.E., and Rockaway, J.D., 1971. Engineering geology of St. Louis County, Missouri: Missouri State Geological Survey, Engineering Geology Series No. 4, 23 p.

MoDNR-DGLS, 2007, Well logs, wells certified, in Missouri Environmental Geology Atlas (MEGA), Division of Geology and Land Survey, Missouri Department of Natural Resources.

Moon, L., Dizhur, D., Senaldi, I., Derakhashan, H., Griffith, M., Magenes, G., and Ingham, J., 2014, The demise of the URM building stock in Christchurch during the 2010-2011 Canterbury earthquake sequence, Earthquake Spectra, 30(1), 253-276.

Nelson, W.J., 1995, Structural features in Illinois: Illinois State Geological Survey, Bulletin 100, 144 p.

Nuttli, O.W., 1973, The Mississippi Valley earthquakes of 1811 and 1812: Intensities, ground motion, and magnitudes: Bulletin of the Seismological Society of America, v. 63, no. 1, p. 227–248.

Odum, J.K., W.J. Stephenson and R.A. Williams, 2010, Predicted and observed spectral response from collocated shallow, active- and passive-source Vs data at five ANSS sites, Illinois and Indiana, USA. Seismological Research Letters, Vol. 81, No. 6, pp. 955-964.

Palmer, J., Mesko, T., Cadoret, J., James, K., and Jones, R., 2006. St. Louis, Missouri surficial materials database. Missouri Department of Natural Resources, Division of Geology and Land Survey, CD-ROM.

Papathanassiou, G., 2008, LPI-based approach for calibrating the severity of liquefaction-induced failures and for assessing the probability of liquefaction surface evidence, *Engineering Geology*, 96(1-2), 94-104.

Pearce, J.T., and Baldwin, J.N., 2008, Liquefaction susceptibility and probabilisticliquefaction potential hazard mapping, St. Louis, Missouri and Illinois: National Earthquake Hazards Reduction Program, Final Technical Report, 51 p. access at http://earthquake.usgs.gov/research/external/research.php.

Petersen, M.D., A.D. Frankel, S.C. Harmsen, C.S. Mueller, K.M. Haller, R.L. Wheeler, R.L. Wesson, Y. Zeng, O.S. Boyd, D.M. Perkins, N. Luco, E.H. Field, C.J. Wills, and K.S. Rukstales, 2008, Documentation for the 2008 update of the United States National Seismic Hazard Maps, USGS Open-file Report 2008-1128, 127 p. (available at http://pubs.usgs.gov/of/2008/1128/).

Petersen, M. D., M. Moschetti, P. Powers, C. Mueller, K. Haller, A. Frankel, Y. Zeng, S. Rezaeian, S. Harmsen, O. Boyed, N. Field, R. Chen, K. Rukstales, N. Luco, R. Wheeler, R. Williams, and A. Olsen, 2014, *The 2014 update of the United States national seismic hazard models*, U.S. Geological Survey, OFR 2014-1091, 255 p. (available at http://pubs.usgs.gov/of/2014/1091/).

Phillips, A.C., 2010, Surficial Geology of Paderborn Quadrangle, Monroe and St. Clair Counties, Illinois: Illinois State Geological Survey, Illinois Geologic Quadrangle Map, IGQ Paderborn-SG, 2 sheets, 1:24,000, report, 7 p.

Phillips, A.C., Grimley, D.A., and Lepley, S.W., 2001, Surficial geology map of Granite City quadrangle, Madison and St. Clair Counties, Illinois, and St. Louis County, Missouri: Illinois State Geological Survey, IGQ Granite City-SG, scale 1:24,000, access at http://www.isgs.illinois.edu/maps-data-pub/statemap/pdf-files/granite_city_sg_sm.pdf.

Romero, S., and Rix, G.J., 2001, Regional variations in near surface shear wave velocity in the greater Memphis area: Engineering Geology, v. 62, p. 137–158.

Romero, S., and Rix, G.J., 2005, Ground motions amplification of soils in the upper Mississippi Embayment: National Science Foundation Mid America Earthquake Center, report no. GIT-CEE/GEO-01-1, p. 461.

Romero-Huddock, S., and G.J. Rix, 2005. Liquefaction potential mapping in Memphis/Shelby County, Tennessee. In Seminar on New Knowledge of Earthquake Hazard in the Central United States and Implications for Building Seismic Design Practice, March 3, 2005, Memphis, Tennessee Speaker Handouts, 7-15-7-32. Redwood City, CA: Applied Technology Council.

Schultz, A.P., 1993. Map showing surficial geology of the St. Louis 30x60 minute quadrangle, U.S. Geological Survey Open-File Report 93-288, scale 1:100,000, U.S. Geological Survey, Reston, VA.

Seed, H.B., and ldriss, I.M., 1971, Simplified procedure for evaluating soil liquefaction potential. Journal of the Soil Mechanics and Foundation Division, 97, 1249-1273.

Seed, H.B., Tokimatsu L.F., Harder, L.F., and Chung, R.M., 1985. Influence of SPT procedures in soil liquefaction resistance evaluations, Journal of. Geotechnical Engineering., 111(12), 1425-1445.

SigmaPlot software, 2006, SigmaPlot for Window, version 10.0.

Toprak, S., and Holzer, T.L., 2003, Liquefaction potential index: Field assessment, ASCE Journal of Geotechnical and Geoenvironmental Engineering, 129(4), 315-322.

USGS. 2011, Groundwater watch. http://groundwaterwatch.usgs.gov (accessed December, 2011).

Weibull, W. 1951, A statistical distribution function of wide applicability. Journal of Applied Mathematics, 18(3), 293-296.

Williams, 2013 ?

Williams R.A., Odum, J.K., Stephenson, W.J., and Hermann, R.B., 2007a, Shallow P-and S-wave velocities and site resonances in the St Louis region, Missouri-Illinois: Earthquake Spectra, v. 23, no. 3, p. 711–726.

Williams, R.A.; Steckel, P., and Schweig, E., 2007b, St. Louis area earthquake hazards mapping project: United States Geological Survey Fact Sheet 2007-3073, 2 p.

Wills, C.J., Petersen, M., Bryant W.A., Reichle, M., Saucedo, G.J., Tan, S., Taylor, G., and Treiman, J., 2000, A site-conditions maps for California based on geology and shear-wave velocity: Bulletin of Seismological Society of America, v. 90, no. 6B, p. S187–S208.

Woolery, E.W., 2005, Ground motion site effects in the Wabash Valley region form the 18 June 2002 Darmstadt earthquake, U.S. Geological Survey Final Technical Report for Award Number 04HQGR0095, 111 p.

Youd, T.L., 1973. Liquefaction, flow, and associated ground failure, U.S. Geological Survey Circular 688 < http://pubs.er.usgs.gov/publication/cir688>.

Youd, T.L., Idriss, I.M., Andrus, R.D., Arango, I., Castro, G., Christian, J.T., Dobry, R., Finn, W.D. L., Harder, L.F., Hynes, M.E., Ishihara, K., Koester, J.P., Liao, S.S.C., Marcuson, W.F., Martin, G.R., Mitchell, J.K., Moriwaki, Y., Power, M.S., Robertson, P.K., Seed, R.B., and Stokoe, K.H., 2001. Liquefaction resistance of soils: Summary report from the 1996 NCEER and 1998 NCEER/NSF workshops on evaluation of liquefaction resistance of soils, Journal of Geotechnical and Geoenvironmental Engineering, 127(10), 817-833.

Publications from this Research

One publication resulted from this research so far. A pdf file of the publication is provided separately.

Cramer, C.H., R.A. Bauer, J. Chung, J.D. Rogers, L. Pierce, V. Voigt, B. Michell, D. Gaunt, R.A. Williams, D. Hoffman, G.L. Hempen, P.J. Steckel, O.S. Boyd, C.M. Watkins, K. Tucker, and N. McCallister, 2017, St. Louis area earthquake hazards mapping projects: seismic and liquefaction hazard maps, *Seis*. *Res*. *Lett*. **88**, 206-223.

Appendix A

May 31, 2011

Comparisons of Soil Amplification Distributions

by Chris H. Cramer, CERI, ccramer@memphis.edu

Eight soil profiles were used to generate site amplification distributions for comparing the effects of variations in possible reference profiles for three basic groups of soil profiles: clay (5m, 10m, and 15m) over alluvium, loess (5m, 10m, and 20m) over till, and loess over sand over till with and without a basal silt layer. The site amplification distributions were generated using the randomization approach that will be used in generating the St. Louis Area Earthquake Hazards Mapping Project (SLAEHMP) seismic hazard maps. Input ground motions, soil profile properties (mainly shear wave velocity - Vs), and dynamic soil properties were randomized using Vs information provided by Bob Bauer. A suite of M7-8 earthquake time histories and a natural lognormal variation of 0.35 in standard dynamic soil properties were used to generate the resulting site amplification distributions. The various soil profiles used are summarized in table A1.

Table A1. Summary for the eight soil profiles used in this comparison.

Profile	Total Soil Thickness
Group 1 - COA:	
5m clay over alluvium	35 m
10 m clay over alluvium	35 m
15 m clay over alluvium	35 m
Group 2 - LOT:	
5 m loess over till (diamicton)	45 m
10 m loess over till (diamicton)	50 m
20 m loess over till (diamicton)	55 m
Group 3- LOSOT:	
5m loess over sand over till (diamicton) w/o basal silt	30 m
5m loess over sand over till (diamicton) w/ 10 m basal silt	40 m

Figures A1-A3 present the median amplification curves as a function of input hard rock ground motion. Each figure shows the median amplification curve for peak ground acceleration (PGA), and 0.2 s and 1.0 s spectral acceleration (Sa). The 16^{th} and 84^{th} percentiles (plus and minus one standard deviation – not shown for clarity) vary from 1.3 – 2.0 times above and below the median curves.

Figure A1 shows the group 1 results, which are for the same total soil thickness but varying the top layer of clay from 5m to 20 m thick. This shows the smallest group variation in median amplification among the three alternative clay thicknesses. The differences are frequency dependent, which is not surprising. PGA has the least, and not very significant, variation among the median amplifications. 1.0 s Sa has a bit more variation over the range of input hard-rock ground motions. 0.2s Sa shows the most

variation, particularly at weak input ground motions (less than 0.1g). The 0.2 s Sa variation is greatest going from 5m to 10m thickness of clay. To me, it is still important to have this level of detail in the Vs reference profiles, because of the frequency dependence of the results. This affirms the need for 5 m resolution in the Vs reference profiles.

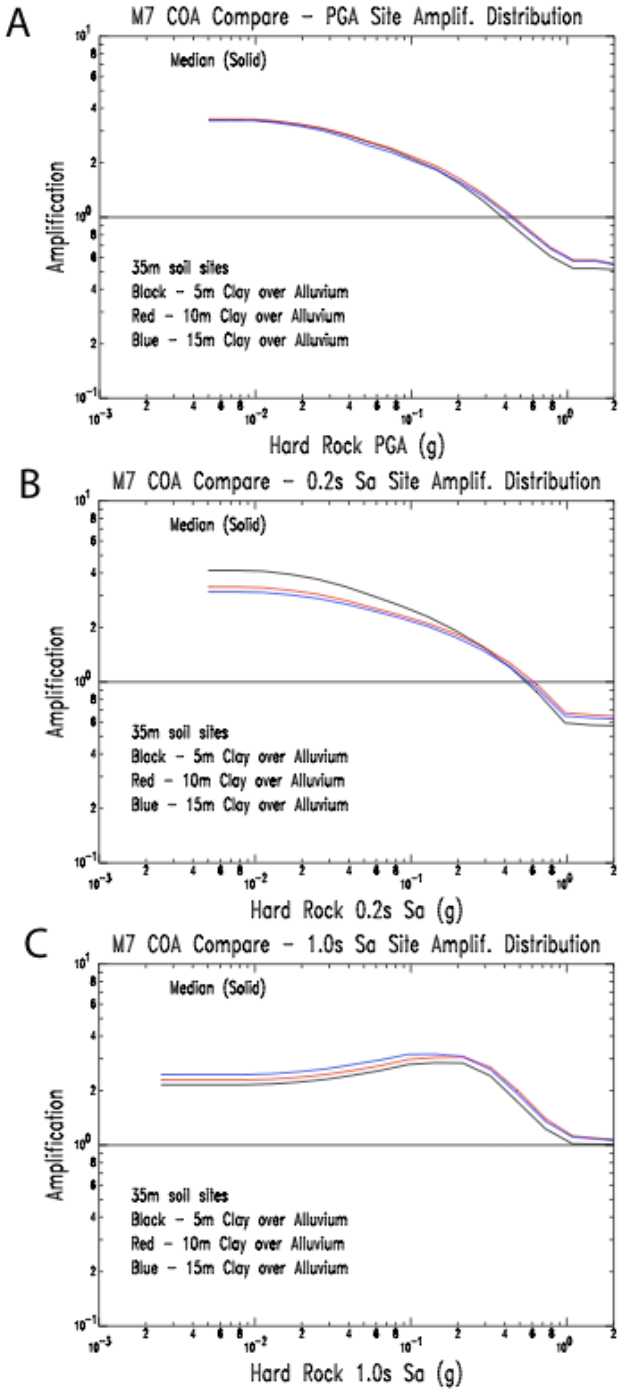

Figure A1. Group 1 comparisons of 5m, 10 m, and 15m thick clays over alluvium for (A) PGA, (B) 0.2 s Sa, and (C) 1.0 s Sa.

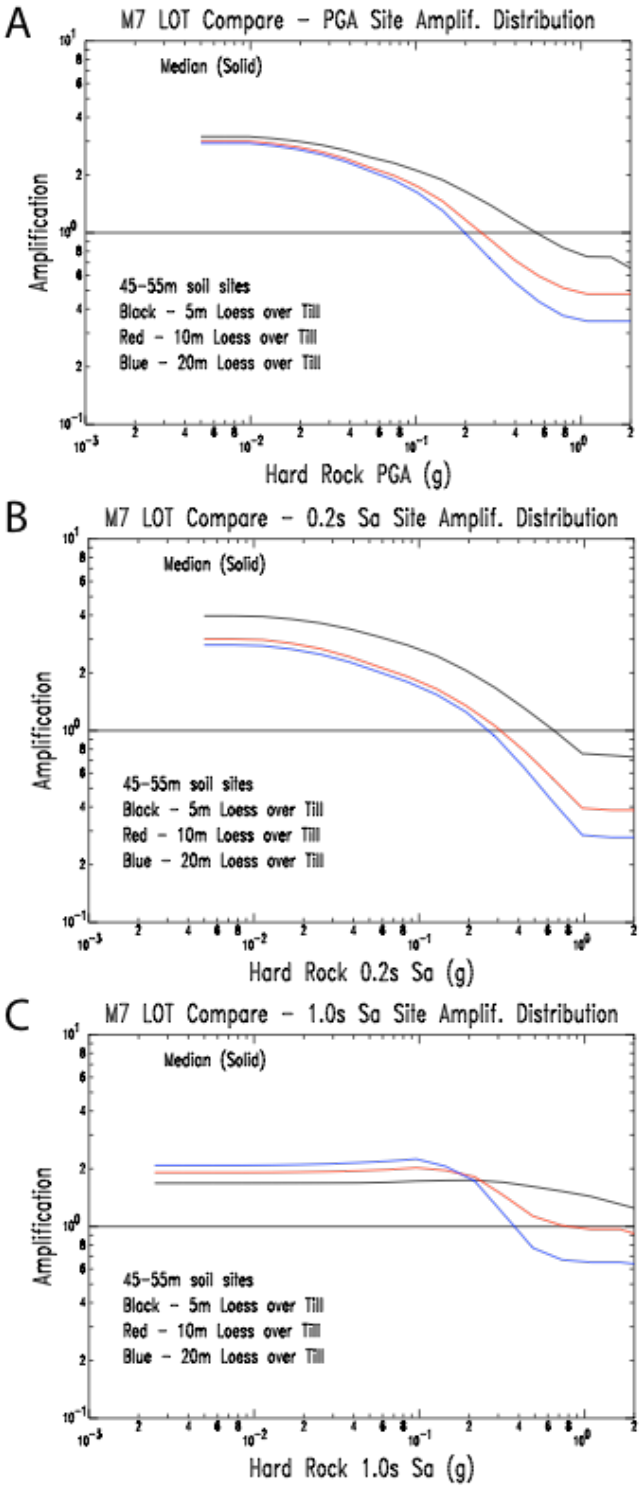

Figure A2. Group 2 comparisons of 5m, 10 m, and 20m thick loess over till for (A) PGA, (B) 0.2 s Sa, and (C) 1.0 s Sa. Note that the total thickness of soils varies from 45 to 55 m.

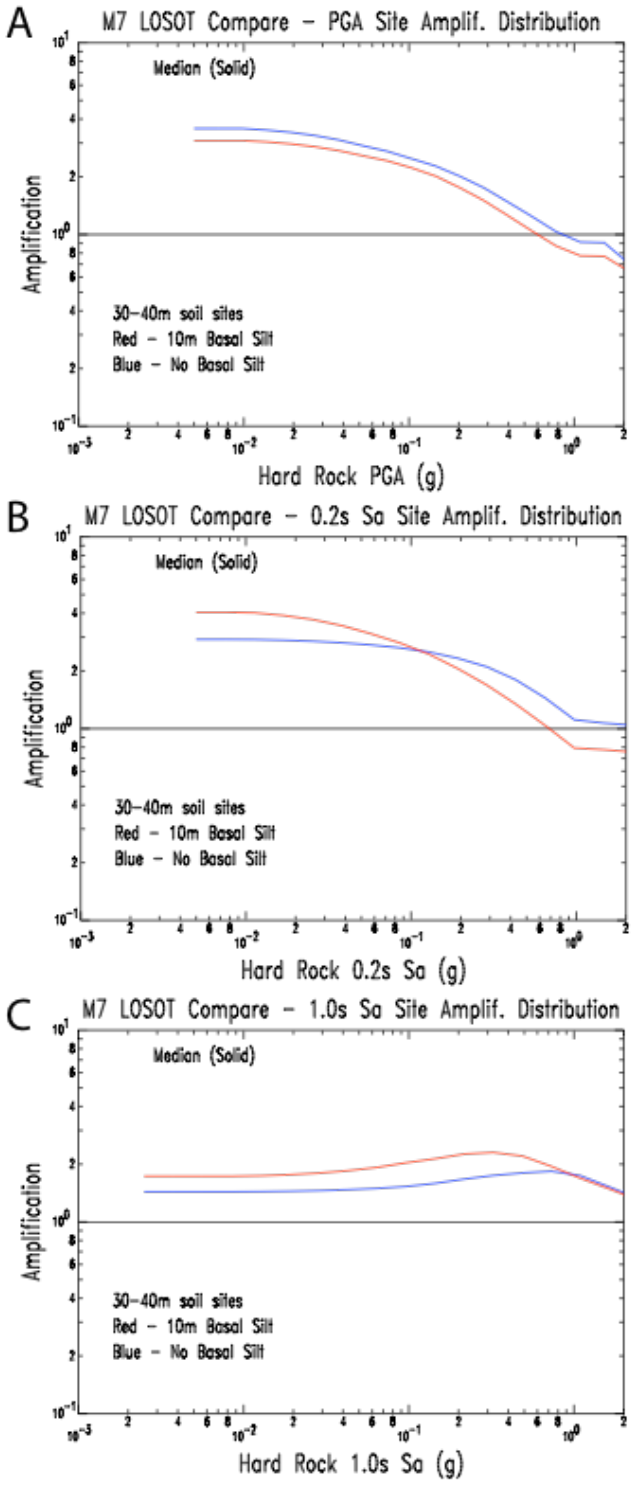

Figure A3. Group 3 comparisons of loess over sand over till with and without a 10 m basal silt layer (A) PGA, (B) 0.2 s Sa, and (C) 1.0 s Sa. Note that the 10 m basal layer is added to the no basal silt profile and increases the total soil thickness from 30m to 40 m.

Figure A2 shows the effect of increasing loess thickness and total thickness of soil. In figure A2 the differences are more dramatic and significant, particularly in the nonlinear soil behavior range (greater than 0.1 g input hard-rock ground motion). The differences are at all frequencies and have a lot to do with the change in total soil thickness. To me, these variations are significant and need to be retained in the soil reference models used by SLAEHMP to generate seismic hazard maps.

Figure A3 presents the impact of the presence of a basil silt layer on a loess-sand-till sequence of soils. The main effect is from the addition of the 10 m basal silt layer. Again, the variation from no basal layer to the presence of a 10 m basal layer is fairly dramatic and significant, particularly for 0.2 s Sa, where the nonlinear soil effect is amplified by the basal layer. Clearly, this level of detail is important to retain in the Vs reference profiles use by SLAEHMP to generate seismic hazard maps.

Appendix B

Illinois shear wave velocity reference profiles per geologic provinces in table 4 of text.

1 - Disturbed ground (5 m) over sand alluvium

Top depth (m)	Vs (m/sec)	St.Dev. (m/sec)
0.	122.	20.
5.	196.	40.
10.	215.	29.
15.	224.	48.
20.	248.	34.
25.	257.	32.
30.	280.	54.
35.	297.	50.
40.	314.	50.
45.	331.	50.
50.	348.	50.

2 - Sand alluvium

Top depth (m)	Vs avg (m/sec)	St.Dev. (m/sec)
0.	172.	37.
5.	196.	40.
10.	215.	29.
15.	224.	48.
20.	248.	34.
25.	257.	32.
30.	280.	54.
35.	297.	50.
40.	314.	50.
45.	331.	50.
50.	348.	50.

3 - Thin alluvial clay (5 m) over sand alluvium

Top depth (m)	Vs avg (m/sec)	St.Dev. (m/sec)
0.	122.	20.
5.	196.	40.
10.	215.	29.
15.	224.	48.
20.	248.	34.
25.	257.	32.
30.	280.	54.
35.	297.	50.
40.	314.	50.

45.	331.	50.
50.	348.	50.

4 - Thick alluvial clay (10 m) over sand alluvium

Top depth (m)	Vs avg (m/sec)	St.Dev. (m/sec)
0.	122.	20.
5.	146.	20.
10.	215.	29.
15.	224.	48.
20.	248.	34.
25.	257.	32.
30.	280.	54.
35.	297.	50.
40.	314.	50.
45.	331.	50.
50.	348.	50.

5 - Thick (15 m) loess over till

Top depth (m)	Vs avg (m/sec)	St.Dev. (m/sec)
0.	174.	42.
5.	204.	41.
10.	241.	55.
15.	333.	137.
20.	507.	60.
25.	598.	75.
30.	420.	195.
35.	365.	103.
40.	449.	76.
45.	39.	90.
50.	456.	54.
55.	556.	54.
60.	456.	75.

6 - Thick (15 m) loess over till (10 m) over basal silt

Top depth (m)	Vs avg (m/sec)	St.Dev. (m/sec)
0.	174.	42.
5.	204.	41.
10.	241.	55.
15.	333.	137.
20.	507.	60.
25.	338.	45.
30.	374.	45.
35.	411.	29.
40.	456.	54.

45.	465.	15.
50.	478.	50.
55.	487.	54.
60.	496.	50.

7 - Moderate loess (10 m) over till

Top depth (m)	Vs avg (m/sec)	St.Dev. (m/sec)
0.	174.	42.
5.	204.	41.
10.	333.	137.
15.	507.	60.
20.	598.	75.
25.	420.	195.
30.	365.	103.
35.	449.	76.
40.	639.	90.
45.	456.	54.
50.	556.	54.

8 - Moderate loess (10 m) over till (10 m) over thick basal silt

Top depth (m)	Vs avg (m/sec)	St.Dev. (m/sec)
0.	174.	42.
5.	204.	41.
10.	213.	60.
15.	333.	137.
20.	338.	45.
25.	374.	45.
30.	411.	29.
35.	456.	54.
40.	465.	15.
45.	478.	50.
50.	487.	54.
55.	496.	50.

9 - Thin loess (5 m) over till

Top depth (m)	Vs avg (m/sec)	St.Dev. (m/sec)
0.	195.	53.
5.	213.	60.
10.	333.	137.
15.	507.	60.
20.	598.	75.
25.	420.	195.
30.	365.	103.

35.	449.	76.
40.	639.	90.
45.	456.	54.
50.	556.	54.
55.	600.	90.

10 - Thin loess (5 m) thick till (20 m) over thick basal silt

Top depth (m)	Vs avg (m/sec)	St.Dev. (m/sec)
0.	195.	53.
5.	213.	60.
10.	333.	137.
15.	507.	60.
20.	598.	75.
25.	338.	45.
30.	374.	45.
35.	411.	29.
40.	456.	54.
45.	465.	15.
50.	478.	50.
55.	487.	54.
60.	496.	50.

11 - Thin loess (5 m) over thin till (10 m) over basal silt

Top depth (m)	Vs avg (m/sec)	St.Dev. (m/sec)
0.	195.	53.
5.	213.	60.
10.	333.	137.
15.	302.	45.
25.	338.	45.
30.	374.	45.
35.	411.	29.
40.	456.	54.

12 - Tributary Valleys

Top depth (m)	Vs avg (m/sec)	St.Dev. (m/sec)
0.	133.	42.
5.	147.	42.
10.	163.	55.
15.	181.	45.
20.	198.	45.
25.	216.	45.
30.	234.	45.
35.	252.	45.

40.	270.	45.
45.	288.	45.
50.	306.	45.
55.	324.	45.

13 - Glacial Ridge

Top depth (m)	Vs avg (m/sec)	St.Dev. (m/sec)
0.	201.	59.
5.	238.	10.
10.	237.	20.
15.	278.	17.
25.	278.	17.
30.	365.	103.
35.	449.	76.
40.	639.	90.
45.	354.	39.
50.	291.	29.
55.	456.	54.
60.	464.	15.
65.	470.	20.
70.	485.	25.

14 & 15 - Disturbed ground – extreme variable conditions, no representative shear wave column

Appendix C

Liquefaction Probability Curve Regressions

Table C1. Regression Statistics for Weibull Equation.

	Geologic Unit	Groundwater Level	LPI	Regression Coefficient				R^2
				a	b	c	X_0	
Low-lying floodplains	Qa	High	LPI>5	0.7851	0.0224	0.6093	0.1199	0.9967
			LPI>12	0.7539	0.0522	0.9356	0.1472	0.9970
		Normal	LPI>5	0.6366	0.1036	1.3630	0.1940	0.9954
			LPI>12	0.5702	0.1289	1.2010	0.2494	0.9968
	Qa(C)	High	LPI>5	0.7886	0.0108	0.6288	0.1091	0.9984
			LPI>12	0.7906	0.0231	0.5745	0.1230	0.9972
		Normal	LPI>5	0.7744	0.0703	1.2870	0.1632	0.9936
			LPI>12	0.7693	0.1048	1.1740	0.2255	0.9947
	Qa(S)	High	LPI>5	0.7968	0.0120	0.7968	0.1108	0.9978
			LPI>12	0.7955	0.0267	0.7067	0.1251	0.9924
		Normal	LPI>5	0.7829	0.0580	0.8447	0.1759	0.9920
			LPI>12	0.7729	0.1139	1.2040	0.2474	0.9928
	Qf	High	LPI>5	0.7843	0.0306	1.3580	0.1196	0.9958
			LPI>12	0.7426	0.0424	1.1970	0.1316	0.9974
		Normal	LPI>5	0.7389	0.0258	0.9114	0.1553	0.9956
			LPI>12	0.7158	0.0422	0.6161	0.1967	0.9884
	Qld	High	LPI>5	0.8038	0.0179	0.5673	0.1193	0.9923
			LPI>12	0.7762	0.0497	1.0670	0.1446	0.9978
		Normal	LPI>5	0.7022	0.0721	1.2410	0.1971	0.9909
			LPI>12	0.6652	0.1079	1.1010	0.2670	0.9969
	Qo	High	LPI>5	0.7667	0.0325	0.9235	0.1218	0.9984
			LPI>12	0.7148	0.0624	0.8399	0.1583	0.9932
		Normal	LPI>5	0.5463	0.1654	1.0880	0.2544	0.9772
			LPI>12	0.4778	0.2013	1.8490	0.3507	0.9903
	af	High	LPI>5	0.7752	0.0146	0.7608	0.1120	0.9994
			LPI>12	0.7802	0.0330	0.7607	0.1313	0.9971
		Normal	LPI>5	0.6299	0.0989	1.7050	0.1872	0.9939
			LPI>12	0.6298	0.1335	1.0940	0.2630	0.9979
Uplands	Ql	High	LPI>5	0.7159	0.0718	1.0530	0.1534	0.9976
			LPI>12	0.6494	0.1076	1.3890	0.1898	0.9964
		Normal	LPI>5	0.2634	0.1608	0.9990	0.3032	0.9964
			LPI>12	0.1558	0.2389	2.4300	0.3793	0.9981
	Qt	High	LPI>5	0.6870	0.0668	0.8854	0.1542	0.9975
			LPI>12	0.6045	0.0911	1.3590	0.1966	0.9930
		Normal	LPI>5	0.2635	0.2030	0.7729	0.3251	0.9944
			LPI>12	0.2206	1.2960	0.4311	0.8354	0.9890
	af	High	LPI>5	0.6796	0.0298	0.9545	0.1218	0.9996
			LPI>12	0.6170	0.0382	1.5250	0.1341	0.9989
		Normal	LPI>5	0.6446	0.0671	0.4885	0.2294	0.9926
			LPI>12	0.5720	0.0513	0.7059	0.3108	0.9989

R	High	LPI>5	0.4425	0.1297	0.7950	0.1943	0.9935
		LPI>12	0.3636	0.1106	0.8186	0.2119	0.9948
	Normal	LPI>5			n.a		
		LPI>12			n.a		

a, *b*, *c*, and x_0 = fitted coefficients; R^2 = coefficient of determination